

NASA
TM
X-71802
c.1

TERRESTRIAL PHOTOVOLTAIC MEASUREMENTS

LOAN COPY: RETURN TO
AFWL TECHNICAL LIBRARY
KIRTLAND AFB, TEXAS

TECH LIBRARY KAFB, NM
0152333



Workshop Proceedings

March 19-21, 1975
Cleveland, Ohio

Organized by

Lewis Research Center

NATIONAL AERONAUTICS AND SPACE ADMINISTRATION

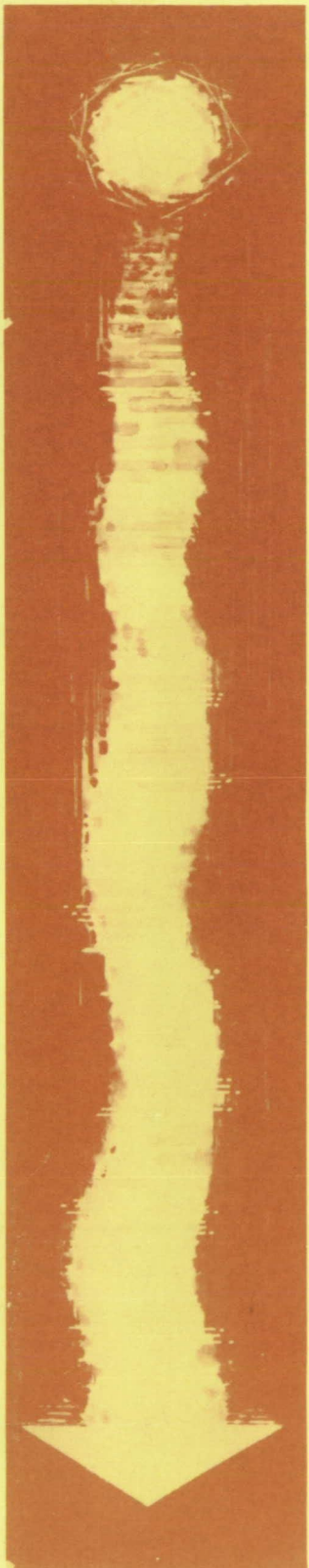
Sponsored by

ENERGY RESEARCH AND DEVELOPMENT ADMINISTRATION



RECEIVED
14 JAN 1976
Technical Library
Weapons Laboratory

NATIONAL AERONAUTICS AND SPACE ADMINISTRATION
RESEARCH & DEVELOPMENT ADMINISTRATION
USA





FOREWORD

A Terrestrial Photovoltaic Measurements Workshop under the joint sponsorship of ERDA and NASA was held at the NASA Lewis Research Center in March 1975. Nearly 100 people attended from all segments of the solar cell community. The workshop was divided into three separate sessions:

- (1) Solar Intensity and Spectrum Conditions for Terrestrial Photovoltaics
- (2) Terrestrial Sunlight Simulation
- (3) Methodology for Measurements and Calibration of Solar Cells

A broad spectrum of short papers was presented; then the attendees addressed key questions in the workshop sessions. The separate sessions were held concurrently.

An interim draft of procedures for testing solar cells for terrestrial applications that resulted from the workshop sessions is available from the NASA Lewis Research Center. A final version of the test procedures manual is planned for the summer of 1976.

This conference was under the cochairmanship of Leonard M. Magid (Division of Solar Energy, ERDA) and Henry W. Brandhorst (Head, Photovoltaic Section, NASA Lewis Research Center).

Technically edited by
Larry N. Scudder
Thomas M. Klucher

NASA Lewis Research Center
Cleveland, Ohio

Page intentionally left blank

Page intentionally left blank

CONTENTS

	Page
FOREWORD	iii
INTRODUCTORY REMARKS	
Daniel T. Bernatowicz	ix
PURPOSE OF THE WORKSHOP	
Henry W. Brandhorst, Jr.	xi
SOLAR RADIATION MEASUREMENTS AT NOAA	
Michael R. Riches	1
SOLAR RADIATION AT NEWPORT, RHODE ISLAND	
John R. Hickey	4
MEASUREMENT OF INSOLATION AT DSET	
Gene Zerlaut	10
MEASUREMENT OF THE SOLAR CONSTANT BY PACRAD ON CONVAIR 990 FLIGHTS IN 1968	
James M. Kendall, Sr.	12
SPECTRAL MEASUREMENTS OF SOLAR INTENSITY AND SPECTRUM CONDITIONS AT HIGH ALTITUDES (5200 TO 14 000 FT) AND ARID (COLORADO) CONDITIONS	
Rolland L. Hulstrom	17
SPECTRAL DISTRIBUTION OF SUNLIGHT UNDER VARIOUS AIR MASS CONDITIONS	
Alfred Seck	25
ESTIMATION OF DIRECT NORMAL RADIATION	
Eldon C. Boes	38
SOLAR CELL PERFORMANCE IN TERRESTRIAL SUNLIGHT	
J. A. Castle	44
VARIATION OF SOLAR CELL EFFICIENCY WITH AIR MASS	
Henry W. Brandhorst, Jr.	51
MICROCLIMATOLOGICAL INFLUENCES ON TWO SOLAR MODULES	
Douglas M. Warschauer	58

	Page
MODERN RADIOMETRY FOR PHOTOVOLTAIC SOLAR CONVERSION	
Jon Geist	67
SOLAR SIMULATOR SPECTRAL AND IRRADIANCE DEGRADATION	
A. R. Lunde	74
PROPOSED STANDARD FOR AM1 SUNLIGHT	
Henry Hadley, Jr.	80
DETERMINATION OF DIFFUSE RADIATION CHARACTERISTICS FOR APPLICATION IN SOLAR ENERGY HARVESTING	
B. H. Armstrong, J. V. Dave, and P. Halpern	86
LOW COST, LARGE AREA SOLAR SIMULATION	
Vincent DeLeo	94
LOW COST, AM2 SIMULATOR	
Henry Curtis	98
AN ANALYSIS OF THE INFLUENCE OF CELL CHARACTERISTICS ON THE SPECTRAL SENSITIVITY OF Cu_2S-CdS SOLAR CELLS	
Allen Rothwarf	106
SPECTRAL EFFECTS IN CdS/Cu_2S SOLAR CELLS	
H. Hadley, Jr.	113
PREDICTION OF TERRESTRIAL SOLAR CELL SHORT-CIRCUIT CURRENTS BY SPECTRAL ANALYSIS	
Henry W. Brandhorst, Jr.	120
TERRESTRIAL SOLAR CELL MEASUREMENTS	
Engene L. Ralph	129
SOLAR CELL MEASUREMENT TECHNIQUES USED AT NASA LEWIS RESEARCH CENTER	
Russell E. Hart	134
A STANDARD FOR SOLAR CELL TESTING AND REPORTING	
John D. Meakin	140
RESULTS OF SESSION I WORKING GROUP - SOLAR INTENSITY AND SPECTRUM CONDITIONS FOR TERRESTRIAL PHOTOVOLTAICS	
John R. Hickey	146
RESULTS OF SESSION II WORKING GROUP - TERRESTRIAL SUNLIGHT SIMULATION	
Henry Curtis	150

	Page
RESULTS OF SESSION III WORKING GROUP - METHODOLOGY FOR MEASUREMENT AND CALIBRATION OF SOLAR CELLS	
Eugene L. Ralph	151
UNIFIED RECOMMENDATIONS OF THE WORKSHOP	
Henry Brandhorst	154
APPENDIX - SUPPLEMENTAL PAPERS	
SPECTRAL DISTRIBUTION OF DIRECT AND DIFFUSE SOLAR ENERGY RECEIVED AT SEA LEVEL OF A MODEL ATMOSPHERE	
J. V. Dave, P. Halpern, and N. Braslau	159
STATIONARY SILICON SOLAR CELL CONVERTER CALCULATIONS	
Werner Luft	168
ATTENDEES	175

Page intentionally left blank

Page intentionally left blank

INTRODUCTORY REMARKS

Daniel T. Bernatowicz

NASA Lewis Research Center
Cleveland, Ohio 44135

I want to welcome you to what we believe is a very important meeting. I am very pleased by your response to this meeting called on such short notice, especially because it indicates you share our feelings as to its importance. In this meeting we must all agree on how we should make our efficiency measurements, then we can compare and discuss our results knowing what each others measurements represent. We had a number of inquiries over the past months from investigators who have just entered the field, asking the best way to make efficiency measurements. I think the longer you are in the field the more you recognize the critical need for a standard way. It's an important problem. How easy a problem it will be to settle in 3 days really depends on us. It's not so much a technical issue, it's more a "people" problem, one of reaching a consensus.

From my past experience with the solar cell community and the fact that so many representatives are here, I'm really confident we will cooperate and that at the end of the 3 days we will be very close to having agreed on the exact way we want to measure efficiency in the first few years.

Page intentionally left blank

Page intentionally left blank

PURPOSE OF THE WORKSHOP

Henry W. Brandhorst, Jr.

NASA Lewis Research Center
Cleveland, Ohio 44135

Absolute measurement of solar cell performance is a difficult task. Furthermore, obtaining agreement between laboratories is even more difficult, but essential. It is imperative that these problems be solved for the terrestrial photovoltaic program. In the space program these problems were solved by finding ways of calibrating solar cells in the space environment, devising artificial light sources that duplicated the spectrum outer space sunlight reasonably well, and finding testing techniques that combined standard cells with artificial light sources to predict the performance of other solar cells in space. We are now confronted by exactly the same problem for terrestrial measurements. Everyone wants to know how good their cell is, how the best available cell will perform. To solve these basic measurement problems is why we've come together. Several areas must be considered. First, the intensity and appropriate spectral distribution of terrestrial sunlight must be agreed upon so we can choose the intensity of a terrestrial sunlight simulator. Most importantly we must agree on a single spectrum for the light source that might be used. We recognize that it's an impossible chore to set a single spectrum that covers all the possible ranges of terrestrial sunlight, but it must be done so all measurements can be made on a common basis. Next, we must agree on a standard testing procedure for performing these solar cell measurements in natural, as well as artificial, sunlight. Included in this procedure are problems of developing a standard cell, choosing the best artificial light source and its intensity, determining the procedures to be used to set intensity of that light source so that a true, accurate reading of short-circuit current is obtained. We must also solve the basic problems of electrical hookups and what area should be used to determine device efficiency. Finally, how do we use pyranometers or pyrheliometers and what role do they play in our measurements? Thus, we must come up with a complete package, an interim method for terrestrial solar cell measurements. It must be an interim method because we can't

begin to answer all the questions in this 3-day workshop. I hope we can reach a consensus, that each working group will come together and answer the questions presented them, and that we, as a total workshop, can agree on an interim method for measuring terrestrial photovoltaic cells. We will also identify many areas of research or many questions that need to be answered in the year before the next workshop. These are an equally important product of our workshop. Thus, our purpose is clear. We must first agree on an interim method, and, secondly, we must identify those areas in need of further work.

SOLAR RADIATION MEASUREMENTS AT NOAA

Michael R. Riches

NOAA/National Weather Service
Silver Spring, Maryland 20910

The National Oceanic and Atmospheric Administration (NOAA) through its component National Weather Service (NWS) operates a solar radiation monitoring network. The current network consists of 60 stations monitoring global (direct plus diffuse) and five stations monitoring direct. Twenty-eight cooperative stations also submit global data.

The equipment in the current network is no longer manufactured or repaired. Therefore, the National Oceanic and Atmospheric Administration and the National Science Foundation (NOAA, NSF) are replacing this network with a smaller, better equipped network (see fig. 1 and list of cities at the end of article). In addition, the NOAA-NSF project will provide the quality control and focal point for solar radiation measurements.

Spectral data are not presently available from NOAA. The data will be taken at a small number of stations in the future program. At present, the Smithsonian Radiation Biology Lab takes spectral data at Barrow, Alaska, Panama, Washington, D. C., and Tallahassee, Florida (joint program with NOAA). Data for the first three stations will be available April 1.

The following is the recommended solar radiation network:

- | | | |
|--------------------------|---------------------------------------|--------------------------------|
| 1. Fairbanks, Alaska | 13. Lake Charles, La. | 25. Medford, Oreg. |
| 2. Montgomery, Ala. | 14. Blue Hill, Mass. ^a | 26. Nashville, Tenn. |
| 3. Phoenix, Ariz. | 15. Caribou, Maine | 27. Brownsville, Tex. |
| 4. Fresno, Calif. | 16. Columbia, Mo. | 28. El Paso, Tex. |
| 5. Los Angeles, Calif. | 17. Great Falls, Mont. | 29. Midland, Tex. |
| 6. Boulder, Colo. | 18. Omaha, Nebr. ^a | 30. Salt Lake City, Utah |
| 7. Grand Junction, Colo. | 19. Greensboro, N. C. | 31. Sterling, Va. |
| 8. Miami, Fla. | 20. Bismarck, N. D. | 32. Burlington, Vt. |
| 9. Tallahassee, Fla. | 21. Albuquerque, N. Mex. ^a | 33. Seattle, Wash. |
| 10. Boise, Idaho | 22. Ely, Nev. | 34. Madison, Wis. ^a |
| 11. Indianapolis, Ind. | 23. Las Vegas, Nev. | 35. Lander, Wyo. |
| 12. Dodge City, Kans. | 24. Cleveland, Ohio | |

^aExisting pyrhelimetric sites.

DISCUSSION

- Q: Do you expect to publish data from the older bulb-type instruments that are being phased out as they wear out if they are still around 2 years from now?
- A: There won't be any around in 1977. We're initiating a recall of all of them to recalibrate them and see if they are fit for the field. There have been 15 brought in to date, so that a 60 station network is sort of a lie because about 10 of them have gone by the wayside. Of the 15 instruments brought in, only one of them was fit to go back to the field. There is even a question as to whether it was actually recoated with Parsons black or whether it is still a lamp black instrument; therefore, I expect by July 1975 there will be no model 180⁰ pyranometers in the network.
- Q: The spectral information is of course of overriding importance for photovoltaic applications. I'd like to know in a little more detail what you said could be available now. You mentioned one possible source now, could you say just a little bit more about that?
- A: I don't know a whole lot about it, but Dr. Kline of the Smithsonian Radiation Laboratory in Rockville, Maryland, is interested in spectral measurements from biological point of view and they have approximately 5 years of this 100 nanometer band information for Washington, D. C., I believe 3 years for Barrow, Alaska, 1 year for Panama, and they are taking data at Tallahassee. These data will not be available until next year. The data that they're taking at Tallahassee, and will be taking at all the other stations very shortly, will be interference filter type data in different wavelength regions and I'm not sure which ones he selected yet. I think that just depends on what NOAA wants and what he wants at the time.
- Q: There is a whole set of data from Dr. Thekaekara at Greenbelt. What's the relationship between that and what you are referring to?
- A: The data that Dr. Thekaekara takes are similar but I don't know who it's available from or whether it's on a continuous basis. I do know that the 5-year data are records from the Smithsonian and are recorded in Washington, D. C. I believe that they represent about $2\frac{1}{2}$ years from downtown at the Smithsonian castle and 2 or 3 years out at Rockville, and they find no difference between the two stations which would be separated by approximately 15 miles. So I would be surprised if the data from Dr. Thekaekara (at Greenbelt) would differ much from these data except that they might be in different wavebands.
- Q: Is there still a problem that the stations shown on your figure are separated from US weather observing points?
- A: No, these stations represent national weather service stations and will be collated with weather stations.

Q: Is this going to be aside from Maine, or is this the same one you have in Caribu?

A: Caribu, Maine, is an official weather service station and does take at present both radiation data and regular weather observations. All present and future weather service stations will take the weather data as well as the radiation data - the 60-station network and the new 35 station network. The hourly data are available from Nashville, and the 3 hourly weather data are published. The co-op network does not necessarily have any data other than the radiation data. We are trying to encourage people who are in the business of taking radiation data for either heating and cooling or photovoltaics to take other weather parameters.

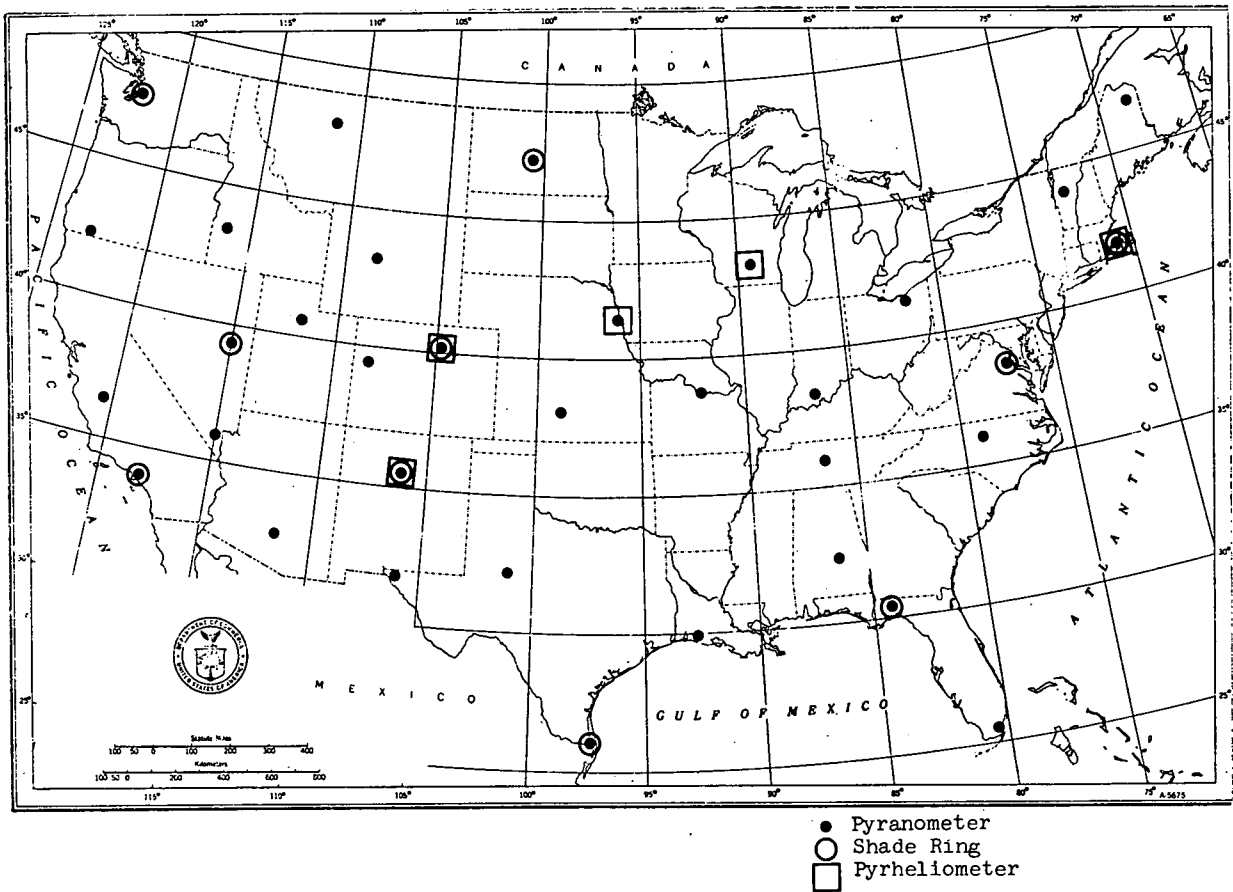


Figure 1.

SOLAR RADIATION AT NEWPORT, RHODE ISLAND

John R. Hickey

The Eppley Laboratory
Newport, Rhode Island 02840

Solar radiation measurements have been made at the Eppley Laboratory for a number of years. The records date back into the 1930's. The global irradiance values, which are the 180° field of view pyranometer measurements, have been reported monthly to the weather service in the prescribed format in the same manner as for National Weather Service stations. The Newport data constitutes a unique set since the primary reason for taking the data is in conjunction with the manufacture, test, and calibration of the instruments which were being used throughout the U. S. network and in many foreign countries. The standards and the basic measuring instrument were well maintained, and the recording and integrating instruments were checked and calibrated on a daily basis. In addition to the hemispherical measurements, normal incidence measurements of the same high quality have been made since 1938. The normal incidence records were kept for clear days on which normal incidence instruments were being calibrated against the standard. No attempt was made for many years to retain or log records of those days on which no calibrations were performed. In the early days, when few normal incidence instruments (pyrheliometers) were manufactured and sold, there were very few days for which the records were retained.

Recently, in response to the new demand for solar radiation data, the Eppley staff has been reviewing the available records in order to establish as complete a data set as possible back to the earliest days. Since this is an in-house project it has been delayed somewhat due to the pressing schedules of our satellite experiment projects for solar energy measurements. First, we have established a policy that all normal incidence records will be maintained in the same manner as hemispherical data. This has been in effect since November 1973. Also, we have started a program of identifying cloudless day data from our strip chart recordings of the pyranometer data. Using the hemispherical radiation data we are also studying the variations in solar radiation at Newport and computing the percentage of possible solar radiation which was measured.

The plots shown in this paper are generally for integral values. Daily integral radiation on a horizontal surface for the year 1970 is shown in figure 1 as a function of date. This plot shows the typical yearly variations of weather for a seacoast area such

as our location. Figure 2 is based on instantaneous solar noon readings on clear days for the years 1961 through 1970. The range of values for any given date is significant and on the average is about 10 percent for those days which have been clear a number of times in the 10-year period. This plot is also interesting for examination of weather systems statistics since it shows areas of persistently clear and persistently cloudy days. We hope to continue this analysis back to the early 1940's. Figure 3 returns to the integral evaluations showing monthly integral radiation for the years 1961 through 1973. It shows a maximum monthly value of about 17 400 langleys for July 1966 and a minimum of 2800 langleys for December 1972. Figure 4 shows yearly integral values for the years 1961 through 1973. The year 1965 is high with a value over 126 000 langleys while the year 1972 shows a low of 109 500. The reasons for the drop in 1967 and the more persistent drop from 1971 to 1972 which remained through 1973 are being researched to assure no change in instrument calibration had inadvertently been applied.

We would also like to bring to the attention of the attendees at this workshop that the Earth Radiation Budget experiment aboard the NIMBUS F satellite should be operational in June 1975. The satellite launch is scheduled for 28 May 1975. The experiment includes ten solar channels for measuring the extraterrestrial solar flux.

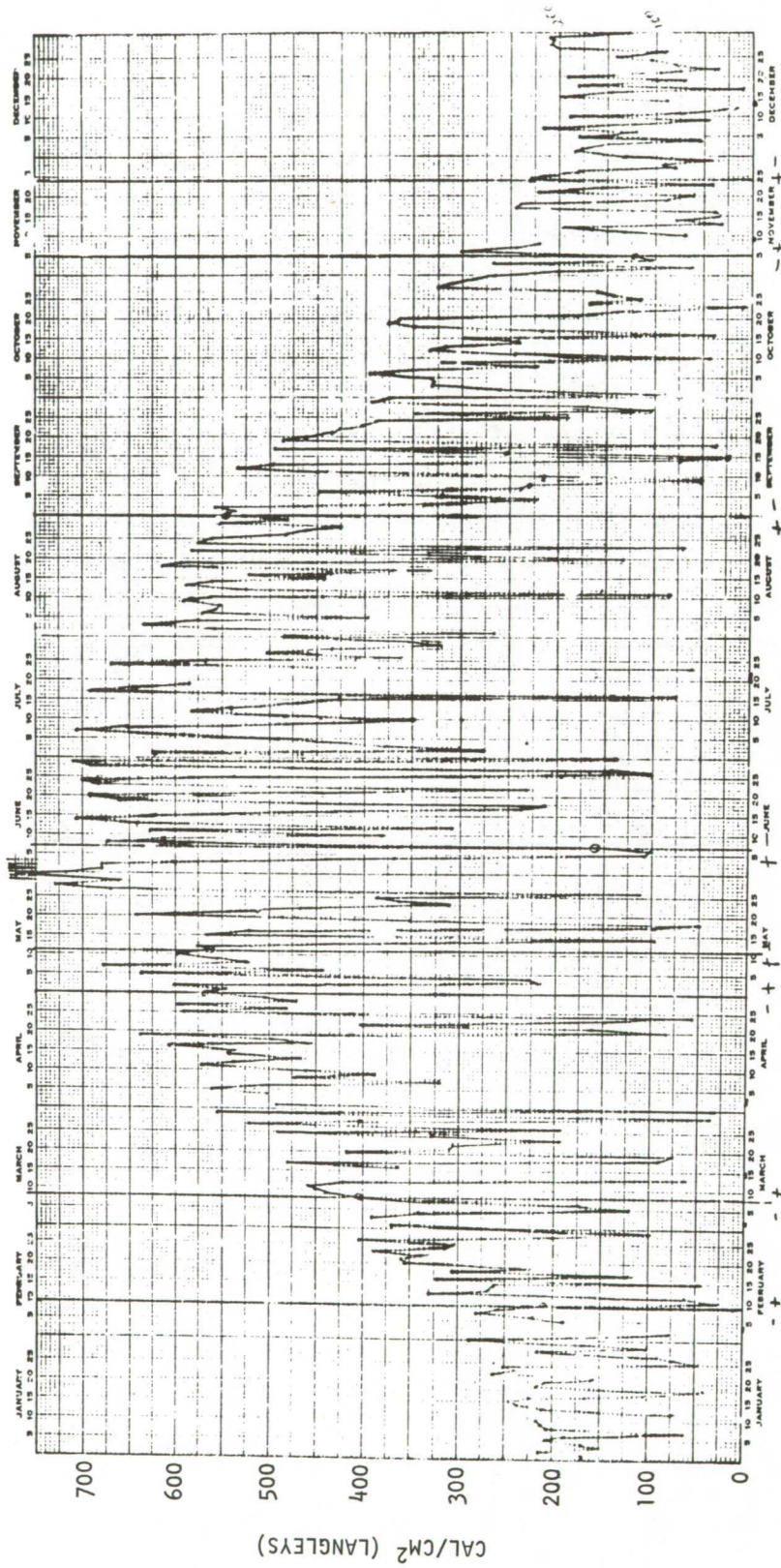


Figure 1. - Daily integrated global solar radiation at Newport, Rhode Island (1970).

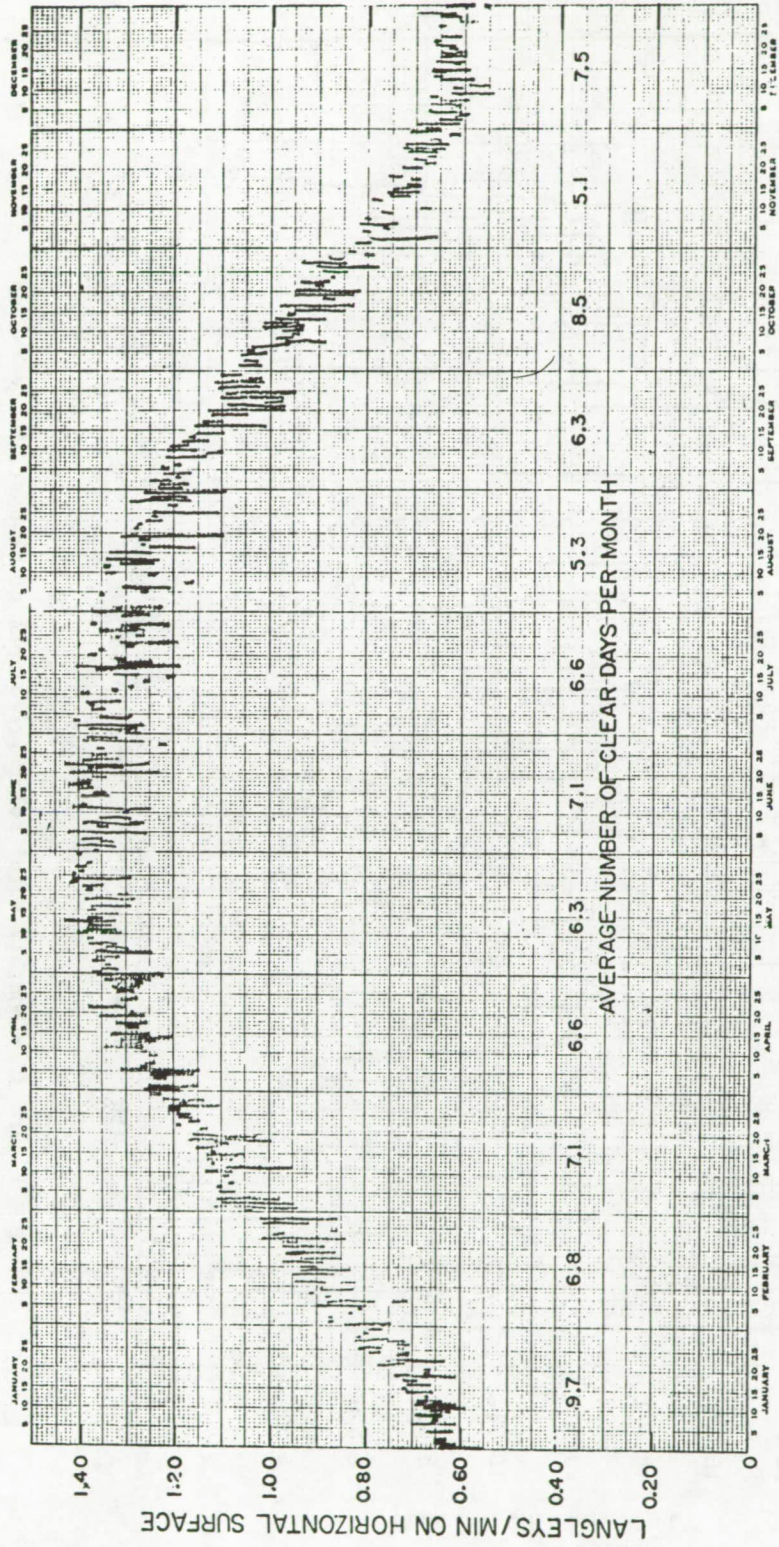


Figure 2. - Range of clear day solar global radiation at Newport, Rhode Island, for solar noon for 1961 through 1970.

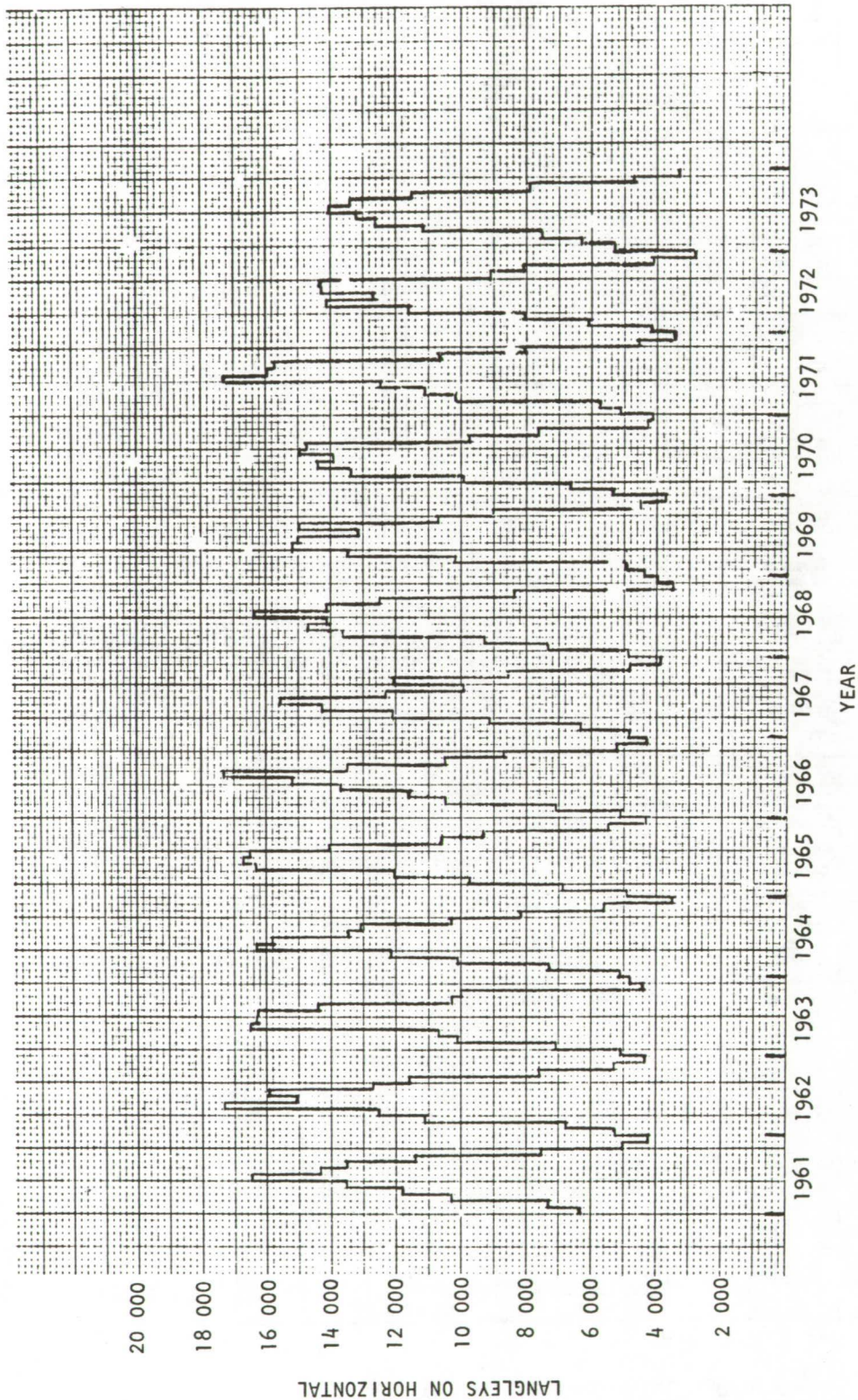


Figure 3. - Monthly total solar irradiance at Newport, Rhode Island, on horizontal surface.

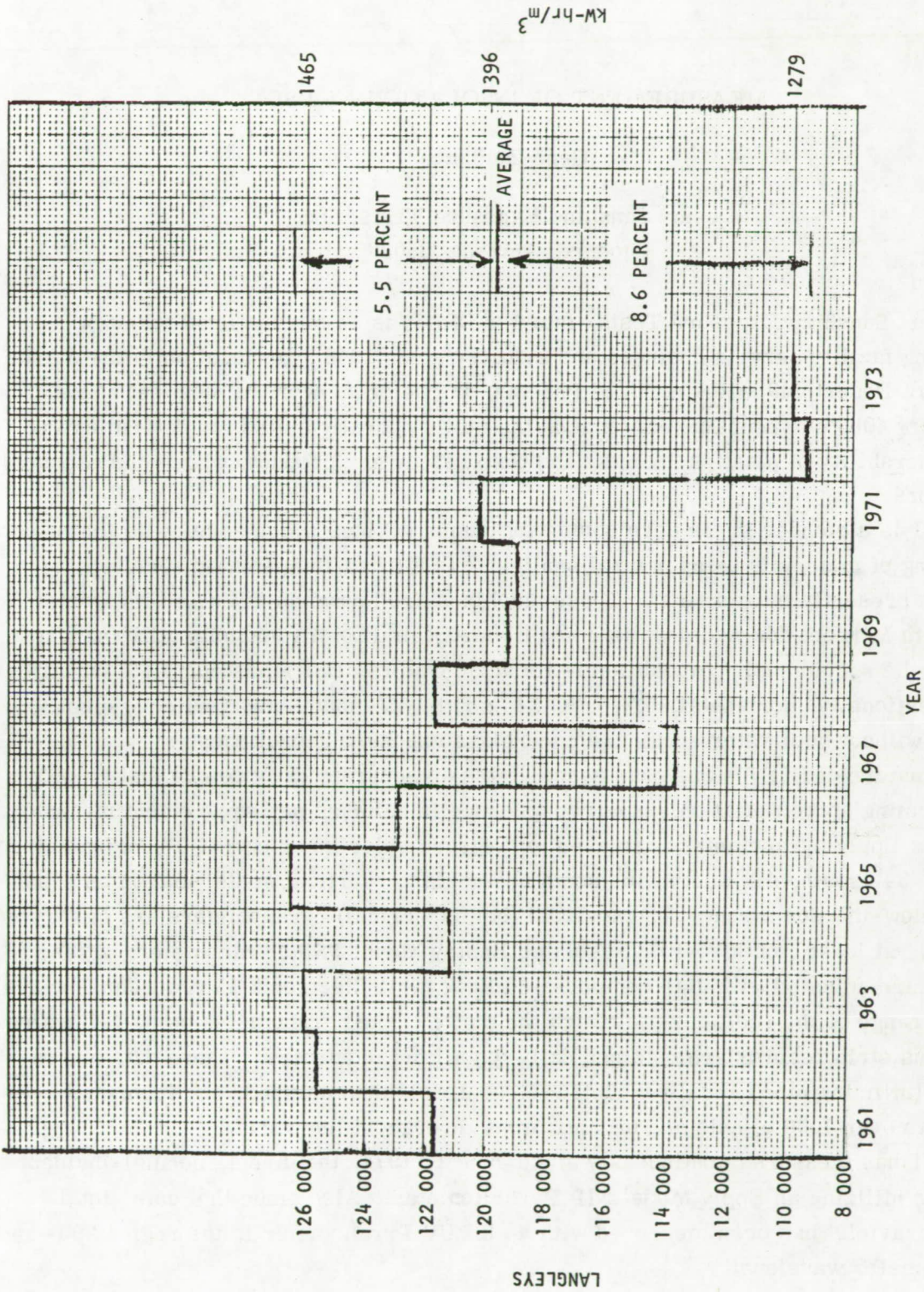


Figure 4. - Yearly total solar irradiance on horizontal at Newport, Rhode Island.

MEASUREMENT OF INSOLATION AT DSET

Gene Zerlaut

Desert Sunshine Exposure Tests, Inc.
Phoenix, Arizona 85020

Desert Sunshine Exposure Tests, Inc. (or DSET) is an internationally known weathering facility serving business and industry since 1948. Its location in the northern Sonora Desert, 40 miles north of Phoenix, in one of the world's sunniest zones (average of 4000 sun hours a year) makes the facility ideally suited for determining the weatherability of plastics, paints, and textiles, or any products whose end use would be outdoors.

DSET is a pioneer in the development of unique devices which accelerate the outdoor weathering of materials using natural sunlight. DSET has 180 patented accelerating machines presently in operation. These machines are known as EMMAs (Equatorial Mount with Mirrors for Acceleration) and EMMAQUAS (EMMA machine utilizing water spray on the specimens). In addition to its accelerators, DSET has complete facilities for conventional 0° horizontal, 5° south, 34° south, 45° south, and vertical exposure with and without both water spray and underglass exposure capacities.

The nature of DSET's business necessitates an accurate daily determination of total incoming solar radiation, usually expressed in calories per square centimeter or langleys. Epply pyranometers are used to measure solar insolation at 0° horizontal, 5° south, 34° south, 45° south, 45° south under glass, vertical south, and on an equatorial follow-the-Sun mount. These global (hemispherical) pyranometers are calibrated regularly, at least monthly with an isolated Epply Model PSP Pyranometer. These readouts are adjusted with dial-compensated Honeywell Electronik 15 recorders, which vary the range of the recorders to match the curve of the pyranometer being calibrated. Continuous strip records are obtained daily for all pyranometers. These data are integrated (utilizing mechanically-coupled integrators), summarized, and furnished monthly to over 1500 clients and organizations throughout the world.

DSET has measured continuously since June 1, 1974, the direct, normal-incident insolation utilizing an Epply Model NIP Pyrheliometer. Also since that date, total global ultraviolet has been measured with an ISI UV Pyranometer in the region 290- and 383-nanometer wavelength.

Facilities have been purchased for constructing a spectral radiometer capable of

measuring spectrally both direct or normal incidence and global insolation in the 290- to 2800-nanometer wavelength region. These measurements will be performed using a Leiss double-prism, single-beam monochromator. A siliclyate-excited, mechanically chopped, photodiode will be employed as the detector, the output of which will be amplified with a PAR Model 186 phase-locked amplifier. Both a 5⁰ collimator and a hemispherical integrator or integrating sphere will be constructed by DSET for the front-end optics. These data, along with routine pyranometric and pyr heliometric data, will be furnished requestors.

DSET will consider making the daily continuously recorded data available to any government or industrial organization on a cost-sharing basis.

MEASUREMENT OF THE SOLAR CONSTANT BY PACRAD ON

CONVAIR 990 FLIGHTS IN 1968

James M. Kendall, Sr.

Technical Measurements, Inc.

LaCanada, California 91011

The PACRAD was flown on the Convair 990 astronomical flights in July and August 1968. A measurement of the solar constant was obtained. Data were taken on each of the nine flights.

The Convair 990 generally flew at 40 000 feet while taking the measurements. A quartz window was mounted in the upper side of the plane to permit direct sunlight to enter the plane to irradiate the radiometer. A platform on which the radiometer was mounted was continuously controlled to keep the radiometer accurately aimed at the Sun.

Table I gives a resume of the 35 measurements (based on 197 readings) made during the nine flights. Several series of measurements were made on each flight. Data for each series are given in the table, each value shown being the average of all readings made in that series. Usually there were about eight readings made in each series. Generally the scatter in the measurements in each of the series was under ± 0.1 percent, and, as can be seen in the table, the scatter between the series was also no greater. When corrected for Earth-Sun distances, the day to day scatter is no more than 0.1 percent.

The measurements themselves thus appear to be consistent within ± 0.1 percent. The greatest uncertainty would appear to come from the uncertainty in the atmospheric transmittance and from the uncertainty in the transmittance of the quartz window. The value for the atmospheric transmittance used (0.9440) was obtained from John Arvesen's (Ames Research Center, Moffett Field, California) experimental measurements of the solar spectrum. He took into account water vapor, ozone, Rayleigh scattering plus other effects including $\sec z$ for the azimuth angle. Arvesen stated that the uncertainty in his measurements is within 0.5 percent. The uncertainty in the value 0.8907 for the transmittance of the quartz window is perhaps 0.4 percent.

There remains the uncertainty in the absolute sensitivity of the PACRAD from considerations given in JPL TR 32-1396, the absolute accuracy should be within ± 0.5 percent. The overall uncertainty of the value obtained for the solar constant would appear to be within about 1 percent. The value given in table I is 137.02 ± 0.8 percent, with the

true value probably lying between 136.0 and 138.0 milliwatts per square centimeter. The radiometer used for measuring the solar constant is of the "blackbody cavity" type and has an inherent accuracy of better than 0.5 percent. As shown in the diagram of figure 1, the cavity receptor is located in a massive copper heat sink, which itself is located in a Dewar flask to minimize heat transfer with the environment and thereby prevent variation of the temperature of the heatsink during the time of measurements. View limiting of the incoming irradiance is restricted to an angle of $\pm 2.5^\circ$ (5° total angle).

Figure 2 shows a photograph of the cavity assembly. The actual receptor of the cavity is located to the right of the mounting ring. The hot junctions of the thermopile are located on the outside of the cavity, while the cold junctions are located on the right side of the assembly and serve as compensation for the time rate of change of the heat-sink temperature.

The radiometer can easily be calibrated at any time desired by applying a known electric heating power to the cone located inside of the cavity. The electric heating is accurately equivalent to heating of the cavity by incoming irradiance.

Figure 3 shows an updated version of the radiometer, and figure 4 shows the radiometer mounted on a Sun tracker for measuring solar irradiance at the World Radiation Center in Davos, Switzerland.

BIBLIOGRAPHY

- Arvesen, John (Ames Research Center, Moffett Field, Calif.) Private Communication.
- Kendall, J. M., Sr.: Primary Absolute Cavity Radiometer. JPL TR 32-1396, July 15, 1969.
- Kendall, J. M., Sr.; and Berdahl, M.: Two Blackbody Radiometers of High Accuracy. Applied Optics, vol. 9, no. 5, May 1970.

TABLE I. - RESUME OF SOLAR CONSTANT MEASUREMENTS

[Transmittance of window in plane, 0.8907±0.4 percent; transmittance of atmosphere above plane, 0.9440±0.5 percent; value of solar constant obtained from these values, $\frac{115.193}{0.8907} \times \frac{1}{0.9440} = 137.02 \text{ mW/cm}^2$.]

Flight	Date (1968)	mW/cm ²	Measured inside plane				Correction Earth-Sun distance	Corrected values in- side plane
1A	7/15	109.4	109.6	110.4	110.4	109.7	1.0331	113.54
3A	7/17	111.3	111.5	111.4	111.5	111.5	1.0331	115.13
4A	7/18	111.2					1.0330	114.87
^a 5A	7/19	111.78	111.8	111.7	111.6		1.0320	115.27
6A	7/30	111.6	111.9	111.9	111.5	111.2	1.030	115.05
7A	8/1	111.9	111.9	111.9	111.6		1.030	115.15
8A	8/2	112.0	112.2	111.8			1.030	115.36
9A	8/6	112.0	112.2	112.1	111.92		1.0287	115.26
10A	8/7	111.81	112.2	112.4	111.8		1.027	115.07
								^b 115.193

^aA better procedural technique was used for the last six measurements. Each value given in the table is itself an average of several measurements.

^bLast six measurements only.

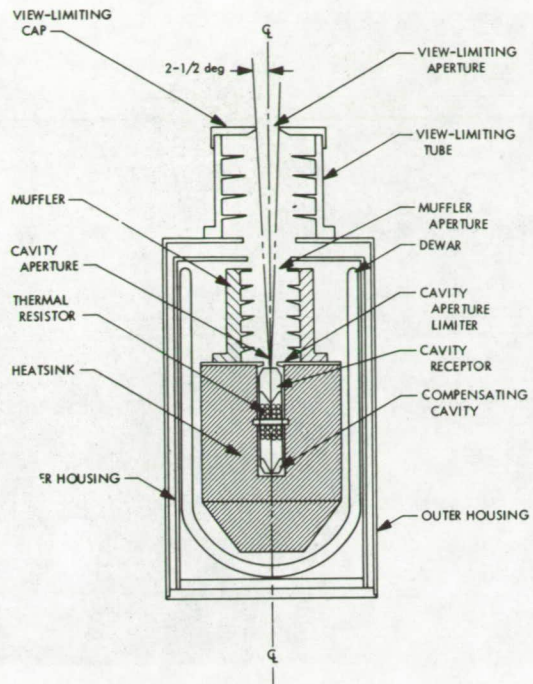


Figure 1.

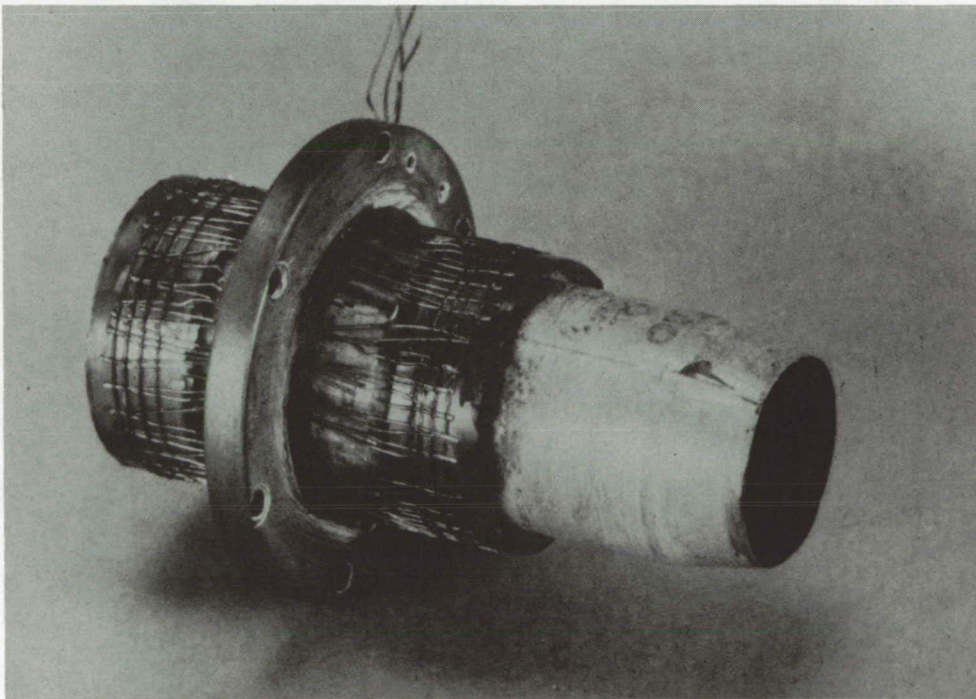


Figure 2.

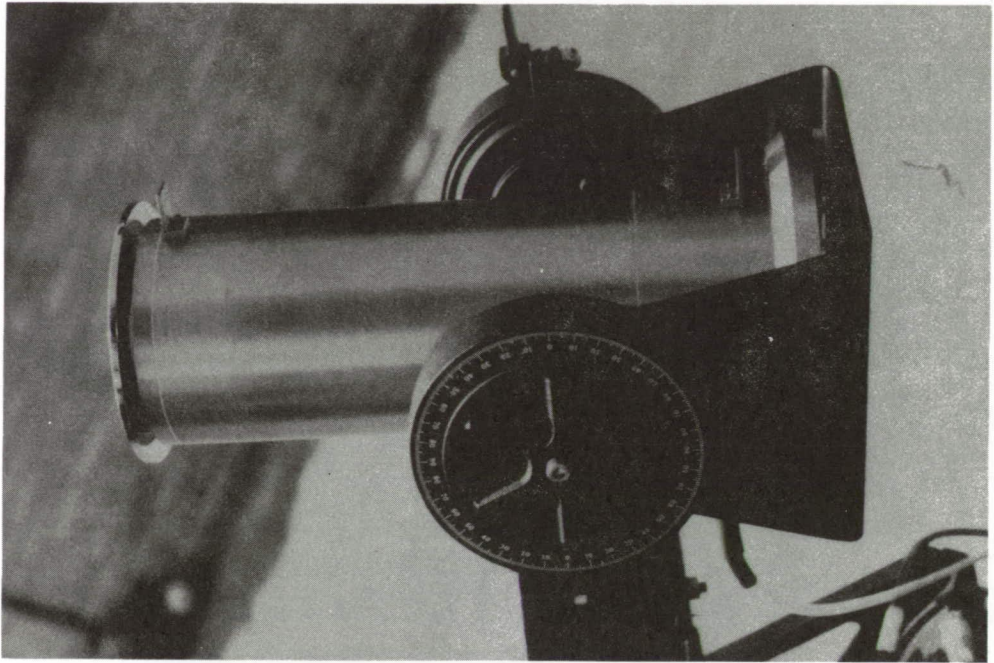


Figure 3.

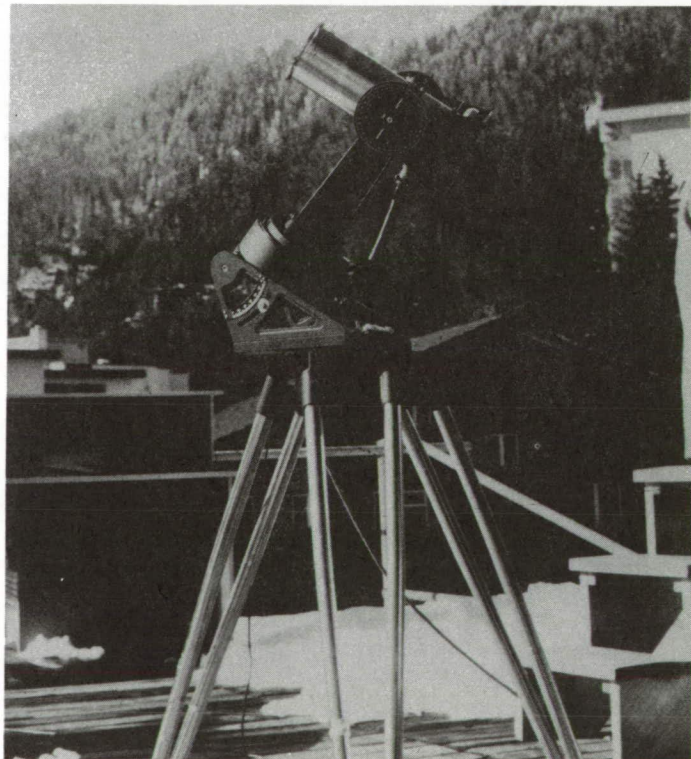


Figure 4.

SPECTRAL MEASUREMENTS OF SOLAR INTENSITY AND SPECTRUM
CONDITIONS AT HIGH ALTITUDES (5200 TO 14 000 FT)
AND ARID (COLORADO) CONDITIONS

Rolland L. Hulstrom

Martin Marietta Aerospace
Denver, Colorado 80201

This paper addresses the Solar Photovoltaic Energy Conversion Program problem of "Solar Intensity and Spectrum Conditions for Terrestrial Photovoltaics." This problem is created by the fact that previous solar cell testing has been done with simulated, extraterrestrial, solar intensity spectrums; however, terrestrial solar cell applications require a knowledge of solar, spectral, intensity under various atmospheric conditions. The following sections present data and analyses for solar spectral intensity (irradiance) conditions for high altitudes (5200 to 14 000 ft) and arid and slightly polluted atmospheric conditions. In addition, basic concepts regarding atmospheric effects on spectral solar intensity conditions and the instrumentation used to make the measurements are discussed.

BASIC CONCEPTS

Two components of solar irradiance exist under terrestrial conditions; they are the direct component and the diffuse component. The direct component is that solar irradiance coming directly (beam) from the solar disk; and the diffuse, skylight component is created by the scattering of solar radiation (out of the direct beam) by atmospheric molecules and particles. The sum of these two components is the total (also known as global, 180°) solar irradiance. Mathematically (for a horizontal surface) this is given as

$$H = I \cos \theta_0 + S \quad (1)$$

where H is the total irradiance, I the normal incident direct irradiance, θ_0 the solar zenith angle, $\cos \theta_0$ the solar zenith angle ($\cos \theta_0$ required to account for the direct

irradiance on a horizontal surface (Lambert's law), and S the diffuse/sky irradiance. All components are wavelength dependent; therefore, a λ subscript will not be used. The direct component can be given as

$$I = I_0 e^{-\tau \sec \theta_0} \quad (\text{Beers-Lambert law}) \quad (2)$$

where I_0 is the extraterrestrial solar irradiance, $\sec \theta_0$ the relative air mass (m) or path length through the atmosphere relative to vertical, and τ the atmospheric optical depth. The atmospheric optical depth is made up of three components due to molecular (Rayleigh) scattering τ_m , particulate scattering (Mie), τ_p , and selective absorption τ_a . The attenuation of the direct beam due to molecular scattering is proportional to $1/\lambda^4$, that due to particulate scattering is proportional to $1/\lambda^{1.3}$, and that due to absorption is highly selective of wavelength (absorption bands). The total optical depth can be given as

$$\tau = \tau_m + \tau_p + \tau_a \quad (3)$$

The magnitude and spectral distribution of the direct solar irradiance is determined by the extraterrestrial solar irradiance distribution (I_0 , solar constant), the atmospheric optical depth τ , and the relative air mass/Sun angle. This is illustrated in figure 1. Shown in figure 1 are model predictions of the magnitude and spectral distribution of direct solar irradiance as a function of altitude (sea level and 3 km), wavelength, and relative air mass (1.0, 2.0, and 4.0). These curves were generated by using equation (2), Elterman's model (ref. 1) (visibility, 23.0 km), for optical depth and Thekaekara's (ref. 2) data for the extraterrestrial solar irradiance (solar constant). Several conclusions can be drawn from the curves shown in figure 1; two of the major ones are as follows:

(1) As the air mass increases - low Sun angles - the magnitude of the solar intensity is decreased and its spectral distribution changes from a "blue" to a "red" distribution.

(2) The effect of increasing altitude is to increase the solar intensity magnitude and shift the spectral distribution toward the "blue" region. In fact, the magnitude and spectral distribution at 3.0 km and at an air mass of 4.0 is similar to an air mass of only 2.0 at sea level.

The magnitude and spectral distribution of the diffuse sky radiation is determined by the molecular and particulate scattering of sunlight. On very clear days the skylight is "blue," due to molecular scattering of the shorter wavelengths, while on turbid days the skylight is grayish, due to particulate scattering. The mathematical modeling of skylight is much more complex than that for the direct beam and involves many more

variables such as solar azimuth, scattering phase function of the aerosol particles, particle index of refraction, ground albedo, etc. In general, the diffuse skylight can make up nearly 60 to 70 percent of the total solar irradiance in the short (400 nm) wavelengths and only about 5 percent in the longer (>750 nm) infrared wavelengths. If cloud cover exists, it is a significant contributor to the skylight and, in fact, can dominate the solar irradiance conditions (see ref. 3). Obviously, as shown in equation (1), one of the most significant factors concerning total solar irradiance is the Sun angle θ_0 , because of the strongly dependent cosine ($\cos \theta_0$) function.

INSTRUMENTATION

A wedge interference filter spectroradiometer was used to make the direct, diffuse, and total solar irradiance measurements. This spectroradiometer, shown in figures 2 and 3, has a half-bandwidth of 15 nanometers from 380 to 750 nanometers (visible range), and 30 nanometers from 750 to 1550 nanometers (infrared range). For the visible range a special silicon junction photocell is used as the detector, and a germanium junction photocell is used for the infrared range. As shown in figure 2, the sunlight enters the instrument through a diffuser, after which it is chopped and passed through a slit, a monochromator, and finally strikes the detectors. The direct solar radiation is measured by using a fiber optics probe with a diffuser cap on one end. This cap is placed in a special collimator attachment that is baffled and has a 2° field of view. The total radiation is measured by positioning the diffuser cap so that it is horizontal and pointed vertically. The diffuse radiation is measured by simply shading the diffuser from the direct sunlight. The entire system is calibrated for irradiance by using NBS standards and for wavelength by using known interference filters. The system is totally portable and can be used in the field, as shown in figure 3. Four complete systems are available so that simultaneous measurements can be made at four geographical locations.

MEASUREMENTS AND CONCLUSIONS

Shown in figure 4 are measurements of direct solar irradiance from Mt. Evans, Colorado, at an altitude of 14 000 feet. The measurements shown are for relative air masses of 1.2, 2.2, and 5.7. As can be seen, the effect of increasing air mass on the magnitude and spectral distribution of the solar irradiance is very pronounced, even for the high altitude and extremely clear atmospheric conditions. These Mt. Evans measurements probably represent a terrestrial extreme for solar irradiance magnitude and "blue" spectral distribution. It is interesting to note that even for the Mt. Evans low

air mass, 1.2, the radiation conditions are quite different from those of the extraterrestrial conditions under which previous solar cell tests have been conducted. Also shown in figure 4 is a comparison between a model prediction (ref. 1) and actual measurements. The model seems to compare favorably in terms of spectral distribution and magnitude from 400 to 450 nanometers. From 450 to 900 the model compares favorably in terms of spectral distribution, but unfavorably in terms of magnitude. Of course, from 900 to 1000 nanometers the model does not compare because of the water vapor absorption band at 942.0 nanometers. In the "window" region from 1000 to 1050 nanometers a favorable comparison is indicated. A typical solar cell response is shown in figure 4 in order to compare the solar cell response with the changes in magnitude and spectral distribution of the solar irradiance. As can be seen, the maximum response of the solar cell is in the near infrared region, which is also the region of least change in the solar radiation conditions. This does not conclusively indicate that the solar cell will not be sensitive to changes in terrestrial solar intensity/atmospheric conditions, but it does indicate that the near infrared response of the silicon solar cell will minimize its sensitivity to changes terrestrial solar intensity spectral conditions.

Shown in figures 5 and 6 are measurements of direct, total, and diffuse solar radiation made at Waterton (6200 ft) and Denver (5200 ft), Colorado. Waterton is located in the Front Range approximately 20 miles southwest of Denver. The measurements were made on the same day, when Waterton had clear conditions and Denver had a "light" layer of pollution. The total solar irradiance magnitude and spectral distribution represent conditions that a solar cell positioned horizontally (flat plate collector) would experience. A solar cell positioned on an inclined, south facing surface would experience the direct plus some portion of the diffuse sky conditions plus reflected sunlight from the ground. As shown, the spectral distributions of the direct and total are similar with the total having somewhat of an enhanced "blueish" distribution due to the blue skylight.

Note that the magnitude of the direct irradiance, for Denver (5200 ft) and Waterton (6200 ft), is nearly as great as the Mt. Evans direct irradiance. This indicates that a seasonal, Mt. Evans - summer (Aug. 16) and Waterton/Denver - winter (Feb. 25), effect is dominating the altitude difference. The atmospheric conditions during the winter are known to be much more transparent than those of summer.

Also shown in figure 5 is a measurement of solar radiation conditions under complete cloud cover. Quite reasonably, the cloud cover creates a "white" spectral distribution. In terms of magnitude, clouds have an extremely variable effect on total solar radiation (see ref. 3). Partly cloudy/sunny conditions would create solar radiation conditions somewhere between the data shown for the clear and cloudy conditions.

REFERENCES

1. Elterman, L.: UV, Visible, and IR Attenuation for Altitudes to 50 Km, 1968.
A. F. C. R. L. Research paper no. 285, 1968.
2. Thekaekara, M.: Evaluating the Light From the Sun. Optical Spectra, March 1972.
3. Hulstrom, R.: The Cloud Bright Spot. Photogrammetric Engineering and Remote Sensing, vol. XXXIX, no. 4, April 1973.

DISCUSSION

Q: I was wondering if in your model work you considered the albedo of the surface and also the multiple scattering that might help us in proving your results?

A: No, I didn't. My model work consisted of about 20 minutes on an HP-55. I just wanted to show some sort of comparison between what you would get with a simple model compared to the elaborate model that you speak about.

Q: Was that just one day on the Mount Evans data. If so, there are, at least from a visibility point of view, tremendous differences in scattering from day to day, and if that was only one day's data, what sort of day was it?

A: It was about mid-August and there were no clouds. If you will compare the data when you get the proceedings you will find I mentioned this in my paper. The direct incidence intensity which we got at Waterton in the winter was not that much lower than the Mount Evans testing done this summer.

Q: You would expect the water peaks to be changing somewhat, wouldn't you?

A: Yes.

COMMENT: I took Thekaekara's data for the AM0 and AM1 and recomputed it in terms of photon flux. My own feeling is, for purposes of photovoltaics, that this is the way we ought to look at it. We care alot more about the photon flux than power. The waterband shows up more prominently because of the weighting that changes with wavelengths. The shifts in spectral distribution that you showed, and that everyone else knows about, show up more graphically and have a relatively greater importance in this plot.

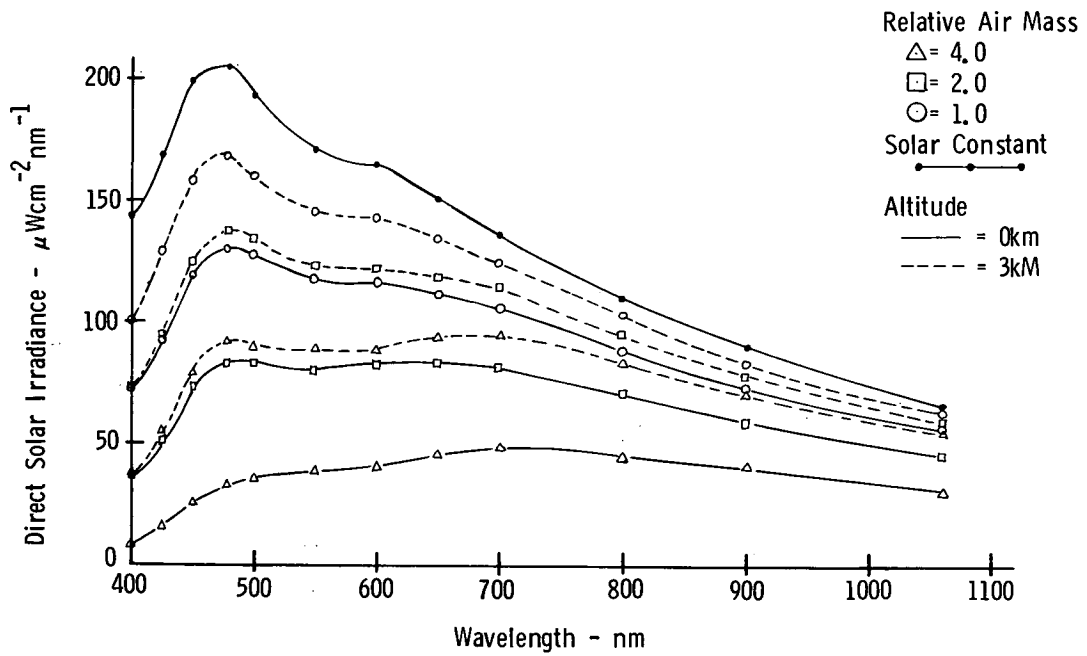


Figure 1. - Model predictions of direct solar irradiance as function of relative air mass, wavelengths, and altitude.

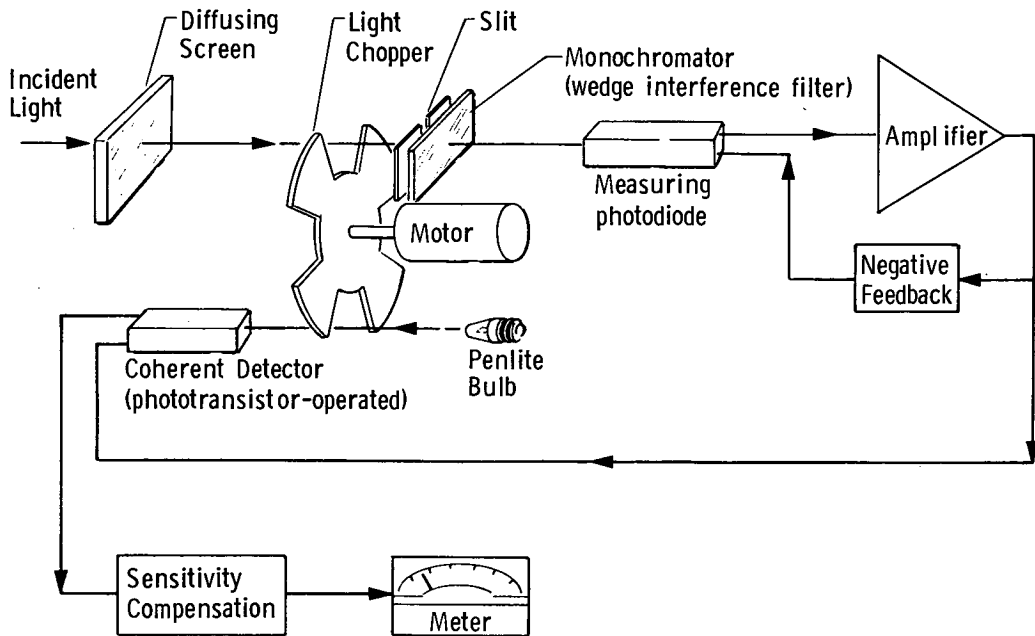


Figure 2. - Spectroradiometer diagram.



Figure 3. - Spectroradiometer field setup.

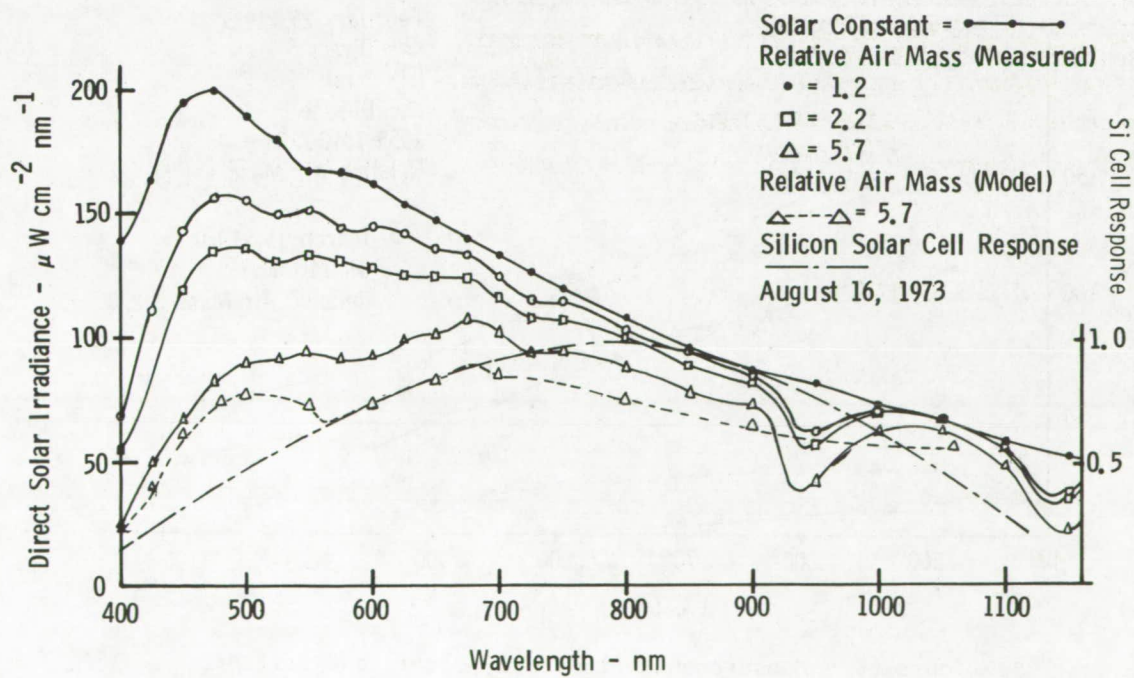


Figure 4. - Measurements of direct solar irradiance from Mt. Evans, Colorado.

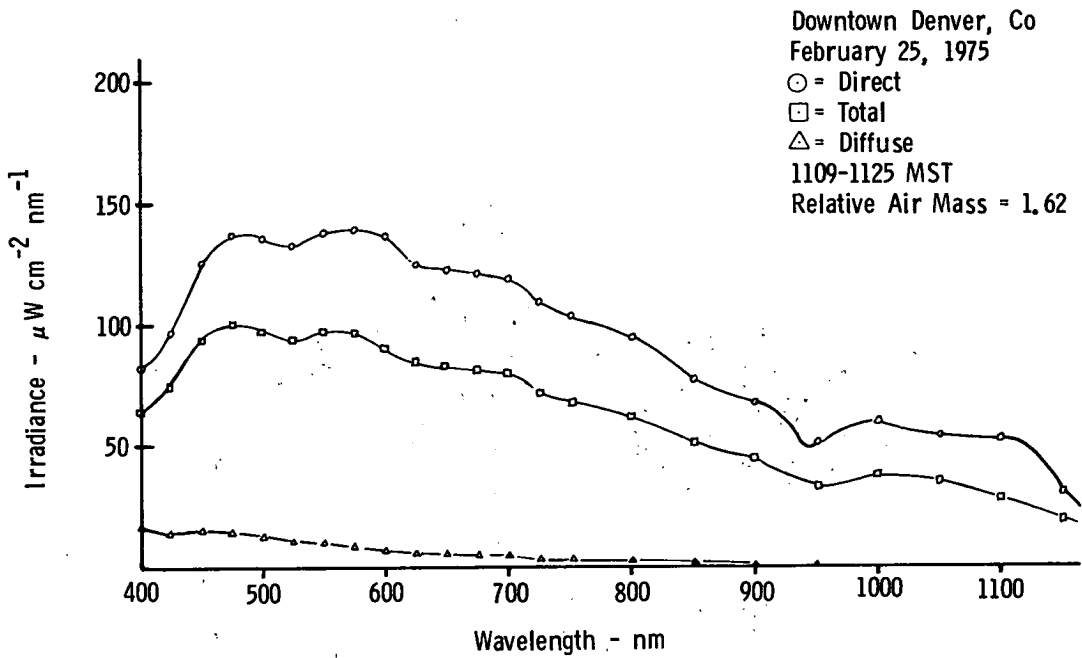


Figure 5. - Measurements of direct, total, and diffuse radiation - Denver, Colorado.

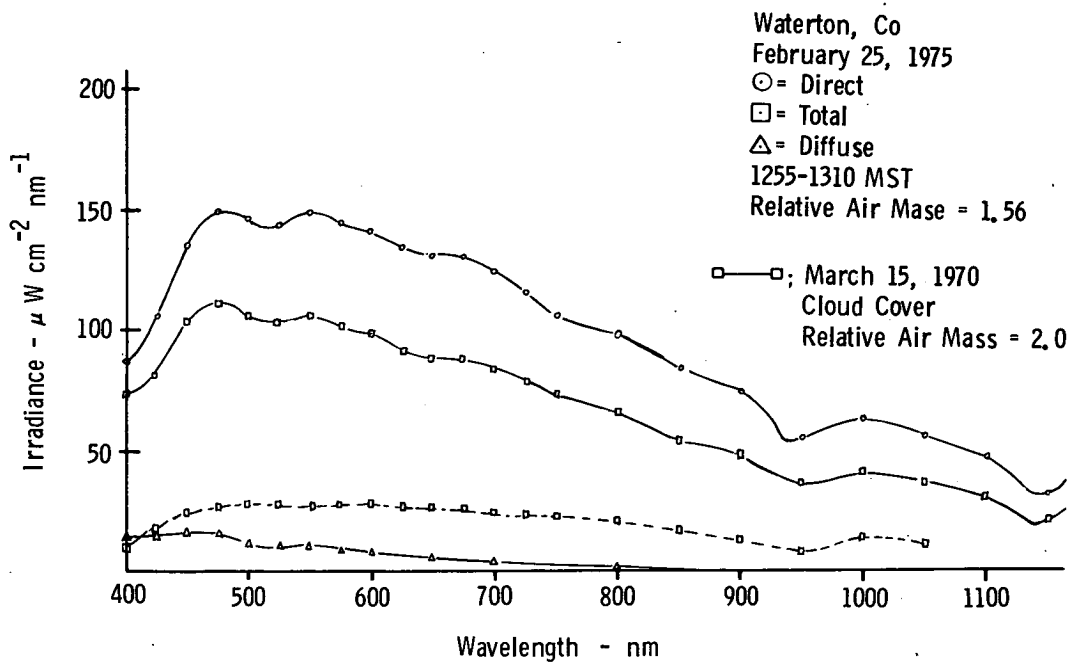


Figure 6. - Measurements of direct, total, and diffuse radiation - Waterton, Colorado.

SPECTRAL DISTRIBUTION OF SUNLIGHT UNDER VARIOUS AIR MASS CONDITIONS

Alfred Seck

Optical Coating Laboratory, Inc.
City of Industry, California 91746

To design optimized silicon photovoltaic energy conversion systems for any site on Earth requires more reliable sunlight energy data than is presently available. The published weather data by the National Weather Service throughout the United States is not adequate and/or predictable. In many instances, the available sunlight energy at a site must be estimated from the data for a nearby location. This approach introduces an additional uncertainty for areas such as mountainous and coastline regions where the local climate changes rapidly over short distances. Various measurements of solar intensity at approximate AM1 conditions (Table Mountain, California) using pyrhelimeter, spectroradiometer, and silicon solar cells indicate discrepancies in resultant data if proper precautions are not taken. Frequent difficulties encountered for measurements and data are the interpretation and/or measurements of atmospheric conditions at the time, instrumentation errors, speed of responds of detectors, spectral response of silicon solar cells, and the quality of spectral distribution components at the time. These are compounded further if measurements are performed near the coastline, because of rapidly changing atmospheric conditions.

TERRESTRIAL SUNLIGHT ENERGY

The solar constant for AM0 is defined as the total amount of energy received from the Sun per unit time per unit area exposed normally to the Sun's rays at the average Sun-Earth distance outside the Earth's atmosphere. The spectral distribution per unit wavelength is similar to Johnson's curve, as shown with dotted lines in figure 1. AM1, on the other hand, is defined as a measure of the total amount of air in the path from the observer to the Sun. It is given, for all practical purposes, by the equation

$$m = \left(\frac{P}{P_0} \right) \sec Z \quad (1)$$

where m is the air mass, P_0 is the local barometric pressure, P is sea level barometric pressure (~ 760 mm Hg), and Z is the zenith angle of the Sun. Although this is not strictly correct (it assumes a homogeneous atmosphere), it is a convenient way to describe the relationship.

Parry Moon, in his classic paper¹, defines solar irradiance as a function of air mass. The irradiance per unit wavelength λ of sunshine at the Earth's surface is given by

$$E_\lambda = E_{0\lambda} e^{-\alpha_\lambda m} \quad (2)$$

where

- E_λ terrestrial solar irradiance at λ
- $E_{0\lambda}$ extraterrestrial solar irradiance at λ
- α_λ absorption coefficient at λ
- m air mass

The absorption coefficients might be derived from Moon and the extraterrestrial irradiance values may be taken from Johnson. The calculated results for one set of atmospheric conditions are shown in figure 2. The specific set of conditions used for absorption coefficient were

$$P_0 = 760 \text{ mm Hg}$$

$$w = 20 \text{ mm precipitable water vapor}$$

$$d = 300 \text{ particles/cm}^3 \text{ dust}$$

$$o = 2.8 \text{ mm ozone}$$

In practice, these factors vary considerably. The precipitable water vapor content of the atmosphere varies as a function of climate and can be between 2 and 100 millimeters. The dust varies between 50 and 1000 particles per cubic centimeter and the ozone is relatively constant between 2 and 4 millimeters. The effects of these variations on short-circuit current density of silicon solar cells as a function of air mass are substantial, as confirmed by the measurements of terrestrial sunlight at Table Mountain, California, in the last 15 years by the solar cell manufacturing industry. These variations may alter not only the scale of figure 3, but its shape as well.

¹Several key articles are referenced in the bibliography attached.

TERRESTRIAL SUNLIGHT MEASUREMENTS

The test site most often employed for solar cell measurements under natural sunlight in the Southern California area is Table Mountain. This site is at an elevation of 7400 feet and is situated in the Angeles National Forest near Wrightwood. The geographical coordinates are $34^{\circ}22'$ and $117^{\circ}41'$ W.

The Table Mountain test site was first used in 1926 by the Astrophysical Observatory of the Smithsonian Institution in their work in determining the variations in the solar constant. This work was continued until 1961 under the direction of A. G. Froiland. During this time instrumentation included a spectrobolometer for measuring the relative spectral energy distribution of sunlight and numerous pyrhelimeters of various types. Measurements were made on virtually all factors of atmospheric absorption and scattering, and extensive records are available on water vapor content, atmospheric scattering, and ozone absorption, as well as spectral distribution, total intensity, and solar constant variations with respect to time and known solar activity. Since 1961 the site has been operated by the U. S. Forest Service and JPL. A number of individual sites with concrete platforms and power outlets are available for industrial concerns and other programs.

The proximity to Los Angeles has often provided smog, with test results showing smog-contributed atmospheric absorption and scattering and instabilities. As a consequence, the spectral distribution of sunlight is affected. Table Mountain is also plagued by an excessive amount of haze (February through June), which has little absorption but which contributes a great deal of scatter. Cloudy and partly cloudy skies occur more than 100 days out of the year. The nominal water vapor content of the atmosphere above Table Mountain is generally quoted as 5 millimeters of precipitable water. This has been seen to vary from less than 1 millimeter to greater than 20 millimeters. On days that are deemed acceptable, a flat radiation detector such as a pyrhelimeter is affected by this water vapor to a much greater extent (typically 2 to 1) than is a solar cell.

The result of these climatic variables is that the ratio between the short-circuit current of a standard solar cell and the incident radiation as measured with a pyrhelimeter varies with a total spread of 10 percent nominally and 30 percent in extreme cases.

In spite of these shortcomings, Table Mountain has been extensively used for large area solar cell array measurements and standard cell calibration. The primary reason is spacial uniformity and temporal stability. There is no area restriction when measuring natural sunlight and the sunlight on Table Mountain on an acceptable day for testing does not vary more than 0.5 percent over a 1-minute time span.

A typical spectral distribution curve for Table Mountain is shown in figure 3. This curve is derived from a series of spectral measurements, a barometer reading, and a few assumptions. It should be noted that this curve is not an average nor should it be

used for this purpose. The selection of an average spectral distribution must be based on numerous data from individual days. Generally such data for a number of years are not available. Consequently, the selection of an average curve is somewhat arbitrary, but must still be based on variations in the specific conditions encountered at Table Mountain or for that matter, some other site. A frequently used method for defining a spectral distribution consists of applying atmospheric absorption coefficients derived from Moon to the solar spectral irradiance outside the Earth's atmosphere as defined by Johnson. However, the data from Moon is for the following conditions:

$$P = 760 \text{ mm Hg}$$

$$w = 20 \text{ mm precipitable water vapor}$$

$$d = 300 \text{ particles/cm}^3 \text{ dust}$$

$$o = 2.8 \text{ mm ozone}$$

These conditions are not at all applicable to Table Mountain and/or some other locations. The result of using these coefficients is a spectral distribution giving too little energy at wavelengths shorter than 0.6 micrometer, the deficiency increasing towards shorter wavelengths, too little energy in the water vapor absorption bands, and too much energy elsewhere. The result for solar cell measurements is an extrapolation factor that is too small. Superimposed on this error is the assumption that the Table Mountain spectral distribution is constant from day to day.

The important constituents of the atmosphere which contribute to the errors of spectral distribution component may be grouped into three categories: (1) permanent gases, including O_2 , N_2 , and O_3 ; (2) water vapor; and (3) dust. Measurements and calculations are used between 0.29 and 2.1 micrometers. The pyrhelimeter window transmission decreases to zero at wavelengths shorter than 0.29 micrometer, and ozone totally absorbs at shorter wavelengths. Transmission data on water vapor and poor for wavelengths longer than 2.1 micrometers, so an assumption is made concerning the energy beyond this point, with due consideration for the characteristics of the pyrhelimeter. The depletion of solar radiation by the "permanent" gases due to the scattering can be expressed as

$$A = e^{-km(P/P_0)} \quad (3)$$

where

A transmission factor for atmospheric scattering

k scattering coefficient (Penndorf)

- m optical air mass
- P_0 atmospheric pressure at Table Mountain
- P atmospheric pressure at sea level (760 mm Hg)

The primary absorption bands for oxygen are the A band at 0.76 micrometer; of less importance the B band at 0.69 micrometer, and two bands at 1.06 and 1.25 micrometers. Data for the transmission of these bands is from Fowle. Ozone absorbs strongly in the Huggins band at wavelengths shorter than 0.35 micrometer and weakly in the Chappius band between 0.55 and 0.7 micrometer. The transmission factors for ozone as a function of wavelength are taken from Wulf. Carbon dioxide has two absorption bands in the wavelength region of interest, 1.99 and 2.05 micrometers. It is assumed that the oxygen and carbon dioxide are distributed evenly throughout the atmosphere such that their absorption coefficients may be extrapolated to any atmospheric pressure. The only calculation necessary to determine the optical air mass at the time of test is to find the angle of the Sun.

Water vapor absorbs at numerous bands in the wavelength region of concern. The principal bands are α at 0.72 micrometer, A band at 0.80 micrometer, ρ band at 0.93 micrometer, φ band at 1.12 micrometers, ψ and ψ' bands at 1.35 and 1.42 micrometers, and Ω band at 1.86 micrometers. Fowle gives the transmission of water vapor for a concentration of 20 millimeters precipitable water vapor and an instrumental slit width of 0.022 micrometer. A-band concentration can be measured with a heliostat-equipped spectroradiometer, and the result is the total precipitable water vapor in the path from the instrument to the Sun. Consequently, no pressure or optical air mass correction is necessary. The scattering might be described by an equation similar to the Rayleigh equation, but the exponent is -2 rather than -4:

$$\tau_w = e^{-k_w \cdot w} \quad (4)$$

where

- τ_w transmission factor for water vapor scattering
- k_w scattering coefficient for water vapor
- w precipitable water vapor, cm

The k_w coefficient might be calculated from an equation from Moon:

$$k_w = 0.00865 \lambda^{-2} \quad (865 \text{ mm Table Mountain})$$

The remainder of the sunlight depletion is caused by the scattering of large particles. The collective term "dust" is used, but these particles range from large molecules of chemical nature to condensation nuclei. The calculation of scattering by this wide range of particles in varying concentrations is exceedingly difficult. For Table Mountain calculations we have assumed that the scattering of particles can be represented by an equation using 1 micrometer size particles. The transmission equation is taken from Moon:

$$\tau_d = e^{-1.02 \times 10^{-4} \lambda^{-0.75} n} \quad (5)$$

where

- τ transmission factor for dust scattering
- n number of dust particles/cm³

Various sources have indicated that dust concentrations between 50 and 1000 particles per cubic centimeter could be found above Table Mountain.

The procedures used to determine the absolute spectral distribution at Table Mountain is straightforward and tedious. The same procedure may be used for other sites except with more caution, particularly near large towns and coastlines. The raw data required are data and time, spectroradiometer curve of the spectral distribution, and pyrhelimeter reading and temperature. The modified and corrected data requirements are - the actual solar constant at the time of test, the solar elevation angle, reduction of local apparent time to true solar time, calculated solar elevation angle at the time and latitude, the absorption coefficients for atmospheric gases, and the transmission of water vapor. In actual calculations the two transmission factors, one for atmospheric scattering and one for water vapor, are combined and then multiplied by the extraterrestrial solar irradiance. The pyrhelimeter data are reduced with proper tilt and temperature corrections, and the result is total energy incident during the test. A concentration is chosen for dust such that the depletion due to this dust scattering will make the observed and calculated total energies equal. This dust transmission factor is applied to the previous curve and a new curve is plotted and integrated to yield the absolute spectral distribution at the time of the test. These procedures have given results repeatable to within ± 2 percent at Table Mountain when related to silicon solar cell short-circuit current at AM0.

As the Table Mountain measurements show, if proper precautions are not taken, the reliability of sunlight radiation data is affected. Extreme consideration must be given in use of flat detectors such as pyrhelimeters and pyranometers. Both of these instruments can be calibrated within ± 1 percent; however, they vary from one to another so individual calibrations are required.

PYRHELIOMETERS AND PYRANOMETERS

A pyr heliometer is used in direct measurements of solar radiation (direct sunlight measurement). A pyranometer is used in global measurement of solar radiation (total sunlight measurement). Mostly, both instruments use thermopile detectors; however, commercially available pyranometers also have silicon cell or bimetallic strip sensors. The source of errors for most flat detectors are sensitivity, speed of response, long term stability, temperature response, wavelength response, and cosine and azimuthal response. Either one of these error sources and/or a combination of them may introduce error greater than ± 4 percent. Extreme caution must be exercised if pyranometers are used. The azimuthal and cosine response may introduce errors of ± 5 percent, especially at large solar zenith angles when the Sun is near the horizon. Taking into consideration all sources of possible error, it is doubtful if some of the published Sun radiation data is reliable. Some of these data may have errors in excess of ± 10 percent.

The computer projected charge data for El Monte, California, and actually recorded charge data during 1973 confirms it. The projected charge data is approximately 15 percent lower in January and approximately 26.5 percent lower in December. The data plots (ampere-hours per day as a function of time) are shown in figure 5.

CONCLUSIONS

It is apparent that the existing weather data and the gathering methods used are not sufficient to design an optimized silicon photovoltaic energy conversion system for a given site. It has been demonstrated that under almost ideal terrestrial sunlight conditions (Table Mountain, California) and controlled measurement techniques it is difficult to achieve repeatable results below ± 2 percent. It is obvious that for accurate solar cell output prediction for a location either the incident irradiation levels must be well defined from the existing available data or an alternative method must be found to obtain sunlight energy data throughout the Earth.

The alternatives which might be considered are: (1) each weather station throughout the United States to monitor sunlight using 2 calibrated solar cells (one collimated and one uncollimated) for a minimum of 5 years, (2) establishment of standard absolute spectral distribution per unit wavelength for air mass ≥ 1 with total irradiance level, and (3) using calibrated quartz-iodide lamps as primary standards to calibrate solar cell secondary standards at AM1 level. This is possible if relative spectral response of solar cells is similar.

The calibration of secondary standards with reasonable repeatability less than ± 2 percent can be attained using sunlight at locations of elevation ≥ 7000 feet and climatic conditions similar to Table Mountain. For optimum photovoltaic conversion, sky radia-

tion data obtained with calibrated silicon solar cells would give a designer an indication of available input energy for the site. After all, it is a solar cell which is used to convert solar energy into electrical energy, not a flat detector.

BIBLIOGRAPHY

Dessens, A.: *Annal. de Geophys.* Vol. 2, 1946, p. 343.

Fowle, F. E.: *The Transparency of Aqueous Vapor.* *Astrop. J.*, vol. 42, 1915, p. 394.

Johnson, F. S.: *The Solar Constant.* *J. Meteorol.*, vol. 11, 1954, p. 431.

List, R. J., ed.: *Smithsonian Meteorological Tables.* Sixth ed., 1951, p. 429.

Moon, Parry: *Proposed Standard Solar-Radiation for Engineering Use.* *J. Franklin Inst.*, vol. 230, 1940, p. 583.

Moon, Parry: *The Scientific Basis of Illuminating Engineering.* Dover Publications, Inc., 1961.

Penndorf, R.: *Tables of the Refractive Index for Standard Air and Rayleigh Scattering Coefficients for the Spectral Region between 0.2 and 20 μm and their Application to Atmospheric Optics.* *J. Opt. Soc. Amer.*, vol. 47, 1957, p. 176.

Thekaekara, Matthew P.: *The Solar Constant and Solar Spectrum and their Possible Variations.* NSF-RA-N-74-062, 1973, p. 86.

United States Air Force: *Handbook of Geophysics.* The Macmillan Co., 1961, chapt. 8.

Wolfe, W. L., et al.: *Fundamentals of Infrared Technology.* The Macmillan Co., 1962, chapt. 4.

Wulf, O. R.: *The Determination of Ozone by Spectrobolometric Means.* *Smithsonian Misc. Coll.*, vol. 85, no. 9, 1931.

DISCUSSION

Q: I would like a clarification on the 20-percent reduction in panels that were not cleaned. That was in the Los Angeles area, wasn't it?

A: Yes.

Q: How did rain affect that or did you make any measurements?

A: It actually increases output from 3 to 5 percent.

- Q: No, I am talking about on that specific panel. Were any measurements made, for example, if it was dusty for 4 or 5 weeks and then rained?
- A: Since we had a zero tilt angle, the panel did not clean off.

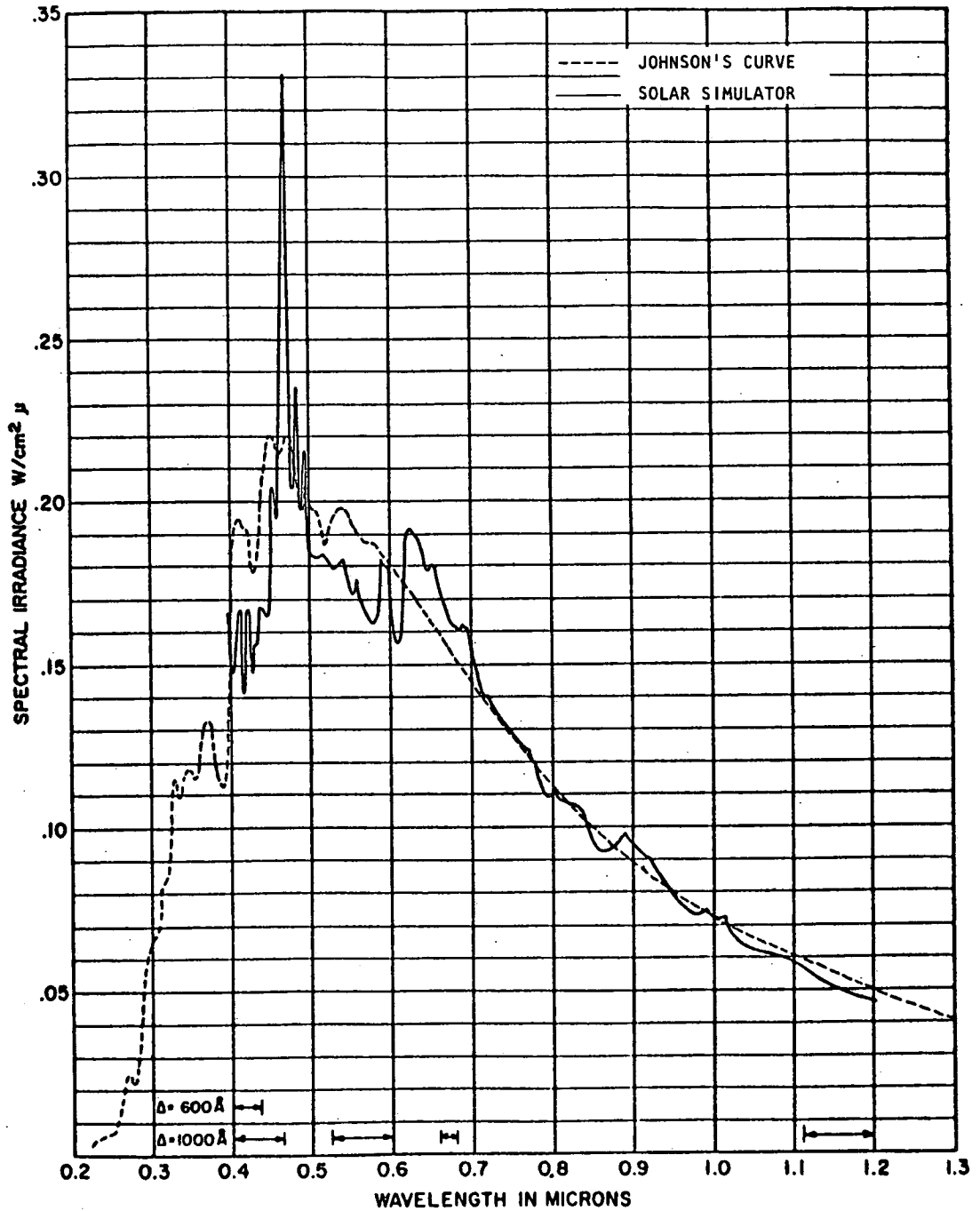


Figure 1. - Centralab's solar simulator.

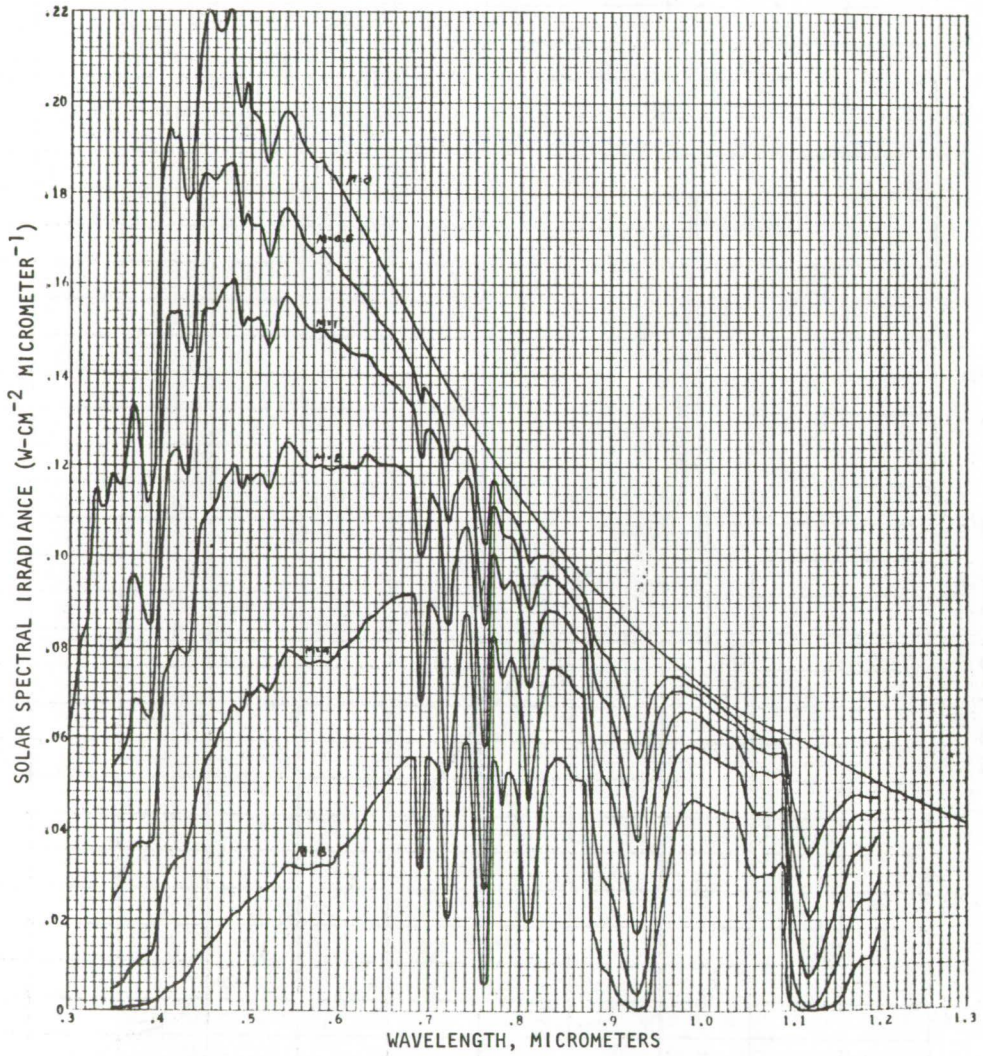


Figure 2. - Solar spectral irradiance as a function of wavelength.

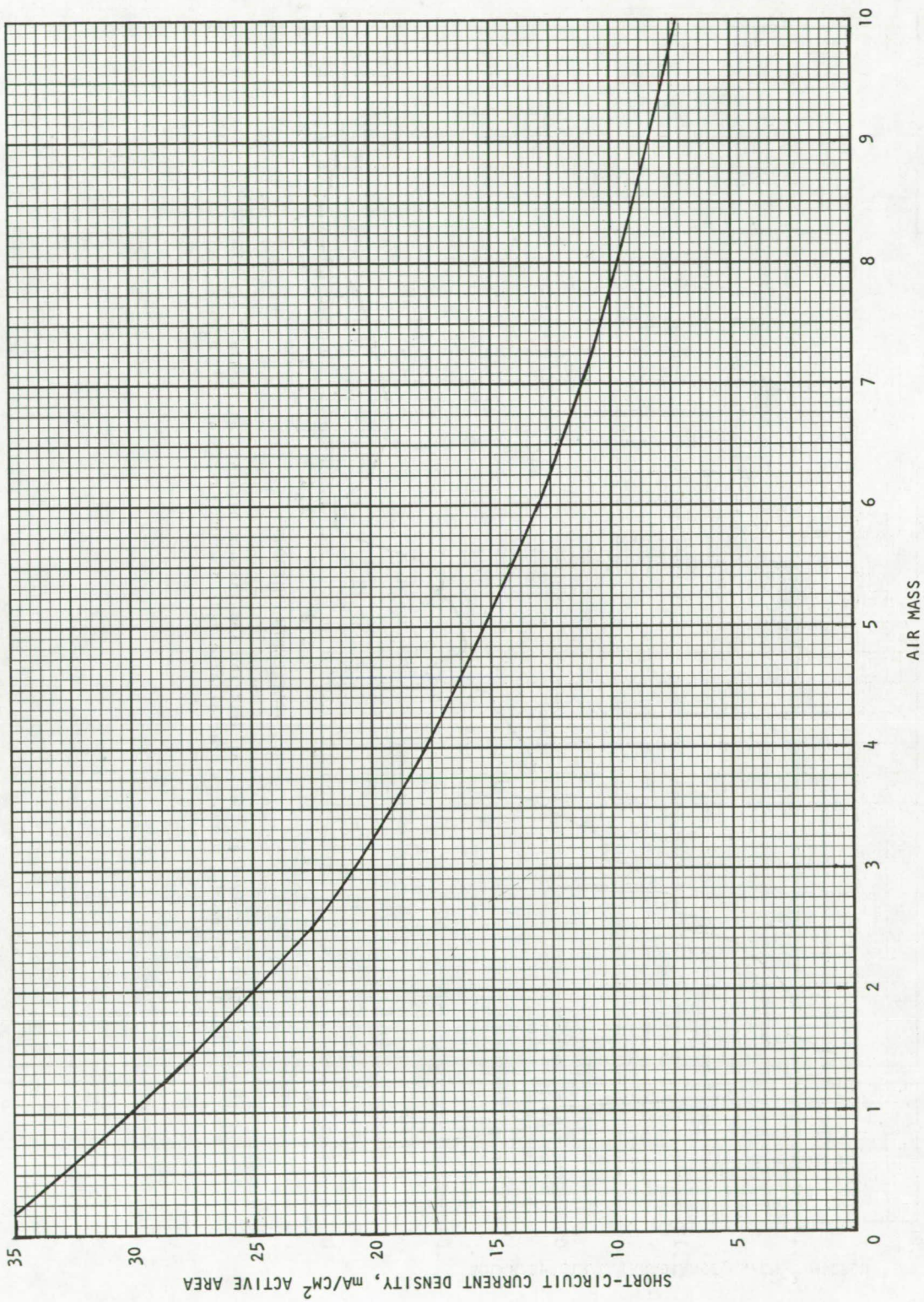


Figure 3. - Short-circuit current density of typical silicon solar cell as function of air mass.

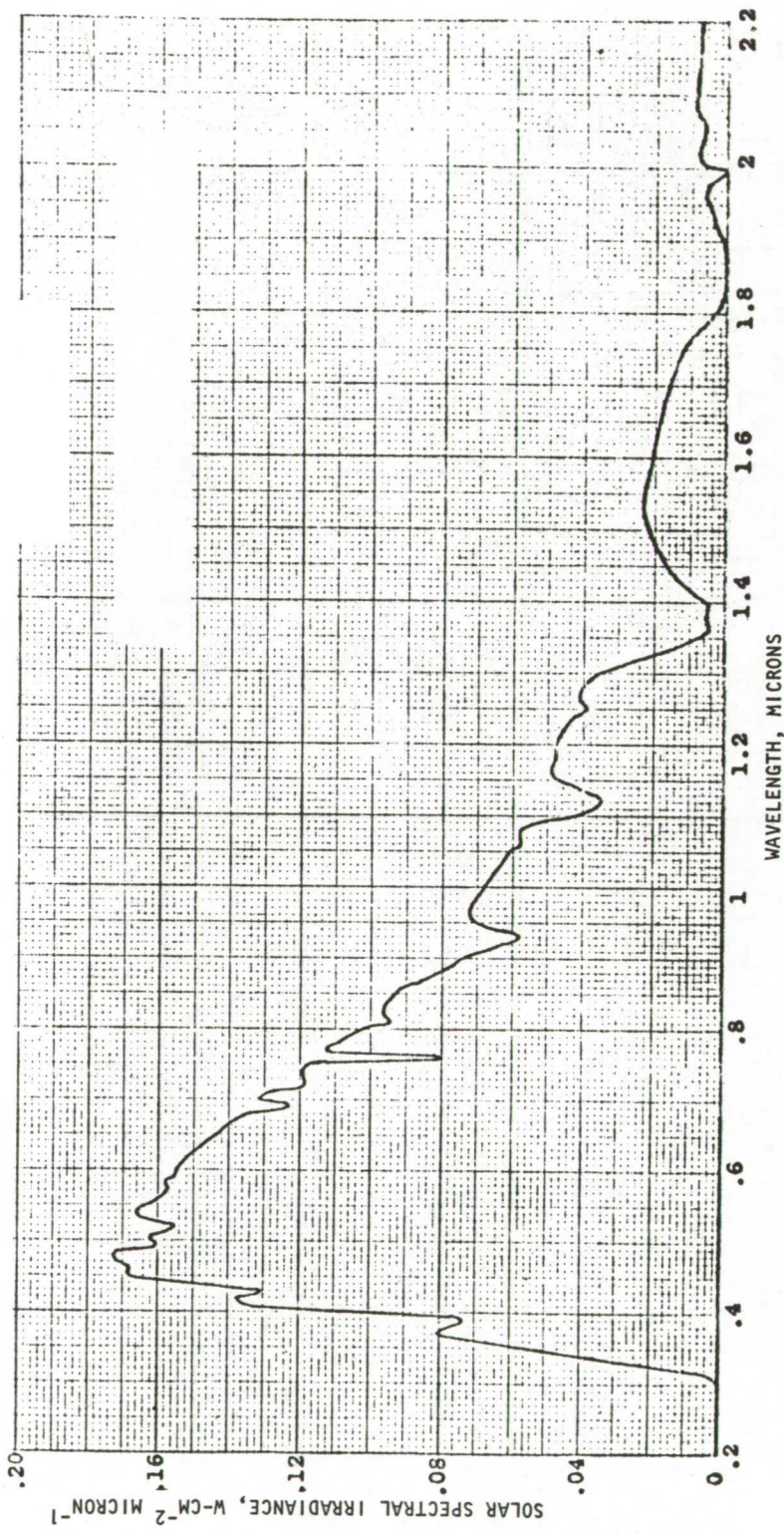


Figure 4. - Typical spectral distribution table mountain, California (June 21).
 $P = 585$ mm Hg; $w = 5$ cm precipitable H_2O ; $d = 200$ particles/cm³; $O_3 = 2.5$ mm;
 $m = 1.03$.

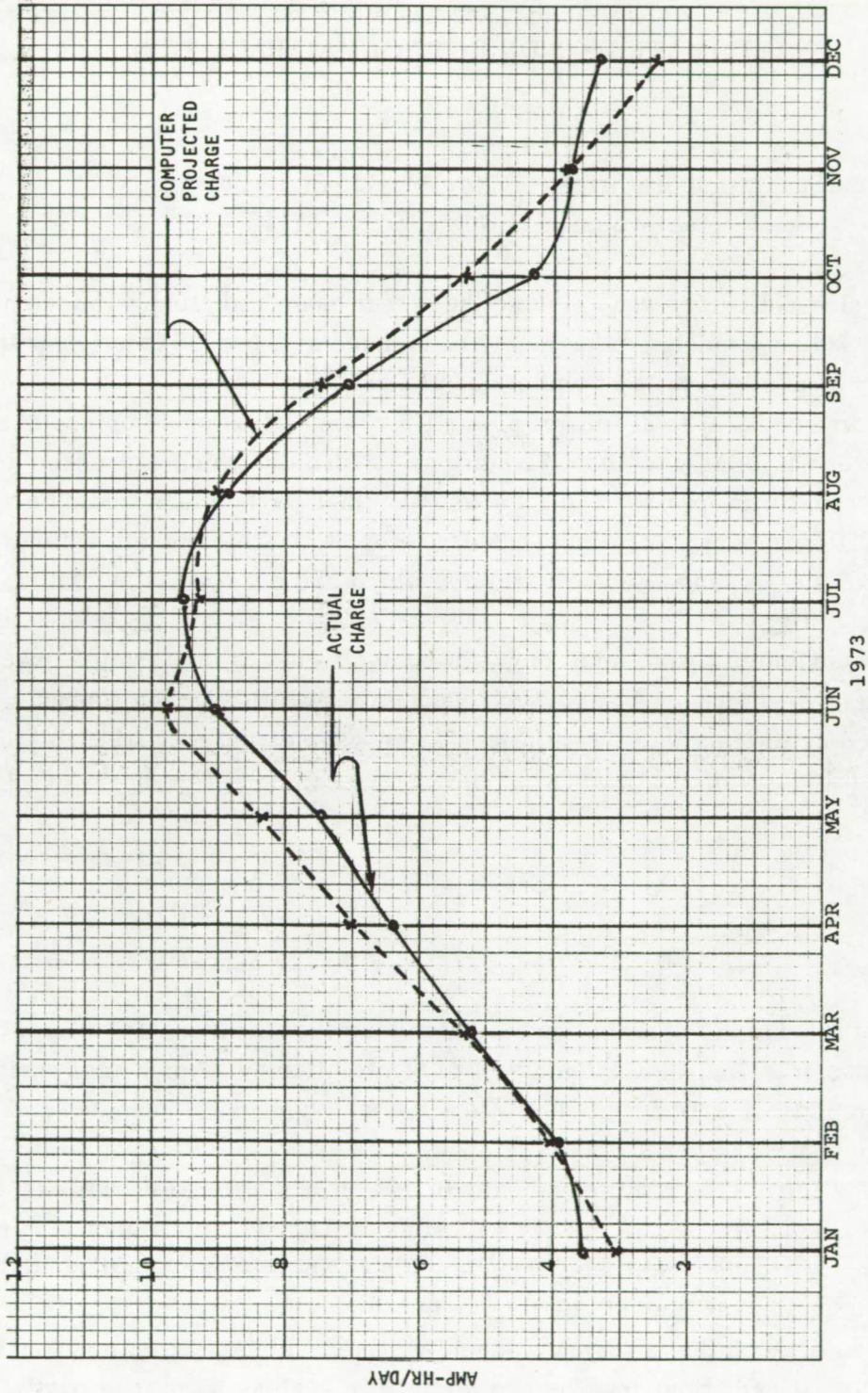


Figure 5. - Site: El Monte, California. Tilt angle, 0°.

ESTIMATION OF DIRECT NORMAL RADIATION

Eldon C. Boes

Sandia Laboratories and New Mexico State University
Albuquerque, New Mexico 87115

Focusing solar collectors can only use the direct beam radiation. Unfortunately, measurements of direct insolation have only been made at a few US locations, and even these data records are intermittent and of questionable quality.

Since measurements of total (direct plus diffuse) insolation on a horizontal surface have been recorded regularly at about 75 stations, a formula which expresses direct normal radiation in terms of total radiation and/or other parameters would be very useful. Quite a few formulas for direct insolation exist, but most are for clear sky conditions, and some use independent variables which are not readily available, such as atmospheric turbidity.

One type of formula in particular is worth noting. This is the formula presented by Jordan and Lie in reference 1 and by Aerospace Corporation in reference 2. The formula is based on the fact that the relationship between direct normal insolation and percent of possible insolation is somewhat linear (see fig. 1). The Aerospace formulation (fig. 2) is

$$I_{DN} = \begin{cases} A \cdot PP + B & \text{if } PP \geq 25 \text{ percent} \\ 0 & \text{if } PP < 25 \text{ percent} \end{cases}$$

where I_{DN} is the intensity of direct radiation on a normal surface, $PP = I_{TH}/I_{EXT, H}$ the percent of possible, I_{TH} the intensity of total radiation on a horizontal surface, $I_{EXT, H}$ the intensity of extraterrestrial radiation on a horizontal surface, and A and B the simple linear regression coefficients.

Although this formula is simple and easy to use, it has several drawbacks. The linear regression equation seems to vary with time of day and with season. Furthermore, under partly cloudy conditions, there simply is not a linear relationship between I_{DN} and PP , or any other kind of relatively simple relationship.

Thus, it was decided that a formula should be tried which takes into account seasonal variation, diurnal variation, and the scatter in I_{DN} values when it is partly cloudy.

The first step was the selection of four 1-week samples of solar data which are representative of the four seasons for Albuquerque. The samples were selected from March, June, September, and December 1962 on the following basis: the total radiation in the sample week equals the long-term weekly average of total radiation for that season. Both the direct and total insolation charts for these weeks were carefully digitized at 10-minute intervals.

The next step was the use of this data to build an estimation technique. The data for each week were divided into four time periods: early AM, late AM, early PM, and late PM. In each period the frequency distribution of I_{DN} as a function of PP was tabulated. Also, for each week those data points (PP, I_{DN}) which seemed to lie on a line were used to compute a linear regression equation.

This information was used to construct four seasonal formulas which use time and PP to estimate I_{DN} . One such formula is described in figure 3 and illustrated in figure 4. Note that quite a few decisions are involved in each estimate. A variation in the PP values is used to determine cloud conditions. The specific decision is whether the current value of PP along with the preceding and succeeding values vary by more than 0.06.

In order to estimate I_{DN} values for a date between seasons the two adjacent seasonal formulas and linear interpolations are used.

Some comparisons of these estimated values with actual data have been made. Figure 5 gives two illustrations. As another example, for 11 days in May 1962, the integral of the estimated I_{DN} values was 4 percent above the integral of the actual I_{DN} values. For 17 days in July the difference was 0.5 percent.

Plans for future work include further comparison and refinement as well as testing and modifying the technique for other locations.

REFERENCES

1. Jordan, R. C.; and Liu, B. Y. H.: The Interrelationship and Characteristics Distribution of Direct, Diffuse and Total Solar Radiation. Solar Energy IV (3), July 1960, pp. 1-19.
2. Aerospace Corporation: Solar Thermal Conversion Mission Analysis. Vol. III - Southwestern United States Insolation Climatology. Report ATR-74 (7417-16)-2, Vol. III (prepared for NSF/RANN), Nov. 1974.

DISCUSSION

Q: I have talked to a Mr. Allen at Aerospace and if you are talking about percent possible the way he talks about it you are talking about percent possible of the extra-terrestrial curve. Is that correct?

A: Percent possible is the total amount under the atmosphere, on Earth on a horizontal surface, divided by the total amount on a horizontal surface outside the atmosphere.

COMMENT: I am not sure if what you are doing has any pertinence to photovoltaic cells. It may be valid for photothermal systems but, as Redfield pointed out, the adsorption of the water vapor on a particular day makes a big difference in what you can get both in adsorption and in scattering. Also, as we find under desert conditions, you can have days where there is a varying amount of dust in the atmosphere. So, although you can get for a given day a total insolation curve which is identical with another day, the actual details are determined by the turbidity of the atmosphere, the amount of water, the cloud cover, etc. And these factors are going to affect both the level, the average level over any given time interval during the day, and the sort of response you will get from solar cells. I don't want to criticize your data as data, I think for total insolation that's fine, but if you are going to go to a solar cell measurement you have to do something different. You have to look at what the spectral distribution is and I think that's a very fundamental problem.

A: I agree completely. I should have said at the outset that I don't plan to do anything or say anything about the spectral decomposition of the radiation available.

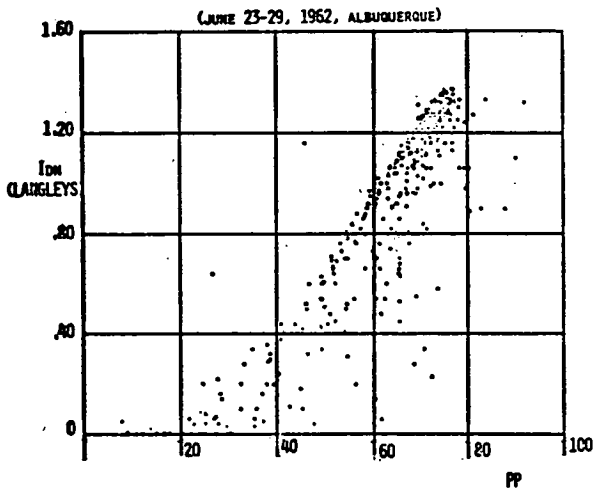


Figure 1. - Typical plot of I_{DN} vs PP.

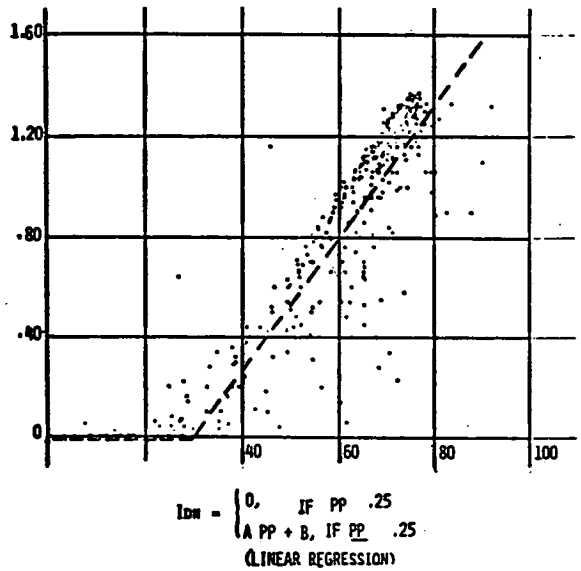


Figure 2. - Aerospace linear model for I_{DN} .

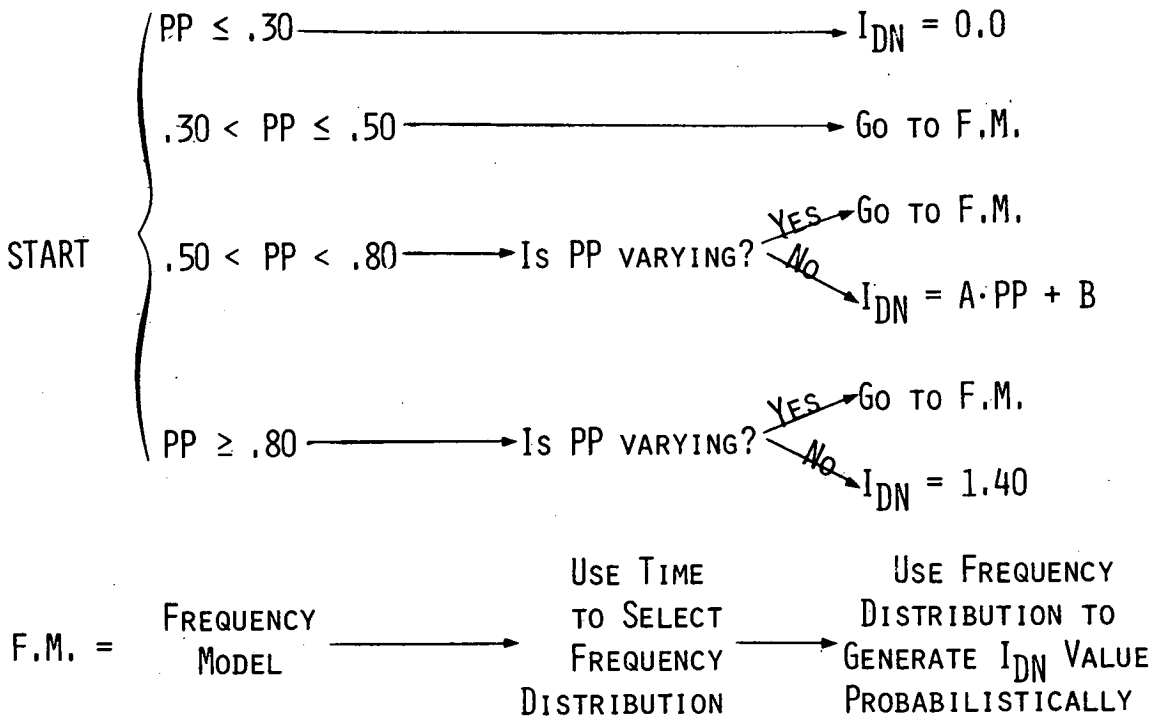


Figure 3. - Estimation formula for June, Albuquerque.

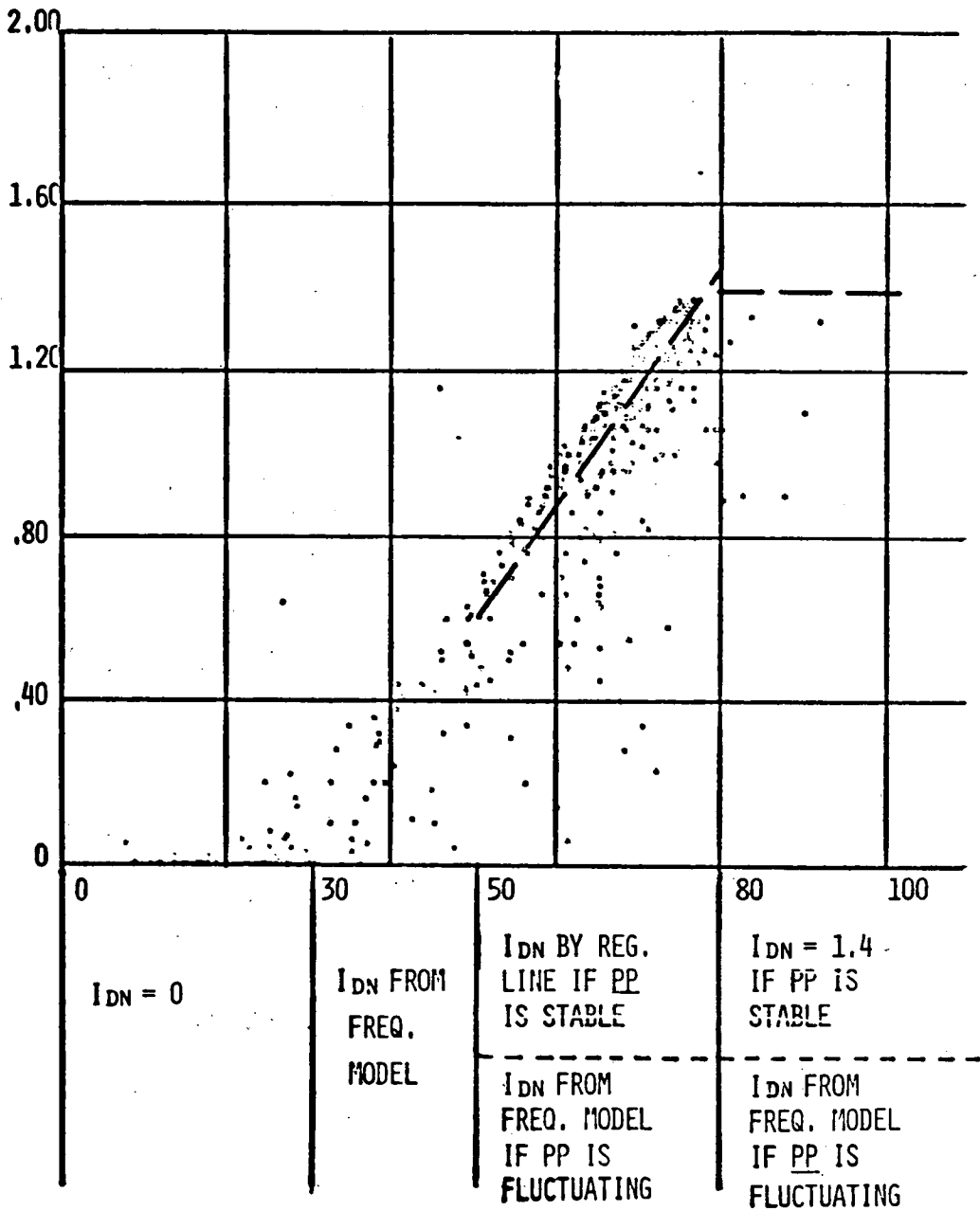


Figure 4. - Estimation formula for June, Albuquerque.

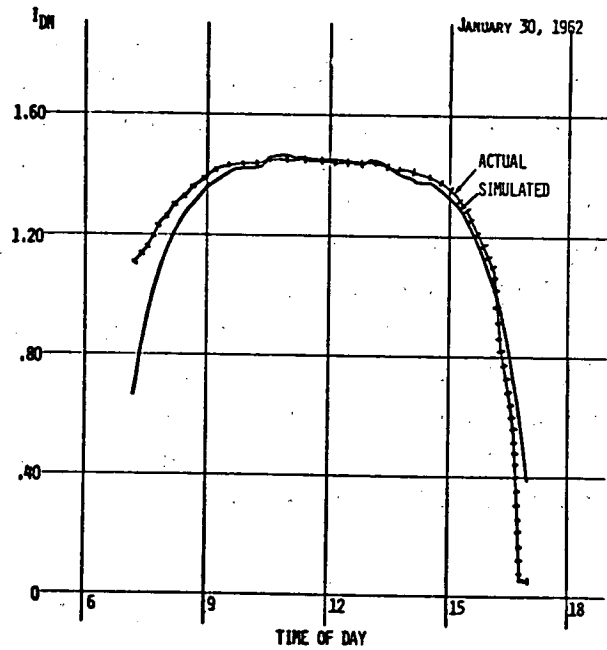
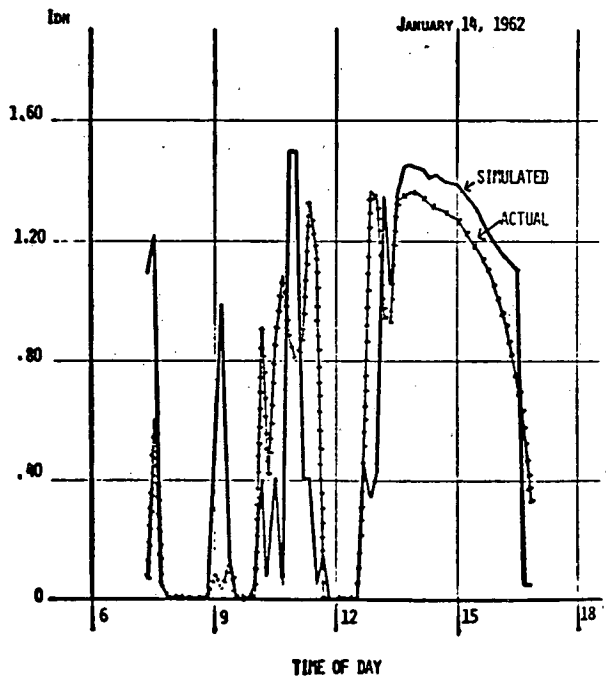


Figure 5. - One-day comparisons of actual and simulated values of I_{DN} .

SOLAR CELL PERFORMANCE IN TERRESTRIAL SUNLIGHT

J. A. Castle

Spectrolab, Inc.
Sylmar, California 91342

Unlike the solar radiation experienced outside the Earth's atmosphere, the spectral distribution and intensity of terrestrial sunlight is continually changing. As a result, predicting the output performance of a terrestrial-based solar cell array is further complicated because of the strong wavelength dependence of the cell response. This paper assesses the magnitude of this problem by looking at the sensitivity of the silicon solar cell output to variations in atmospheric conditions.

Varying quantities of the atmosphere's constituents are responsible for the changing spectral distribution of the insolation. The most important of these constituents are ozone, carbon dioxide, water vapor, and dust particles. Another important variable affecting radiation from the Sun is the distance the radiation must traverse through the atmosphere to reach the surface. The monochromatic slant-path transmission can be written from Lambert's law as

$$T_{\lambda} = e^{-\tau_{\lambda} m}$$

where τ_{λ} is the monochromatic extinction optical thickness at wavelength λ along a vertical path from the Earth's surface to space, and m is the air mass which equals the ratio of the length of the slant path to the length of the vertical path (ref. 1). For solar zenith angles of less than 65° , a good approximation for the air mass at sea level is $m = \sec z$. For larger angles atmospheric refraction should be accounted for. For altitudes above sea level, where the pressure P is less than at sea level (P_0), the value of air mass is multiplied by the factor P/P_0 .

Scattering and absorption by the atmosphere lead to substantial changes in the spectrum. For cloudless conditions the greatest variation is caused by changes in the concentration of aerosol or dust (ref. 2). Molecular or Rayleigh scattering is caused by nitrogen, oxygen, and other molecular components where the scattering particle is small compared with the wavelength of the radiation. Large-particle or Mie scattering is caused by dust, aerosols, water droplets, and other particles of diameter comparable to the wavelength of the radiation. Absorption in the ultraviolet is caused by ozone,

which produces an abrupt termination of the solar energy reaching the Earth's surface at a wavelength near 0.29 micron. In the visible spectrum ozone produces a very weak absorption from 0.44 to 0.74 micron. In the near infrared the spectrum is attenuated by a series of absorption bands primarily dominated by water vapor and carbon dioxide. An air mass 1 spectral model as derived by Moon (refs. 2 and 3) is given in figure 1 showing location of the absorption bands. Figure 2 gives the spectral irradiance at sea level for various path lengths (air masses) through the atmosphere.

The silicon solar cell is strongly wavelength dependent responding to radiation in the wavelength range of 0.4 to 1.1 microns. The maximum response is in the near infrared at approximately 0.8 micron. Figure 3 shows the spectral response of a "conventional" N/P cell with a SiO₂ A/R coating (ref. 4). Also depicted for comparison purposes are the response curves of two newer more efficient space cells.

It is generally accepted that the solar cell sensitivity improves with increased atmosphere; for example, the short circuit current under 100 milliwatts per square centimeter will only increase approximately 16 to 20 percent with an increase of 35 percent in solar radiation for the space AM0 conditions. The reason, of course, is a result of the changing spectrum of the radiation. As we approach an AM0 spectrum much of the added incident radiation occurs at wavelengths associated with water absorption bands, outside the useful spectral range of the solar cell. Conversely, as we increase the path length through the atmosphere, we would expect to experience additional cell sensitivity.

To obtain some quantitative numbers of this change, the "conventional" silicon solar cell sensitivity has been computed for AM0 through AM5. Table I has been constructed breaking the solar spectrum into nine separate bands (ref. 5). The energy contained within each wavelength band is expressed as a percentage of the total energy available. The relative output of the "conventional" solar cell for each of these spectrums was then determined. These outputs, normalized to the AM1 case, show an increase in cell sensitivity with increasing air mass.

It is noted that for the atmospheric conditions assumed the cell is only 85.5 percent as sensitive at AM0 as it is under the AM1 conditions. This decrease in sensitivity, or conversely the increase in sensitivity, from AM0 to the AM1 conditions falls in the range of actual values experienced at Table Mountain during the last 13 years.

In conclusion, we find that the sensitivity of the solar cell short-circuit current with respect to incident radiation increases with increasing path length through the atmosphere. Solar cell standards for terrestrial purposes are normally standardized during clear periods favoring times near solar noon and when the irradiance level approaches 100 milliwatts per square centimeter. These conditions are desirable for obtaining good calibration values that can be repeated with reasonable consistency. These conditions are not, however, typical of the overall weather conditions that a photovoltaic power system would experience in usage. The insolation data that would be used to predict the

performance of such a system would most likely have been gathered using pyranometers and pyrhemometers. These instruments exhibit a flat spectral response over the major portion of the solar spectrum. These factors combined should have the affect of maximizing the spectral error in predicting the system performance. Perhaps this conservative error will offset other errors such as those associated with the cosine or directional response. Certainly, calibration procedures, performance predictions, and solar simulation methods must be carefully critiqued to minimize or at least account for errors resulting from these spectral characteristics.

REFERENCES

1. Gates, D. M.: Spectral Distribution of Solar Radiation at the Earth's Surface. Science, vol. 151, no. 3710, Feb. 1966.
2. Moon, P.: Proposed Standard Solar Radiation Curves for Engineering Use. J. Franklin Inst., vol. 230, Nov. 1940, p. 583.
3. Handbook of Geophysics. Revised ed., USAF, ARDC, sec. 16, Macmillian Co., 1961.
4. Ralph, E. L.; and Scott-Monck, J.: Development and Space Qualification of New High-Efficient Silicon Solar Cells. International Conf. Photovoltaic Power Generation, 1974.
5. Bonner, M. G.; and Sapsford, C. M.: Measurement of Solar Radiation by Silicon Solar Cell. Solar Energy, vol. 10, no. 4, 1966.

DISCUSSION

- Q: I have heard alot of speculation about this difference between the pyranometer and the solar cell. As you suggested, if we put pyranometers and solar cells together in different parts of the country and compare solar cell outputs for the same pyranometer reading, how much variation are we really talking about - 1 percent, 2 percent, or a larger value because, it's a critical issue? If it's only a couple of percent, then you could probably live with it in engineering design. If it's a large number, then you will have to have better data. Until you answer that question it's going to be very difficult to make a decision - it's all speculation at this point.
- A: I think there are probably a number of people starting to look at this now and maybe we can answer it. Perhaps Henry in his paper will help answer it. It doesn't look like it's a great big percentage, and it also looks like you would tag a maximum percentage error on it. In other words, going from AM1 to AM2 was a larger error

than going from AM2 to AM3. What we're saying is as we deplete the energy in these water absorption bands then all of a sudden with further attenuation of the climatic or weather condition you are going to set something that is generally not going to change the sensitivity of the cell as the intensity goes down. So I think maybe we can bracket what the problem is; perhaps, also, the problem is not as large as we might worry about when we don't have the facts.

COMMENT: I would just like to say that if we do use solar cells we are implicitly talking about a silicon solar cell and we have to keep in mind as one of your slides shows that even the thickness of the cell itself is going to influence its performance.

COMMENT: Absolutely, that's why I do not think you would want to implement a complete network, for example. I think for our cells, and other manufacturers that are presenting going silicon, that they will have to understand that.

COMMENT: I don't think there were any data on the output of silicon cells as they relate to pyranometer readings. Stan Leonard in his mission analysis asked, for the purpose of the mission analysis, if he would use the pyranometer data as they exist to predict the output if he should go back and pick out all the pertinent weather data (such as turbidity) and try to revamp the data. I believe what he did was to take the atmosphere model calculations and calculate the direct solar intensity involved with a silicon spectral response. He did this for various air masses, different geographic locations, and atmospheric conditions. I remember the conclusion was something like this. For cases where the insolation is high there is not a great deal of difference, perhaps a few percent or less. There was quite a substantial difference when the insolation is low, 20 percent or that sort of number. So his conclusion in this case is that for the purpose of a mission analysis it seems quite adequate to use it.

COMMENT: I would like to bring up again the point that Mr. Bernatowicz made. That being that we have two main needs. One is for an index of performance measurement where as much accuracy as possible is required. But if we are talking about computing power outputs of arrays for actual power generation, then perhaps we should find out what sort of accuracy the utilities need and in fact what sort of precision they can put on the output of even a conventional oil powered station before they build it. If they can only get within 10 percent then need we spend a lot of effort in being able to forecast photovoltaic outputs to 5 percent.

TABLE I. - SILICON SOLAR CELL SENSITIVITY
WITH AIR MASS VARIATIONS

Wavelength band, μm	Optical path length ratio, m					
	0	1	2	3	4	5
	Percent of total energy available ^a					
Up to 0.4	9.0	4.3	2.7	1.7	1.1	0.5
0.4 to 0.5	14.4	14.6	12.9	11.2	9.6	8.1
.5 to .6	13.8	16.3	16.0	15.6	14.6	13.6
.6 to .7	11.8	14.5	15.5	15.9	16.2	16.4
.7 to .9	17.3	20.6	22.4	23.3	24.5	25.5
.9 to 1.1	10.8	12.7	13.7	14.8	15.8	16.9
1.1 to 1.4	9.3	9.2	9.6	9.1	9.2	9.5
1.4 to 1.8	6.1	6.4	6.6	7.2	7.8	8.4
Greater than 1.8	7.5	1.4	1.2	1.2	1.2	1.1
	100.0	100.0	100.0	100.0	100.0	100.0
Solar cell ^b output sen- sitivity (relative)	0.855	1.000	1.039	1.053	1.064	1.071

^aEnergy data based on spectral distribution data published by Moon.

^bSolar cell sensitivity data based on applying conventional relative response curve against energy distribution and normalizing with respect to relative output response to AM1 spectrum.

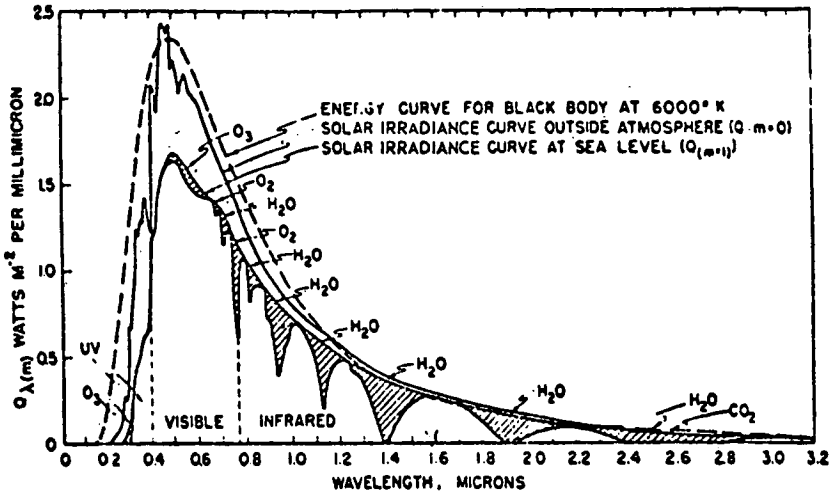


Figure 1. - Spectral distribution of solar energy outside the atmosphere and at sea level (ref. 2).

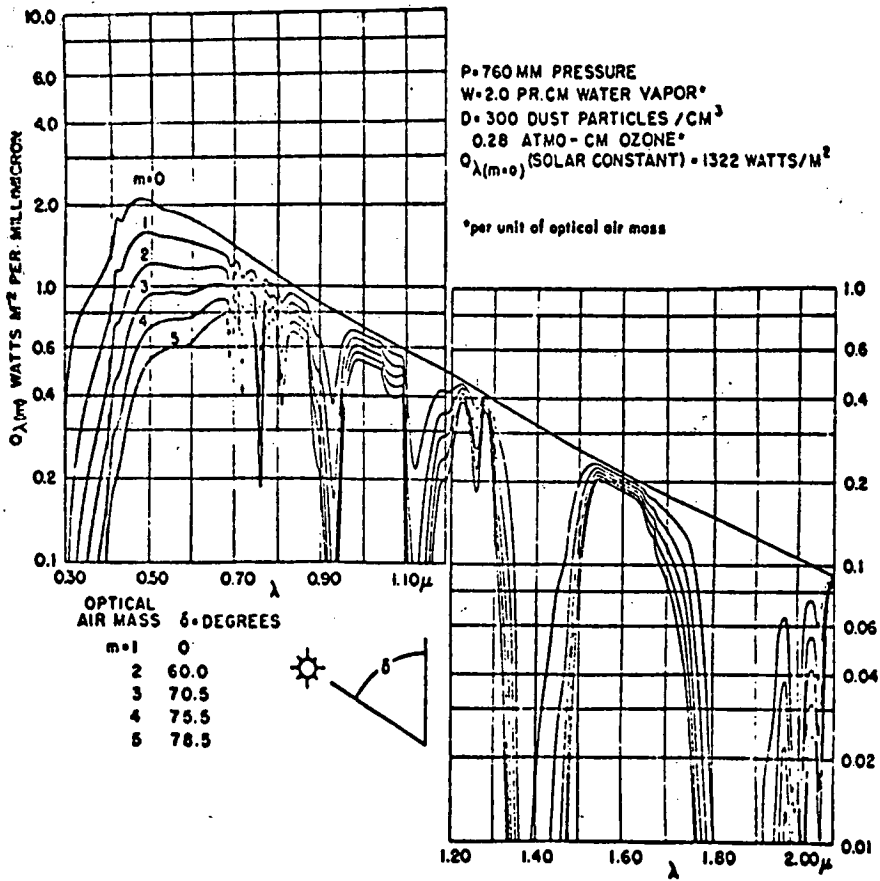


Figure 2. - Solar spectral irradiance curves at sea level with varying optical air masses.

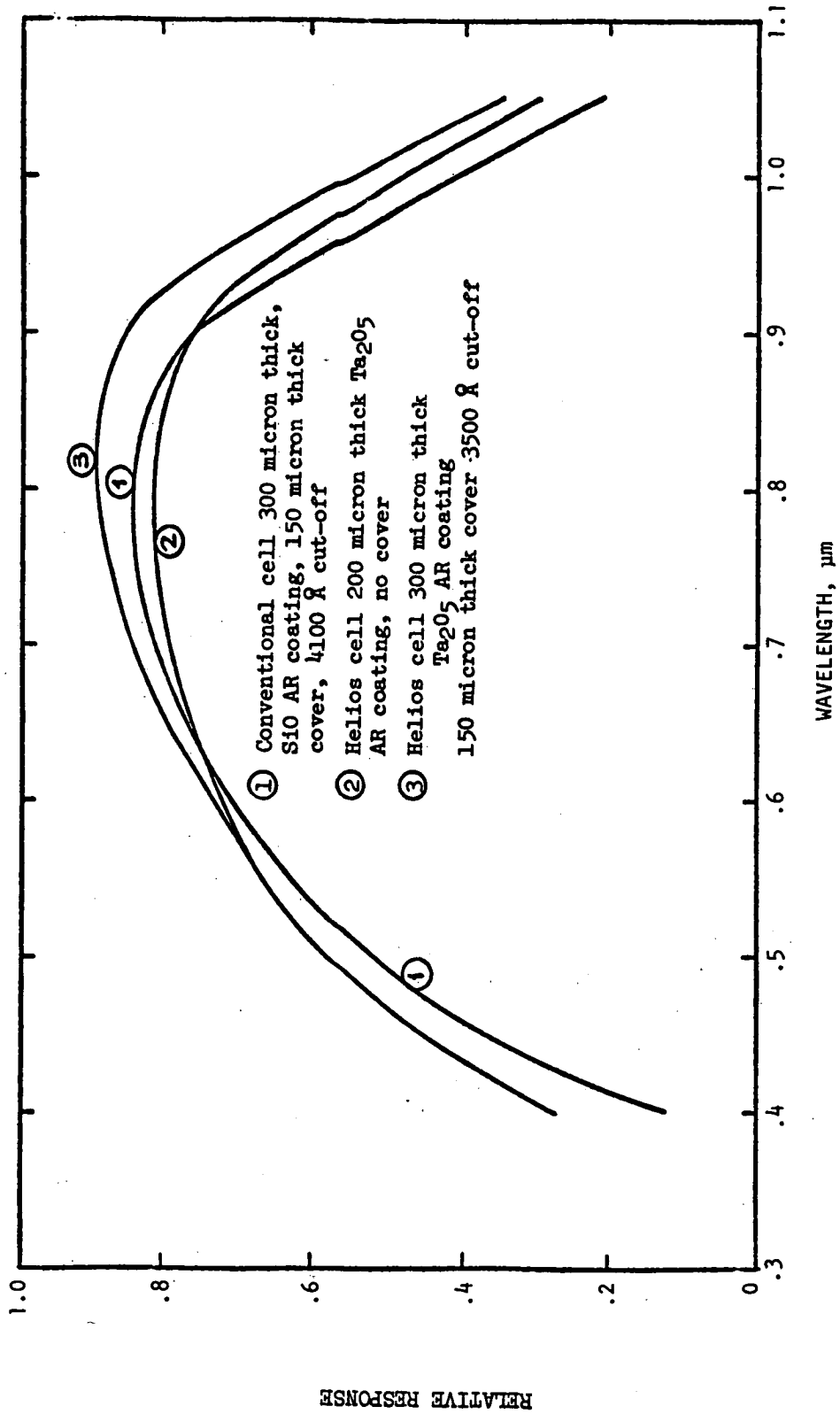


Figure 3. - Spectral response of shallow junction Helios field cells compared to conventional cells.

VARIATION OF SOLAR CELL EFFICIENCY WITH AIR MASS

Henry W. Brandhorst, Jr.

NASA Lewis Research Center
Cleveland, Ohio 44135

In contrast to outer space sunlight, terrestrial sunlight is constantly changing in intensity and spectral distribution. These changes are caused by the variable thickness of the atmosphere (air mass) through which the sunlight passes and the variation in atmospheric condition. Thus, intensity and spectral variations may have important implications for the performance of the terrestrial solar cell array. They also complicate the selection of a "representative" spectrum to be used in artificial sunlight simulators. Little detailed data exist on the effect of this change in the sunlight spectrum on the performance of various types of solar cells. The purpose of this paper is to provide data on the variation of solar cell short-circuit current and efficiency with air mass. The solar cells studied include silicon, gallium arsenide, and cadmium sulfide.

EXPERIMENT PROCEDURES

The solar cells were measured under direct natural sunlight in Cleveland, Ohio, from December 1974 to March 1975 primarily on days with clear sky and few clouds. Measurements were also made with substantial amounts of haze and cloudiness, and a few cells were even measured through heavy cirrus cloud layers. Measurements were made from early morning to near sunset to afford a wide variation in air mass. Solar intensity was monitored with a normal incidence pyrheliometer (NIP) whose output was recorded while the current-voltage (I-V) curve was being traced. Insofar as possible, measurements were made when no clouds passed near the Sun so that neither the solar cell nor the NIP was changing.

Solar cells as large as 2 centimeters by 2 centimeters were mounted at the end of a 10:1 collimating tube. Collimation was used to eliminate the variable of scattered light. Cells were secured to the plate with a vacuum hold-down. Plate temperature was controlled to $25^{\circ} \pm 2^{\circ}$ C. Separate voltage and current probes contacted the top surface of the cells (except for the CdS cell which was encapsulated under glass). No separate voltage contact was made to the back of the cell; however, four wires were used between

the base plate and the data acquisition system. A variable load and x-y plotter were used to trace the I-V curve. The solar cell, collimating tube, and pyrhelimeter were mounted on a clock-driven Sun tracker. Each cell was measured on several different days. The cells studied included a conventional silicon cell, a silicon cell irradiated with 1×10^{16} electrons per square centimeter, a gallium arsenide cell manufactured in about 1964, a gallium aluminum arsenide - gallium arsenide cell, and a glass-encapsulated Kapton-covered Clevite-type cadimium sulfide cell. Atmospheric conditions varied from a clear, blue sky to a heavy haze. Intensity of the normally incident sunlight ranged from 15 to 90 milliwatts per square centimeter. The air mass was determined from the solar elevation and barometric pressure at the time of measurement. The values obtained ranged from 1.3 to 4.5.

RESULTS AND DISCUSSION

Figures 1 to 3 show the variation of solar cell short-circuit current with intensity. In all cases a line or curve extending through the origin is obtained. Because of this linear relationship, the ratio of short-circuit current density (band on total cell area) to input power density (mA/mW) was calculated for all the points. The mean value of this ratio and the standard deviation are listed on the curves. Mean values range from 0.312 milliampere per milliwatt for the silicon cell to 0.116 milliampere per milliwatt for the gallium arsenide cell. Standard deviations of this ratio were less than 2 percent. On days when the lighting conditions were rapidly changing because of haze or cirrus clouds, the solar cell responded far more rapidly than the pyrhelimeter, which contributed to the spread in results.

Despite the wide variative in intensity for these data, the spectral distribution within the response band of the solar cell is not changing sufficiently to alter significantly the ratio of short-circuit current to sunlight intensity. Thus, it is possible to make current measurements under any known sunlight intensity with the confidence that the short-circuit current for other intensities can be obtained with little error by simple linear extrapolation.

The variation of solar cell efficiency with air mass is shown in figures 4 to 6. Cell efficiency appears to be independent of air mass over the range of air mass and solar cell types studied.

This observation follows because efficiency was independent of intensity so long as the intensity was above 20 milliwatts per square centimeter. Over this intensity range the open-circuit voltage varied by about ± 4 percent. The low-variation coupled with a slight change in the fill factor accounts for the constancy of efficiency with intensity and hence air mass. Average measured cell efficiencies range from 12.0 percent for the silicon cell to 4.26 percent for the gallium arsenide cell. Error values shown on the

figures are standard deviations. Only the radiation damaged silicon cell shows a deviation of more than 2 percent. Measurements on this cell were made when the atmosphere was most variable. Hence, errors in pyrhelimeter readings probably contributed substantially to this deviation. Thus, it appears that considerable freedom also exists in selecting an air mass for terrestrial solar cell measurements.

CONCLUSIONS

For the five types of solar cells measured in this study it has been shown that short-circuit current is directly proportional to intensity within a standard deviation of about 2 percent and that efficiency is independent of air mass within about 2 percent. These relationships permit great freedom in selecting a spectral distribution/intensity to be used as a guide for the artificial light sources used to simulate terrestrial sunlight. Similarly, a great deal of freedom is also permitted for air mass and intensity levels to be used in making cell measurements in terrestrial sunlight.

DISCUSSION

- Q: Would it be reasonable to assume that since we know spectral distribution is shifting with air mass and you don't see any significant change here with air mass that the efficiency and currents are relatively insensitive to spectral distribution for the cells that you have tested?
- A: It's an implication of these data and I don't know how firmly I want to stand behind them because I know what the calculations show.
- Q: I want to pursue that first question a little farther. Hasn't it been established that the AM0 efficiencies are lower than the AM1 efficiencies? And, as the gentleman back here pointed out, aren't the spectral distribution changes from AM0, AM1, AM2, AM3, etc. like the curves we have seen here to the extent the blue and the UV content in the solar spectrum are decreasing? And, also, isn't the usable energy available in the solar spectrum actually increasing? That's the standard argument. So I don't understand your results. I would have expected the efficiency to increase as you went from AM1 to say AM3. Not as radically perhaps as from AM0 to AM1, but at least some increase.
- A: Once you take the big drop getting down to AM1 through the atmosphere, then it appears that, even though we have these spectral distribution changes, the power in the visual portion of the spectrum, against which we are calculating the efficiency, is going in the same ratio as the short-circuit current. I was hoping to show a gradual increase with air mass also but it didn't happen.

- Q: Doesn't this resemble an attempt to extrapolate on a Langley plot a broad band filter to AM0 where you don't get much curvature until you go from AM1 to AM0?
- A: Yes, we do not have the data quoted here as current against air mass because the atmospheric conditions were so variable that we couldn't do that. But, yes, this is what the Langley technique did, and it can be good say up to AM2 or AM3.
- Q: Did you say you monitored the incoming intensity with an Epply NIP?
- A: Yes.
- Q: So the intensity of the radiation does not quite have the spectral match to your solar cell response?
- A: No, it doesn't. It's a blackbody detector.
- Q: The results of the tests done on Solar 1 in Newark do, in fact, show that the December to March period is a very flat period and that any seasonable spectral effects begin to show thereafter. Maybe we will be getting some changes soon.
- A: We are aware of the results you published and that's why I say take everything with a grain of salt.
- Q: Since you have these cells have you made any spectral response measurements?
- A: Yes.
- Q: Are they flat or do they show a typical fall off in the red?
- A: These cells are typical. They show the fall off in the red.
- Q: It seems strange, then, that you should be able to calculate, if you know the spectral content of your various air masses, what the short-circuit current should be.
- A: The problem we have is what the atmospheric composition is for any given moment in time between us and the Sun when we are monitoring the cell current. For the same air mass we have seen a range of a factor of 5 or 6 in intensity for identical air masses. Clearly, to model the current for a given air mass is meaningless unless you have an atmospheric model.

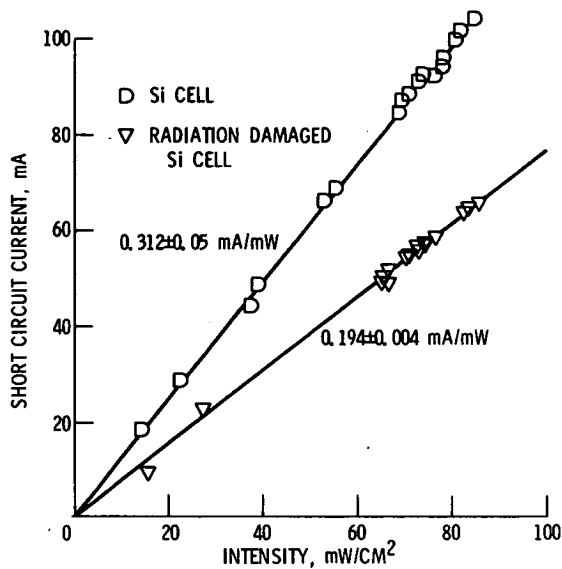


Figure 1. - Variation of silicon solar cell short circuit current with intensity.

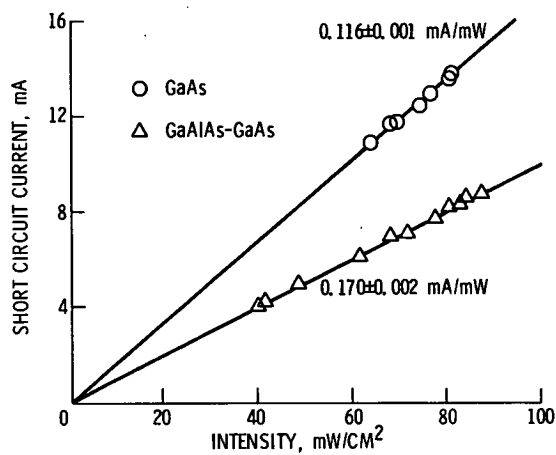


Figure 2. - Variation of gallium arsenide solar cell short circuit current with intensity.

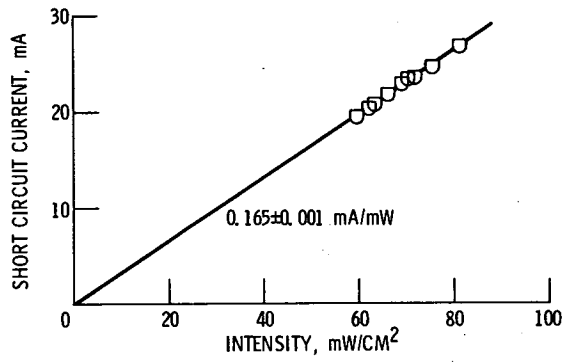


Figure 3 - Variation of cadmium sulfide solar cell short circuit current with intensity.

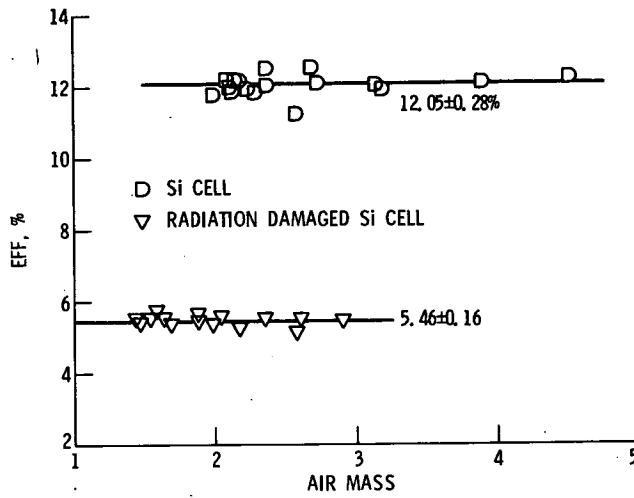


Figure 4 - Variation of silicon solar cell efficiency with air mass.

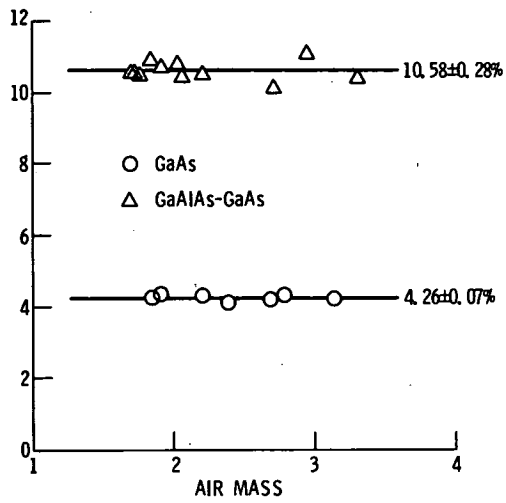


Figure 5. - Variation of gallium arsenide solar cell efficiency with air mass.

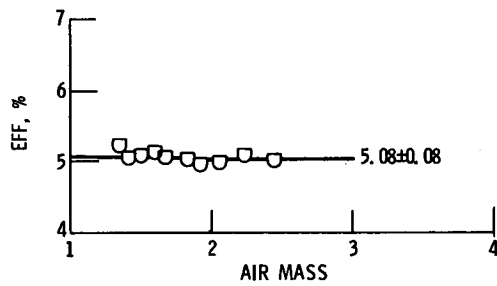


Figure 6. - Variation of cadmium sulfide solar cell efficiency with air mass.

MICROCLIMATOLOGICAL INFLUENCES ON TWO SOLAR MODULES

Douglas M. Warschauer

Naval Weapons Center
China Lake, California 93555

A given photovoltaic solar cell has behavior which is a function of load and insolation. An array may be constructed of cells connected in series-parallel to provide specified currents and voltages at given values of insolation and load. From an engineering point of view a useful concept is that of a photovoltaic solar module: a black box capable of providing solar-derived electrical energy continuously to a load. Present modules generally consist of a solar cell array to generate current, a diode to prevent back current, a battery in parallel with the array to provide storage, and perhaps a voltage regulator to provide stability. Such a circuit, without a voltage regulator, is shown in figure 1. The battery is charged when the array voltage exceeds the battery voltage. The behavior, which is inherently nonlinear, is strongly dependent on the number of photovoltaic cells, their mode of interconnection, the charging efficiency of the battery, its capacity and past history (polarization), and the details of the diurnal fluctuation of insolation. Two arrays, "Brand B" and "Brand X" (shown in figs. 2 and 3), were purchased specified to supply a 0.8 to 0.9 ampere peak at 12 volts nominal with a 4 ampere-hour load per day for local China Lake (Inyokern) conditions. Forty ampere-hour batteries were recommended by the manufacturer of each array as providing sufficient capacity to take care of periods of low insolation. Brand B was connected in accord with figure 1 to wet cells having a 12 volt, 40 ampere-hour capacity with a 68.5 ohm resistive load. Brand X was connected to a 12 volt, 40 ampere-hour sealed gelled electrolyte cells with a 66.6 ohm resistive load. The arrays were mounted side by side with the same orientation.

China Lake has a year-round daily average of 585 calories per square centimeter insolation, and, averaged over a long period, has about 92 percent of ideal clear air conditions. There are isolated times during the winter when the deviation from ideal is large (February has an 18-year average of 432 cal/cm^2 ; the period to be described here average 368 cal/cm^2). A period of 35 days, whose daily insolation values are shown in figure 4, was selected for discussion here. The behavior of the modules during this period is considered instructive enough to report. Brand B module supplied on the average 4.68 ampere-hours and brand X supplied 4.02 ampere-hours (including, in this

case, performance to end of February) of daily load over the period and thus exceeded the specification by 17 and 0.5 percent, respectively.

Figure 5 illustrates that although the diurnal insolation varied considerably during the period concerned the integrated solar insolation approximates a straight line. Figures 6 and 7 show that the panel ampere-hours and the load ampere-hours also exhibit approximately linear behavior. One might infer from figures 5 to 7 that a linear model for the behavior is sufficient to determine average performance, although the deviation of load ampere-hours from linearity for brand X beyond February 18 is suspicious.

These suspicions are verified if one examines the difference between panel and load ampere-hour curves of figure 8 in which no linearity is observable. Brand B has continued to charge and provide adequate power to the load, while brand X in point of fact has fully discharged its batteries toward the end of the period shown, even though the ampere-hour difference is 28 and not the 40 that the battery capacity seems to imply. Figure 9 shows the observed voltage and current at selected times over the 35-day period. Note the wide fluctuation in both voltage and panel current. These are highly dependent on such factors as just how much radiation was incident at the time of measurement, whether the batteries are polarized, etc. With the daytime voltage fluctuating between 12.5 and 16.7 volts the panel, battery, and load powers are all strongly dependent on the product VI rather than I alone as would be the case in a constant voltage system, which a module on first inspection appears to be.

A conclusion that might be drawn from this brief inspection is that a solar module is a highly nonlinear device whose performance is a function of the cell and array characteristics, the efficiency of charge storage, the past history as represented in battery voltage and state of polarization, and the time-dependent details of insolation. Furthermore, it is obviously not satisfactory to use average behavior to determine the parameters of a module, particularly if a heavy intermittent load is drawn or a short time period is involved, as may be the case in military use, for example. Two days of exactly equal insolation might lead to positive or negative net charging dependent on whether the insolation ever reached the value needed for the array voltage to exceed the battery charging voltage. Figure 10 shows three pyranometer curves taken locally having almost the same total insolation, but characteristics which would lead to different module behavior. Thus, an intensive study of modules is needed, in which, from a theoretical point of view, a computer model should be used to take account of the time-dependent variation of all the relevant parameters. When actual field studies are to be done, it is desirable that a pyranometer be mounted adjacent to the module under test and continuous recording of insolation, panel current, load current, and battery voltage be taken and interpreted in order to predict the behavior of a module.

DISCUSSION

- Q: I question your threshold charge voltage. Why is there a threshold there? On a day that maybe you had half the insolation you indicate that maybe it wouldn't charge. If it's designed with a voltage near or below the maximum power point it should definitely charge under those conditions. You should have enough voltage, even though the insolation is lower.
- A: If you made an array out of a given number of solar cells and you designed them for China Lake conditions, I think you would put a certain number of them in parallel with one another and then you would series groups of these. If you were designing primarily for conditions like we have here today you would probably rearrange that series-parallel configuration to take into account the fact that the days are generally gloomier or you might get very little charging. So you must design the panel to fit with the batteries that are going to be used. As far as I can see, you get no charging if the insolation at any given time falls below a certain amount. Our ampere-hour meters just stop dead at that time. The brand B panel in our case happens not only to be charging very well during periods of bad weather like we were having here but under the more ideal conditions that we usually have. I think we generally are always overcharging which I don't think is a desirable situation. Maybe that's what you are talking about. If you design such that you are always overcharging then you don't have any problems.
- Q: Yes, that's what I'm saying. If you design at the proper voltage, even at low insolation, you will get your full charge.
- A: But then if you have open cell batteries, you are driving the water off all the time.

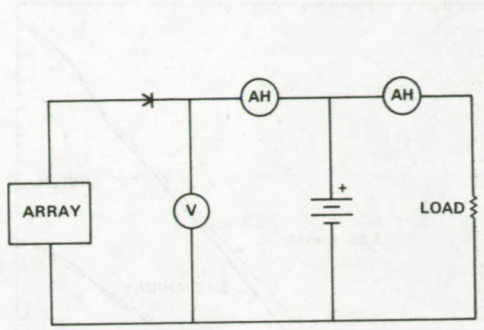


Figure 1. - Solar module circuit diagram.

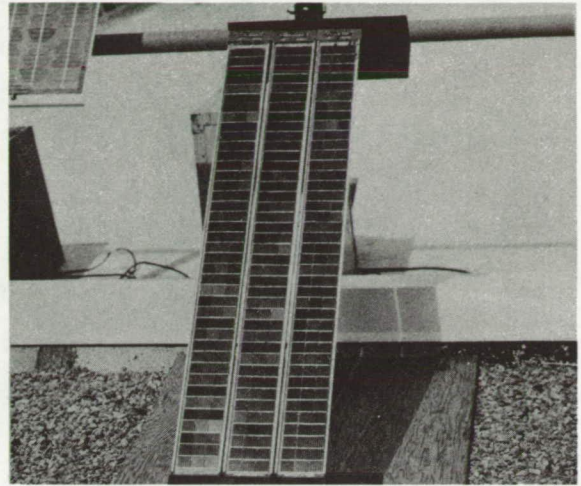


Figure 2. - Photovoltaic cell array of "Brand B".

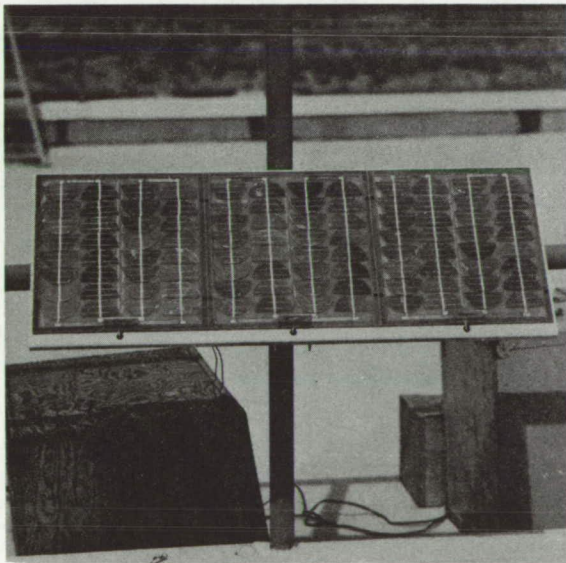


Figure 3. - Photovoltaic cell array of "Brand X".

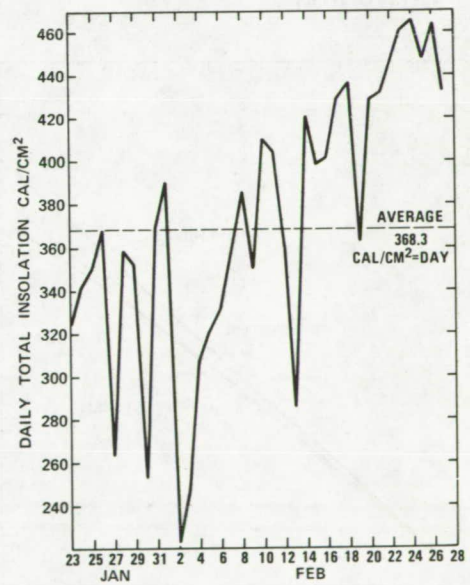


Figure 4. - Daily total insolation for 35 day 1975 period at China Lake (Inyokern), California.

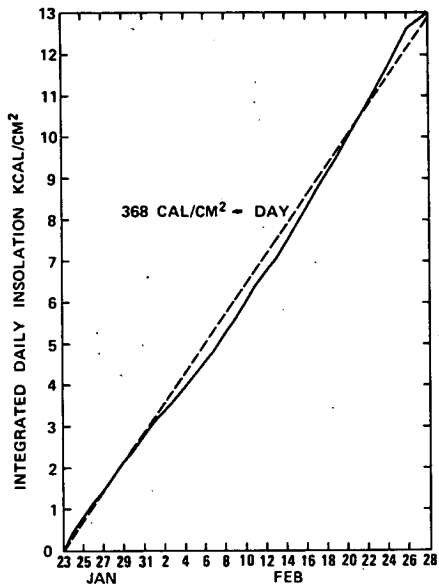


Figure 5. - Cumulative daily insolation for 35 day 1975 period at China Lake (Inyokern), California.

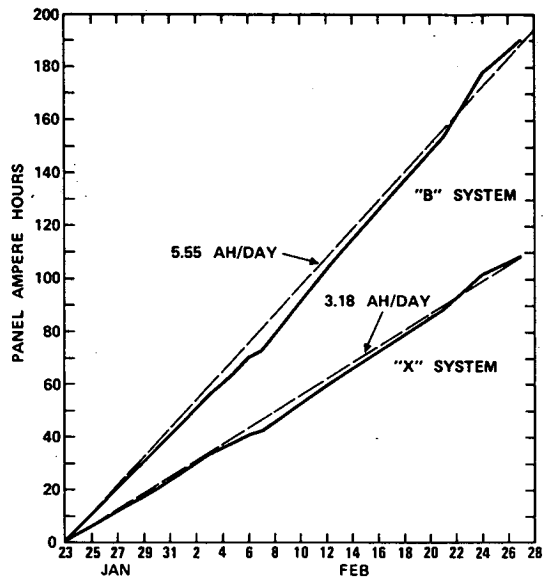


Figure 6. - "Brand B" and "Brand X" panel ampere-hours.

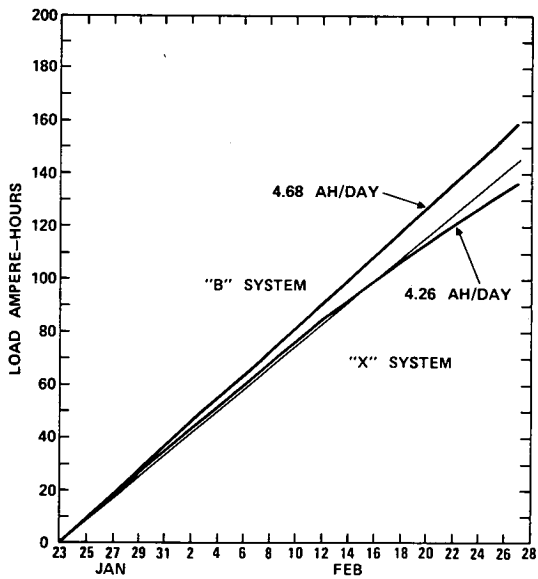


Figure 7. - "Brand B" and "Brand X" load ampere-hours.

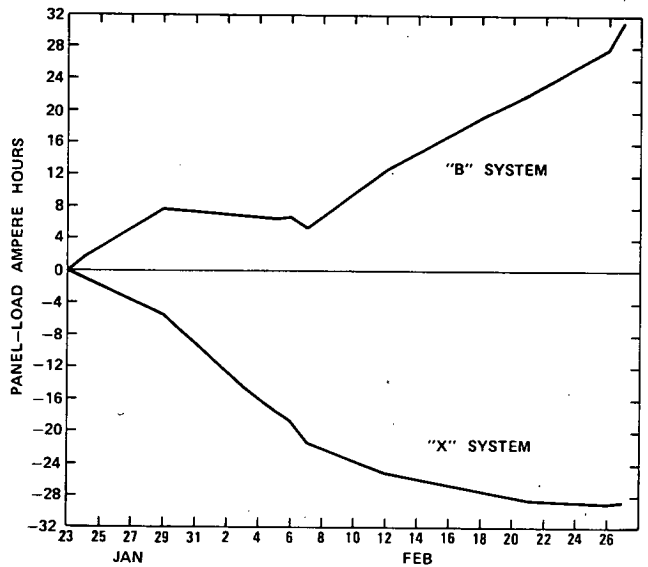


Figure 8. - Net panel minus load ampere-hours.

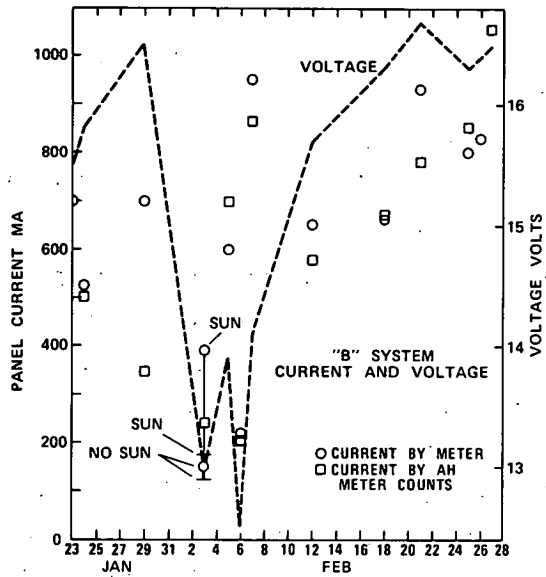


Figure 9. - Observed values of panel current and voltage during 35-day period. Spread of current and voltage values for Sun and no Sun conditions shown for one day.

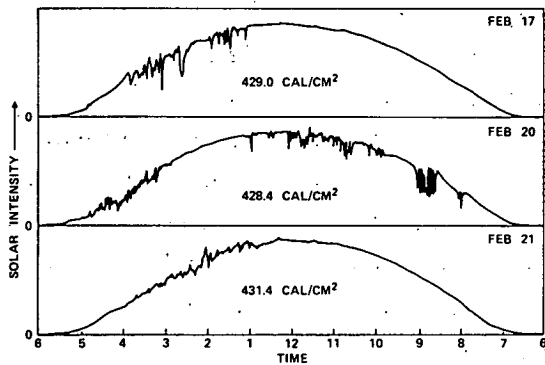


Figure 10. - Daily isolation curves for three days of approximately equal total daily insolation during the 35-day period.

GENERAL DISCUSSION FOLLOWING SESSION I

Q: Are there enough existing data now that we should be working on and can those data be rehabilitated or is there a way we could be more aggressive within the national program to look for these data?

COMMENT: I think the comment was made earlier that we are going to all this trouble to find out what a solar cell does in the sunlight. I wonder why the NOAA program doesn't have a direct and diffuse solar cell measurement as part of their program rather than going through all these calculations to get to what we could get so simply with a easy measurement. It seems like these turbidity calculations and calculations of direct arc the only way we can go now because that's historically the way the data were taken. We will go in an around about way to get there, but I think we could do it very simply and get the data we want with a very inexpensive measurement.

COMMENT: Spectral data are used only in research and other than the congressional charge to characterize the atmosphere NOAA doesn't actually have a need yet for solar radiation data. So this is one problem people face when they ask somebody from NOAA to monitor radiation. The opinion often is if you need it so badly at your particular location why don't you put it in at that location. We feel that we are going to monitor, through the congressional charge, an overall network. It's been pointed out here several times that you are going to have to take point measurements in certain locations. We do want to get into the spectral business. But first there are some questions we do need answers to. What breakdown do you people need in the sense of what bandwidths? How many do you need? At what frequency do you need them - every minute, hour, or daily total? For what time period are you going to need them? Will 1 year of data to serve from now on, as a statistical year be enough or do you need them for 10 or 20 years? About what network size do you think is reasonable to represent the United States and get reasonable data for planning purposes? NOAA can't, and I don't think ERDA can either, afford to monitor at every location that we would really like to because of the budgeting problems.

COMMENT: Again, I want to state that I have only been thinking about this for about a week. I should also point out that I am from China Lake which is in the middle of the desert in California where we get about 3 inches of rain a year, about as little as you get anywhere in the country. Also, we are near Mount Whitney, which is the highest peak in the continental United States, and you can see roughly 100 miles to Telescope Peak which overlooks Death Valley so the conditions are presumably ideal. They may be ideal for

a full year. If you look at the weather conditions as compared to extraterrestrial insolation we get about somewhere between 72 and 76 percent solar insolation. On the other hand, if you want the percent possible total insolation, which is available at the surface of the Earth, I think our conditions represent about 92 percent of the total possible. But that's only an off the top of the head estimate in that it includes all these things that have been discussed here such as turbidity, forward scattering, water vapor absorption, etc. I have been coming to the conclusion, and this is not a very firm conclusion, that you have to do what Ralph says: You have to have not only pyranometers but you must also have standard solar cells for recording. In fact, the ideal thing would be to have continuous recording of a pyranometer and a solar cell side by side so that if a cloud goes over you see it on both machines simultaneously. But then you really ought to be looking at the spectral data, too. I have come to the conclusion that there are two ways of looking at it. One way is to look at the day by day insolation and pick out for each month the very clearest day that you have and then, if you want let's say a standard year for a given location, you are going to have to construct 30 or 31 day months out of your very best day and establish a standard in this way. I think what you have to do is take both the total insolation and also spectral data day by day and then construct hypothetical years out of these very best days out of each month. I think what will happen is that over a period of 1 year, 3 years, or 5 years your standards will drift for awhile as you get clearer days coming along, but I don't see any other way now of doing what has to be done.

COMMENT: I think the thing we are talking about now is very important. I think the workshop is going to have to address itself to this question. There are generally two kinds of data that we need. Some data from which we can make good efficiency measurements (that is, quote standards) not necessarily representative of what happens in Phoenix or Maine on the seventh of May or whatever. Just a standard method that everybody agrees that that's the number they are going to use as an index of performance of a solar cell. The other kinds of data are those for designing a system for an application; that's when you look at the weather data and get an overall average and figure out what size system is needed. They are different kinds of problems. They may turn out to be different kinds of problems for NOAA, and if you don't keep them separated you aren't going to have a good conversation.

COMMENT: I think to a certain extent people should remember that when you're asking for measurements of a national character you are not asking for measurements for your specific discipline alone. As a member of a calibration laboratory we work with everything from ultraviolet sensitometry of diazo reproduction to measurements of solar furnaces. Basically, the division is one of spectrally selective detectors versus flat plate or black or gray detectors. Jon Geist is here and talked on that a number of times. If you take a look at one of the larger industries that's interested in spectrally

selective detectors it's the photographic industry which is highly competitive. Somehow or other they manage to get their own data.

COMMENT: NOAA for years has been trying to measure solar radiation in many forms but priorities haven't allowed it. We now have a chance to start a very good program and we need, or Dr. White, Head of NOAA, needs, some definite statements from people like you on what we should be providing you. We really haven't gotten this. We could use a statement from you on what you need in terms of numbers and details. For example, at what frequency do you need these data, how often do you need them, over what time period do you need them, and what kind of distribution do you need across the United States? I think if groups, user groups, can come up with this information NOAA can go a long way in providing the data. Not only from NOAA itself, but there are many federal agencies that collect data. Most of them collect the data on a small budget, and some of the agencies don't even know they are actually collecting it because maybe it's only \$10 000 out of a budget of millions. I think if we get requirements out of the user community the federal government can go a long way. It will be surprising I think how many data there actually are lying around on bookshelves in the U. S. Maybe the data are of good quality, and thus you would come up with a fantastic federal network. But I think the requirements have to get into the literature so that people know what they really are and so that people can budget for them.

MODERN RADIOMETRY FOR PHOTOVOLTAIC SOLAR CONVERSION

Jon Geist

National Bureau of Standards
Washington, D. C. 20234

A new approach to spectral radiometry is being developed at NBS. The new approach is based on recent advances in electro-optical technology and may prove useful in radiometry measurement problems arising in photovoltaic solar conversion research and applications. In order to appreciate the significance of these developments, it is useful to review the introduction of new technology into radiometry. For this purpose, it is convenient to concentrate on three optical components that play a key role in spectral radiometry and to distinguish four periods in the history of radiometry as shown in the following table:

Sources	Spectral analyzers	Detectors
Arc		Thermopile Photograph
1860		
Filament* Blackbody* Discharge*	Prism* Grating*	Bolometer Photoconductor* Photoemissive
1910		
	Interference filter	Photovoltaic Photomultiplier* Pneumatic
1960		
Laser LED	Interferometer Acousto-optic	Pyroelectric

This table identifies the period during which the various components were introduced into radiometry rather than the date at which they were invented. For instance, the

Michelson interferometer was invented and used in certain spectroscopic applications long before 1960. However, it was not until the interferometer was combined with the computer that it could be used for radiometry. The asterisks in the table indicate the technology that is the basis for radiometry as currently practiced, particularly in standards work.

Three important points are evident from the table. First, radiometry as presently practiced is based almost entirely on 19th century technology. Second, very little happened in radiometry between 1910 and 1960. Indeed, this second point is one of the explanations for the first point. And finally, most of the developments in radiometry during the period between 1910 and 1960 were associated with detectors. This is at least partially due to the fact that 19th century technology was not able to provide detectors that were accurate, sensitive, and reasonably convenient to use. In fact this very lack of detectors that are both accurate and sensitive is a fundamental premise of the classical (presently accepted) approach to accurate spectral radiometry. As a consequence, the classical approach places an inordinate burden on sources such as lamps and black-bodies, as will be shown later in the paper.

The development of a new approach of spectral radiometry awaited technological advances in three areas. Accurate, sensitive detectors, tunable δ -function (monochromatic, uni-directional, spatially concentrated) sources of sufficient power to be accurately measured with the detectors mentioned previously, and characterizable optical components (particularly spectral analyzers) were needed. Modern silicon photovoltaic detectors (ref. 1) and electrically calibrated pyroelectric detectors (ref. 2) combine to satisfy the first requirement, tunable continuous wave dye lasers (ref. 3) fulfill the second requirement in the visible region of the spectrum, and interference (ref. 4) and acousto-optical (ref. 5) filters satisfy the third.

To demonstrate the new approach, we have measured the spectral irradiance (power per unit area and wavelength) at 602 nanometers from a quartz halogen coiled coil filament lamp that had already been calibrated for spectral irradiance by another group at NBS (ref. 6) using the classical approach. This type of lamp with this type of calibration is the most widely requested radiometric standard available from NBS. The classical approach to this calibration is illustrated in figures 1 and 2.

The new approach (described in more detail in ref. 7) is illustrated in figure 3. The top part of the figure represents the measurement of the spectral response of a silicon photovoltaic detector that is covered by a narrow band pass interference filter. The beam from the dye laser is directed through a wedged beam splitter onto the filtered photodiode F. The first surface reflection from the beam splitter is collected by a monitoring detector M. The current $i(\lambda)$ from the filtered detector and the current $m_p(\lambda)$ from the monitoring detector are both measured as a function of wavelength over the range of the dye laser. The filtered detector is then replaced by an electrically calibrated radiant power meter P which serves as the primary reference. The cur-

rent $m_c(\lambda)$ from the monitoring detector and the power $p(\lambda)$ incident on the power meter are both recorded as functions of λ . If the monitoring detector is linear, or if $m_b(\lambda) = m_c(\lambda)$, then the spectral response of the filtered detector $r(\lambda)$ is given by

$$r(\lambda) = \frac{f(\lambda)}{m_b(\lambda)} \frac{m_c(\lambda)}{p(\lambda)} \quad (1)$$

for $\lambda_1 \leq \lambda \leq \lambda_2$, where λ_1 and λ_2 are, respectively, the lower and upper bounds of the wavelength range through which the dye laser can be tuned. The bottom part of the figure represents the measurement of spectral irradiance $e(\lambda_0)$ at wavelength λ_0 with the filtered detector, which is calculated as

$$e(\lambda_0) = K_0 I \left[A \int_{\lambda_1}^{\lambda_2} r(\lambda) d\lambda \right]^{-1} \quad (2)$$

where K_0 is a correction factor (ref. 7, p. 310) accounting for nonideal behavior of the narrow band-pass filter, I the current from, and A the area of the aperture of the filtered detector when irradiated by the lamp.

The estimated uncertainties of the two approaches are comparable, both about 1 percent, and the results obtained from two independent measurements on each of two different lamps agreed to within 1 percent. A comparison of the two approaches shows that the new approach involves a much shorter measurement chain than the classical approach, and it exemplifies the over dependence of the classical approach on sources such as black bodies and incandescent lamps. Also, possibilities for improved accuracy are higher for the new approach, based as it is on new technology, than for the classical approach, which, of course, is based on mature technology.

It must be emphasized that the new approach is still being developed, and is available, at present, only in the visible region of the spectrum. Future development will include extending the wavelength range with yet to be developed tunable continuous wave lasers or with presently existing tunable pulsed lasers, replacing interference filters with tunable acousto-optic filters, development of new quantum detectors for radiometry, and continued improvement of electrically calibrated pyroelectric detectors.

REFERENCES

1. P. G. Withersell and M. E. Faulhaber, *Appl. Opt.* **9**, 73 (1970).

2. R. J. Phelan and A. R. Cook, Appl. Opt. 12, 2494 (1973); J. Geist and W. R. Blevin, Appl. Opt. 12, 2532 (1973); R. J. Phelan, R. L. Peterson, G. P. Klein, C. A. Hamilton, and G. W. Day, Proc. EOSD Conf., 117 (1973).
3. O. G. Peterson, S. A. Tuccio, and B. B. Snavely, Appl. Phys. Lett. 17, 245 (1970); J. M. Yarborough, Appl. Phys. Lett. 24, 629 (1974).
4. A. F. Turner, J. Phys. 11, 457 (1950); P. H. Lissberger and J. Ring, Optica Acta 2, 45 (1955).
5. S. E. Harris, S. T. K. Nieh, and D. K. Winslow, Appl. Phys. Lett. 15, 325 (1969).
6. W. E. Schneider, R. Stair, and J. K. Jackson, Appl. Opt. 6, 1482 (1967); Unpublished report that accompanies the NBS calibrated lamp standards of spectral irradiance.
7. J. Geist, B. Steiner, R. Schaefer, E. Zalewski, A. Corrons, Appl. Phys. Lett. 26, 309 (1975).

DISCUSSION

Q: What did you say the wavelength range was of the acoustic filter?

A: The acoustic filters have been used up to about 2 microns already (e. g., from about 0.25 to 2) although not with a single filter but with maybe two to cover that range.

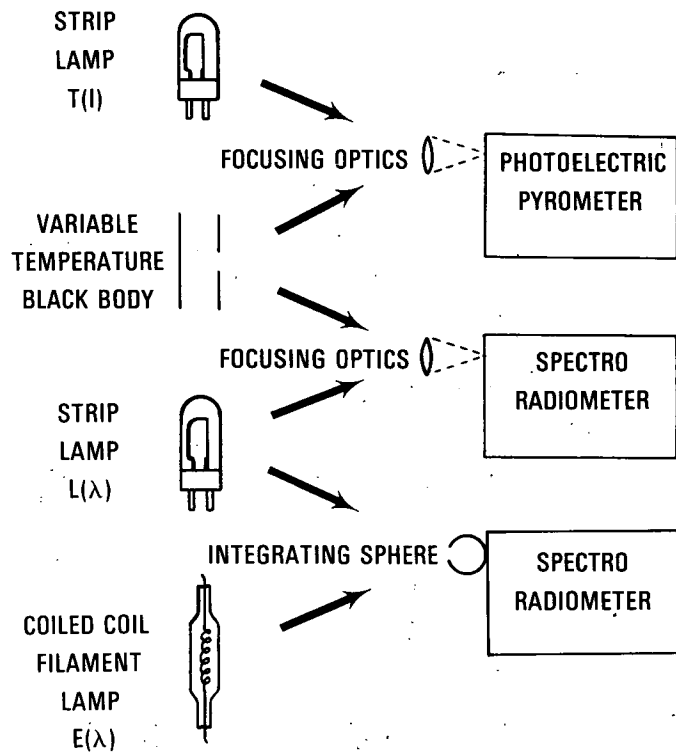


Figure 1. - Classical approach to measuring spectral irradiance from quartz-halogen, coiled-coil filament lamp starting with strip lamp whose brightness temperature at a single wavelength has been measured as function of lamp current.

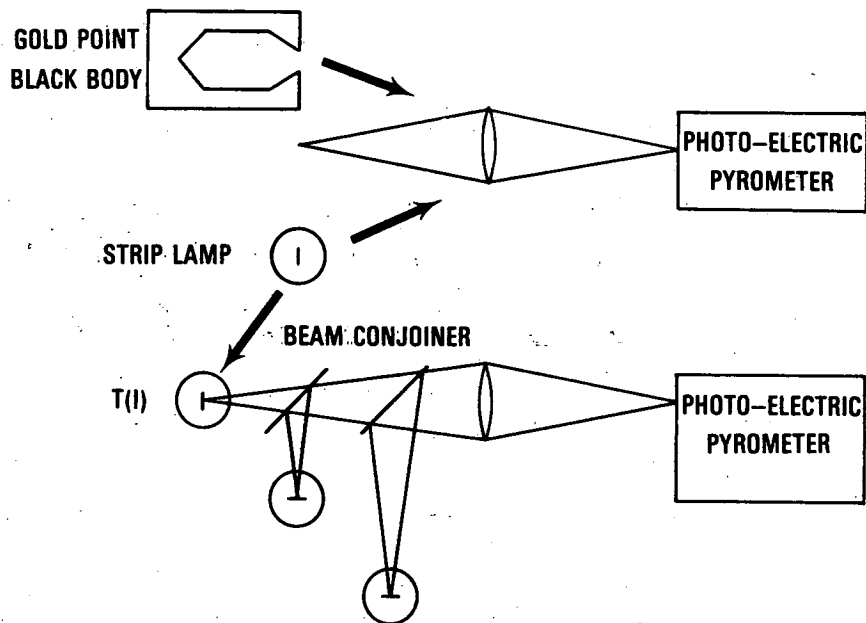


Figure 2 - Classical approach continued: measurement of brightness temperature of a strip lamp as function of lamp current starting with a blackbody at temperature of freezing gold.

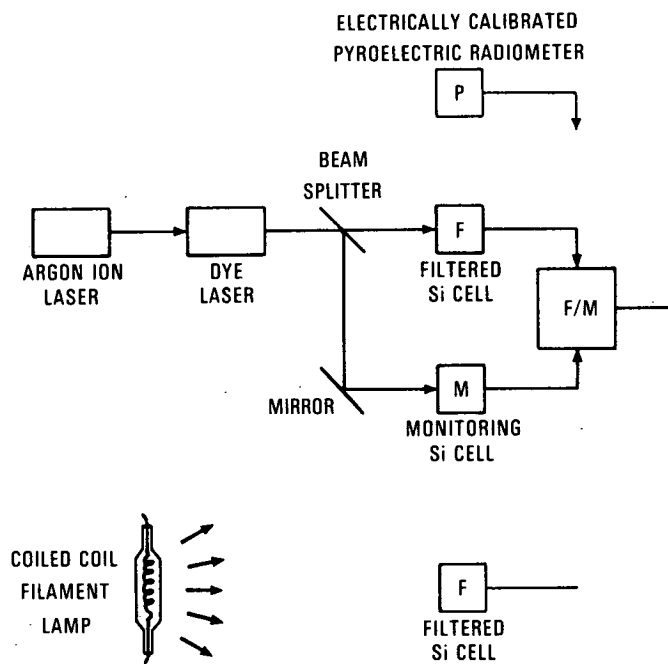


Figure 3. - New approach to measuring spectral irradiance from a quartz-halogen, coiled-coil filament lamp, starting with an electrically calibrated pyroelectric radiometer.

SOLAR SIMULATOR SPECTRAL AND IRRADIANCE DEGRADATION

A. R. Lunde

The Boeing Co.
Seattle, Washington 98124

Measurement techniques of a solar simulator are essential when determining the performance and degradation rate of solar cells. The spectral response of a solar cell covers only a portion of the solar spectrum. For example, the solar cell responds in the spectral range of 0.4 to 1.1 microns. Its output is characteristic of the incident spectrum and total irradiance. It is necessary to reproduce the initial environmental condition in order to determine solar cell performance and degradation rate. Therefore, the total incident energy and the spectral energy in the solar cell region must be known. This paper describes briefly the measured changes of a solar simulator during a solar cell degradation study and discusses how these changes might influence the test results.

TEST ENVIRONMENT

The purpose of the test was to determine the degradation rate of solar cells. The cells were exposed to simulated occultation environment. Periodic solar cell performance was determined by comparison to a standard balloon flown solar cell. The thermal cycle consisted of a 1-hour exposure to the simulated solar beam and 1/2-hour dark cycle. The solar cells were mounted inside a vacuum chamber (see fig. 1) which was maintained at a pressure of 1×10^{-6} torr or lower. The solar cells were surrounded with liquid nitrogen shrouds maintained at 100 K. Thermocouples were attached to the solar cells for temperature indications. During the test the performance of the X-25L solar simulator was monitored. This consisted of measuring the spectral energy distribution from 0.25 to 2.50 microns with a Beckman spectroradiometer. The solar irradiance was set daily during the dark cycle by rotating the simulator to illuminate a standard cell and adjusting the lamp power to the same indicated solar cell irradiance. The lamp power and total irradiance were also recorded using a TRW differential radiometer.

SOLAR SIMULATOR PERFORMANCE

The performance of the X-25L solar simulator was determined from the spectral energy distribution plots, the total irradiance, and the lamp power. It should be reiterated that the irradiance was set daily by maintaining a constant output from the balloon flown standard solar cell. This would allow the total irradiance to change as the spectral energy distribution was changing due to lamp and mirror degradation. The lamp, collector, and folding mirrors were changed periodically when the lamp power reached the maximum allowable operating level of 4.2 kilowatts.

RESULTS AND CONCLUSIONS

Figure 2 shows the amount of energy contained in the two regions of 0.5 to 0.8 micron and 0.5 to 1.0 micron as functions of number of cycles. This is presented to indicate that the energy contained in the solar cell response region is relatively constant over the test time. The scatter of these data is related to the method of measurement and data reduction. The deviation of the 0.5 to 0.8 micron region was ± 1.07 percent, and the deviation of the 0.5 to 1.0 micron region was ± 1.25 percent from the total irradiance. It is noted that only the last 3000 cycles of data are presented because it was not until this time that all the data were taken and could be presented in a meaningful manner. Presented in the same figure is the lamp degradation rate. It can be seen how the lamp power steadily increased while the spectral energy contained in the specified wavelength bands remained fairly constant. Figure 3 relates the total irradiance change against the number of cycles while the standard solar cell maintained a constant irradiance. A very definite pattern of a decrease in total irradiance is seen as related to solar simulator degradation. Then, after a new lamp, collector, and mirrors were installed the total irradiance would return to the original level. The total irradiance decreased approximately 4 percent between lamp and reflective surface changes. This could result in a temperature drop of 10° F (5.5° C) in the solar cell temperature for a cell initially operating at a temperature of 140° F (60° C). The important factor to consider is that a decrease in total irradiance will reduce the operating temperature of the test cells. This in turn will result in increased efficiency of the cells (ref. 1). The net effect is a decrease in the degradation rate of the solar cells over the operational life of a lamp, collector, and folding mirror. It also points out the need for control of repeatability of refurbishment of the solar simulator reflective optics.

In summary, the characteristic performance of a solar simulator is essential in determining the state of performance of the solar cells. It is suggested that total irradiance, spectral irradiance in the response region of the standard solar cell, and temperature of the test cells be known to adequately evaluate the solar cell performance.

REFERENCES

1. Ralph, E. L.: Performance of Very Thin Silicon Solar Cells. Presented at Sixth Photovoltaic Specialists Conference, March 1967.

DISCUSSION

Q: I am afraid I did not understand the last figure. Could you explain more what the differences are between the irradiance that was held constant and the one being plotted?

A: The solar simulator irradiance was set by turning the solar beam on to a balloon flown standard solar cell and maintaining the cell output at a constant value, by varying the power of the lamp. There was a certain amount of degradation of the reflective optics and the lamp. At the same time we would also take readings of the total irradiance. This is done with a total radiometer that looks over the entire spectrum. The total irradiance was always decreasing with time to a point where after the lamp power reached 4.2 kilowatts, which is our limit, we would have to change the lamp and put in refurbished optics. At that time we would return to a different irradiance level. So the total irradiance was continuously changing while we were maintaining a constant irradiance as seen by a solar cell. The fluctuation at this time is about 4 percent while earlier in the program we had as much as a 10-percent fluctuation.

Q: Are solar cells reversible? When the temperature changes the sensitivity changes, is that correct?

A: Yes.

Q: Then, if the temperature comes back again does the sensitivity return to the original sensitivity?

A: I don't claim to be a solar cell expert, but if the cell isn't degraded any I think it would. However, solar cells do degrade so it depends on how long its been exposed and to what its been exposed.

COMMENT: I think basically that, once the temperature has gone through its excursion and comes back to 25^o C, the sensitivity is exactly the same.

COMMENT: Everybody has been plotting various energies against wavelength and it seems to me that in the energy business we ought to be plotting against photon energy or wave number or something so that the area under the curve makes more sense. Perhaps that's one of the things the group might be thinking about.

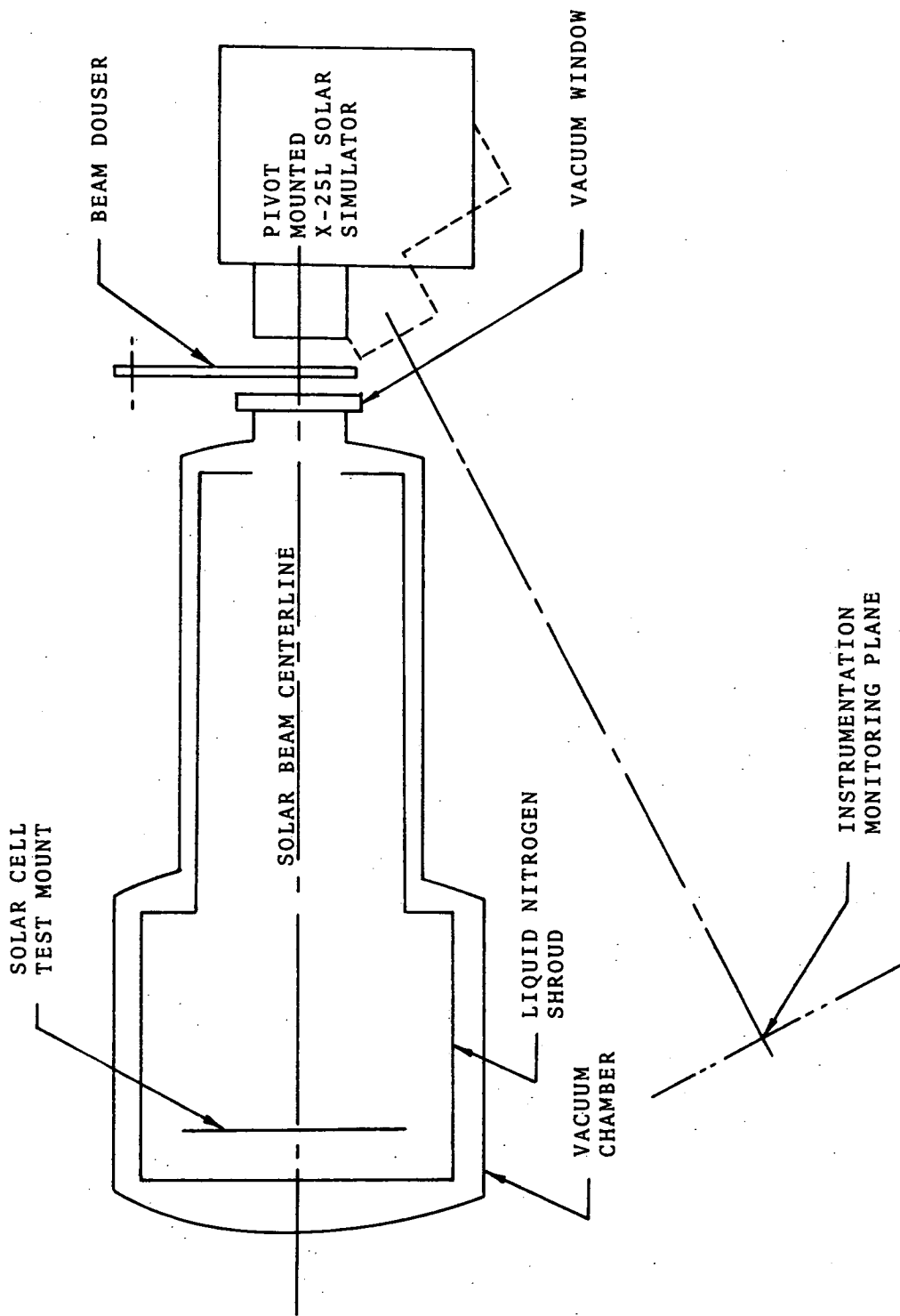


Figure 1. - Schematic - test setup.

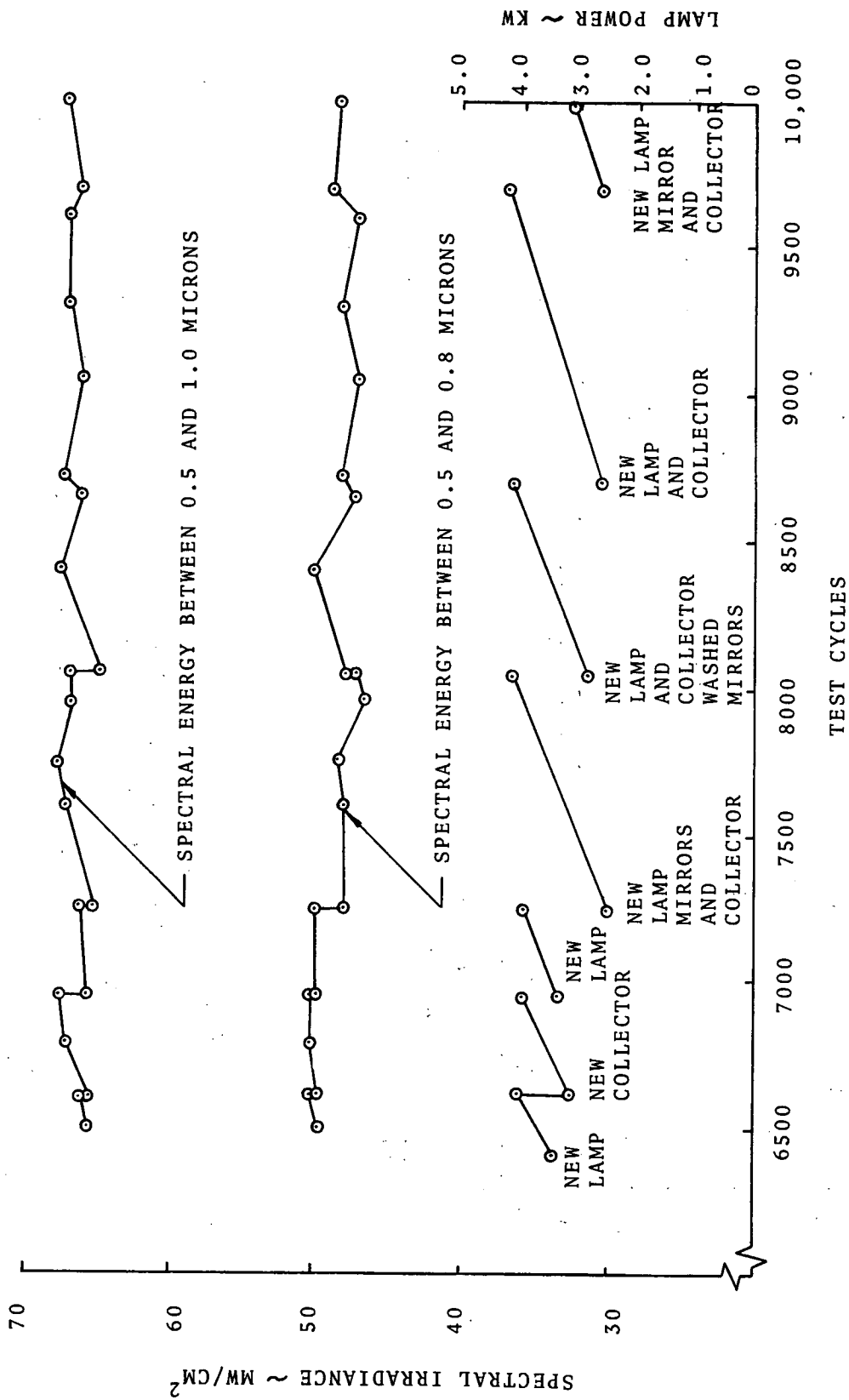


Figure 2. - Spectral irradiance and lamp power.

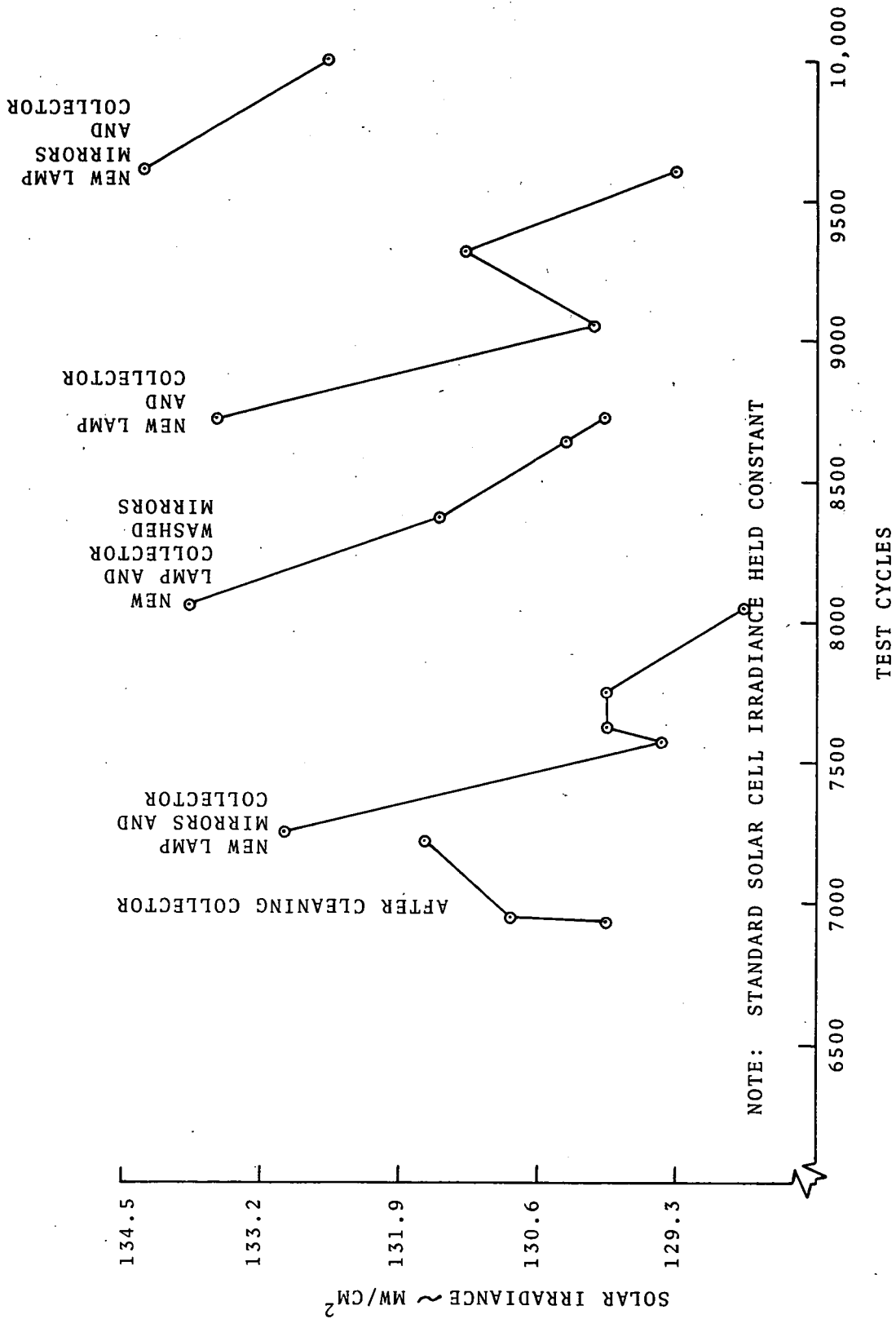


Figure 3. - Total irradiance change.

PROPOSED STANDARD FOR AM1 SUNLIGHT*

Henry Hadley, Jr.

Institute of Energy Conversion
University of Delaware
Newark, Delaware 19711

In order to test the electrical characteristics of solar cells under terrestrial conditions, it is clearly necessary to have a reproducible source of "sunlight." Because of the variability of spectral response between different types of solar cells (for instance Si, Cu_2S -CdS, or GaP-GaAs), nonlinear quenching and enhancement effects as observed in Cu_2S -CdS cells, and variations between individual cells of the same type, this source should simulate terrestrial sunlight both in total power density and spectral distribution as closely as possible.

In designing or evaluating a solar simulator, it is necessary to have a standard definition of the characteristics of terrestrial sunlight as a comparison. However, a precise definition is not possible. Variability in atmospheric conditions, seasonal changes, slant path and surrounding reflecting surfaces all contribute significantly to the variability of terrestrial sunlight. The spectral distribution of extraterrestrial (AM0) sunlight, on the other hand, has been reasonably well defined by various authors, and definitions of the total intensity and spectral distribution may be found in the literature.

Attenuation of this extraterrestrial sunlight through the atmosphere has two main sources: scattering, both molecular (from particles small compared to the wavelength) and Mie or large particle scattering, and absorption by various atomic and molecular transitions.

Atmospheric absorption is primarily due to water vapor, ozone, molecular oxygen, carbon dioxide, nitrogen, and their disassociated constituents. The absorption spectra of all these constituents are all well known. Considerable variations occur in concentration and distribution with altitude resulting in major changes in calculated atmospheric absorption.

Mie scattering is due to dust, water droplets, and other aerosols. Considerable local variations occur which are predominant for lower altitudes; Rayleigh scattering

*Supported by the National Science Foundation, Research Applied to National Needs, under Grant AER72-03489, formerly GI-34872.

dominates when the atmosphere is exceptionally clear.

The necessary data thus exist to permit the calculation of the direct solar radiation under any air mass condition for a given atmospheric composition. Using various atmospheric compositions Gates (ref. 1) has calculated such distributions for a number of air masses from Johnson's AM0 data. Figure 1 shows the mean value atmosphere AM1.0 curve compared to the Johnson AM0 curve (ref. 2).

The effects of the various absorption and scattering mechanisms may be seen. For $\lambda < 0.290$ micron, almost complete absorption results from the ozone and disassociated oxygen (Schumann-Runge bands). The Hartley (0.180 to 0.340 μ) and Huggins (0.320 to 0.360 μ) ozone bands produce structure in the blue. In addition, the weak Chappuis band (0.440 to 0.740 μ) reduces the peak intensity of the AM0 curve. In the red and near infrared, there is considerable structure due primarily to the complex absorption spectra of water vapor. Also, molecular oxygen produces a strong but narrow absorption band at 7596 Å and another at 1.27 microns. Finally, the scattering from aerosols reduces the overall intensity.

Under actual deployment conditions, solar cells will receive not only direct solar radiation but also a significant contribution from diffuse scattered skylight. This additional flux adds considerable energy in the blue region of the spectrum as shown in figure 2 (ref. 3). Addition of this diffuse skylight to the direct radiation produces the global radiation of actual deployment conditions shown in figure 3.

It is proposed that for evaluating solar simulators the characteristics of terrestrial sunlight be as defined by a curve of global radiation calculated in the manner used by Gates from a well defined AM0 spectral distribution and a "standard atmosphere" containing specified amounts of the scattering and absorbing materials. Gates has recommended 1 centimeter precipitable water, 0.35 centimeter per kilometer ozone liquid equivalent, and 200 particles per cubic centimeter aerosol concentration. The AM1.0 global curve for these conditions is shown as figure 3 and has a integrated flux of 91.7 milliwatts per square centimeter. The tabulated energy distribution is given in table I. This definition will have the useful advantage of being easily calculated for the different slant paths (air masses) encountered in actual terrestrial conditions, thus providing references for evaluating solar simulators under a variety of cell deployment conditions.

REFERENCES

1. D. M. Gates, Science, 151, 3710, 523 (1966).
2. F. S. Johnson, J. of Meteorology, 11, 431 (1954).
3. D. Deirmendjian and Z. Sekera, Tellus, 6, 382 (1954).

DISCUSSION

Q: On your last figure, what is your average value for the total insolation?

A: The total insolation depends on the particular standard atmosphere that is chosen. The total insolation for that curve was 91.7 milliwatts per square centimeter. The values of water vapor and so on that you choose for a standard atmosphere can vary the total insolation over 5, 10, or 15 percent. The strongest variations seems to come, according to Gates, from the aerosol concentration and the water vapor equivalent in the atmosphere.

TABLE I - AMI DIRECT AND GLOBAL SPECTRAL DISTRIBUTIONS FOR STANDARD ATMOSPHERE OF 1.0 CENTIMETER H₂O,
0.35 CENTIMETER PER KILOWATT OZONE, AND 200 PARTICLES PER CUBIC CENTIMETER AEROSOL

[Total direct radiant energy, 86.5 mW/cm²; total global radiant energy, 91.7 mW/cm²; W (λ) is intensity in mW/cm²/μ
(values ±1 mW/cm²/μ).]

λ (mμ)	W _D (λ)	W _G (λ)	λ (mμ)	W _D (λ)	W _G (λ)	λ (mμ)	W _D (λ)	W _G (λ)	λ (mμ)	W _D (λ)	W _G (λ)	λ (mμ)	W _D (λ)	W _G (λ)
285	1	12	540	141	152	815	89	89	1090	49	49	1410	1	1
290	2	14	545	142	152	820	86	86	1100	48	48	1420	3	3
295	12	25	550	140	150	830	87	87	1110	35	35	1430	6	6
300	21	35	560	138	147	835	88	88	1120	23	23	1440	7	7
310	28	46	570	137	145	840	87	87	1125	19	19	1450	8	8
320	35	54	580	136	143	845	85	85	1130	18	18	1460	10	10
330	42	65	590	135	142	850	80	80	1135	21	21	1470	10	10
340	55	76	600	134	140	855	70	70	1140	22	22	1480	9	9
345	60	81	610	132	137	860	61	61	1145	21	21	1490	11	11
350	61	88	620	130	135	865	49	49	1150	19	19	1500	14	14
355	62	82	630	127	131	870	50	50	1155	20	20	1510	17	17
360	60	80	640	125	127	875	52	52	1160	22	22	1520	19	19
365	58	77	650	119	122	880	53	53	1165	24	24	1530	20	20
370	59	77	655	114	117	885	50	50	1170	23	23	1540	20	20
375	62	79	660	111	114	890	48	48	1180	29	29	1550	20	20
380	67	83	665	113	115	895	47	47	1190	36	36	1560	19	19
390	73	89	670	114	116	900	48	48	1195	37	37	1570	19	19
400	79	102	675	113	115	905	50	50	1200	36	36	1580	18	18
410	87	111	680	111	113	910	49	49	1210	35	35	1590	18	18
420	98	121	685	109	111	915	38	38	1220	35	35	1600	17	17
430	106	126	690	108	110	920	35	35	1230	33	33	1650	16	16
435	111	131	695	107	108	930	30	30	1240	28	28	1700	15	15
440	112	132	700	108	109	940	31	31	1250	24	24	1750	14	14
445	110	131	705	109	110	950	33	33	1260	24	24	1780	13	13
450	111	132	710	107	108	960	35	35	1270	27	27	1800	12	12
460	119	139	720	97	98	970	38	38	1280	29	29	1810	10	10
470	135	153	730	82	82	980	55	55	1290	32	32	1820	5	5
475	139	157	740	66	66	990	66	66	1300	28	28	1830	1	1
480	141	158	750	62	62	995	66	66	1310	26	26	1840	0	0
485	143	159	760	66	66	1000	65	65	1320	25	25	1850	1	1
490	144	159	770	82	82	1010	60	60	1330	24	24	1875	2	2
495	140	154	775	87	87	1020	56	56	1340	20	20	1900	1	1
500	138	152	780	92	92	1030	54	54	1350	11	11	1920	3	3
505	139	152	785	94	94	1040	51	51	1360	1	1	1940	5	5
510	141	154	790	93	93	1050	52	52	1370	1	1	1960	7	7
515	140	152	795	95	95	1060	52	52	1380	2	2	1980	6	6
520	138	150	800	93	93	1070	50	50	1390	1	1	2000	5	5
530	139	150	810	92	92	1080	48	48	1400	0	0			

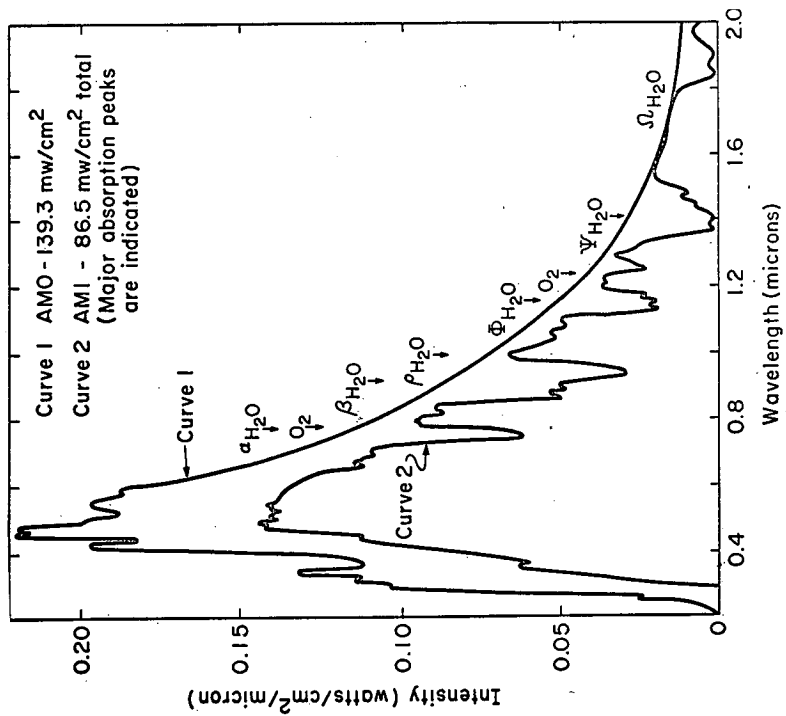


Figure 1.

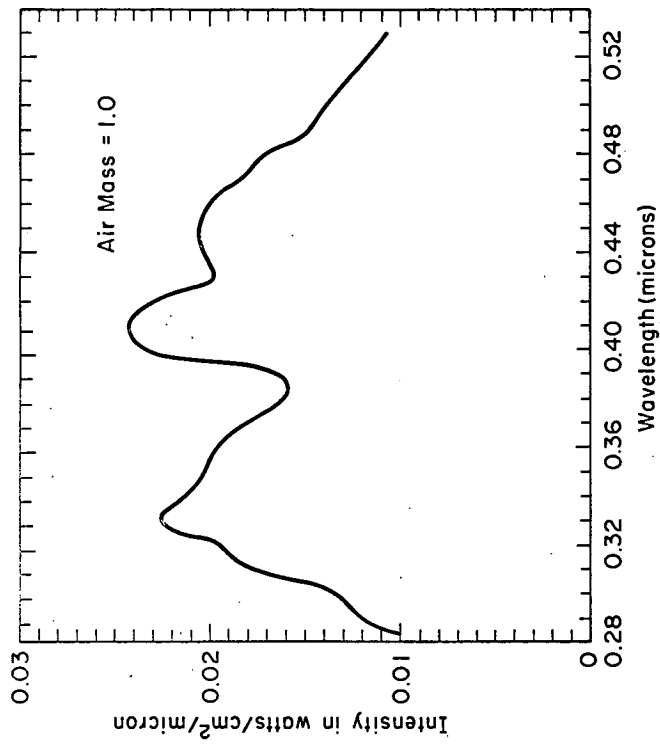


Figure 2.

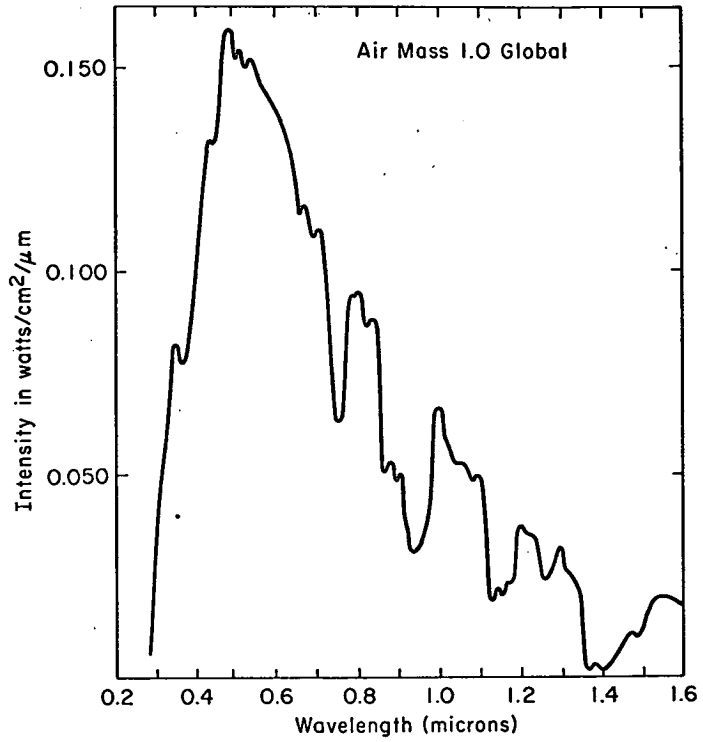


Figure 3.

DETERMINATION OF DIFFUSE RADIATION CHARACTERISTICS

FOR APPLICATION IN SOLAR ENERGY HARVESTING

B. H. Armstrong, J. V. Dave, and P. Halpern

IBM Scientific Center
Palo Alto, California 94304

The absorption and scattering of sunlight by the constituents of the atmosphere results in the attenuation of the direct solar radiation incident at the top of the atmosphere. A good fraction of this energy removed from the direct solar beam reappears in the form of diffuse radiation (or "skylight") in all directions due to the phenomenon of multiple scattering.

For solar energy harvesting, flat-plate collectors mounted in horizontal positions or tilted towards a preferential direction are commonly used. The efficiency of such a collector depends on several factors, for example, spatial and spectral distribution of the diffuse radiation, position of the Sun, time of day, day of year, and geographic latitude of the site. The importance of diffuse radiation to efficient harvesting of solar radiation under turbid atmospheric conditions is well recognized, and the development of collectors which accommodate diffuse radiation has been reported in the literature. However, the detailed characteristics of diffuse radiation are not well known, even though adequate theory now exists for calculating these characteristics. This paper briefly reviews the current solar radiation data and the relevant radiative transfer theory and points out the realistic atmospheric models which can provide the needed description of diffuse radiation.

LIMITATIONS OF CURRENT DIFFUSE RADIATION KNOWLEDGE

The current understanding of diffuse solar radiation is primarily based on the analysis of measurements of the spectrally integrated (wave length region, 0.3 to 5 μm), total (i. e., direct as well as diffuse) insolation made regularly at many weather stations. The instruments used for measuring these quantities are normal incidence pyrheliometer (direct solar energy), hemispherical pyranometer with occulting disk (diffuse sky energy), hemispherical pyranometer (total equals direct plus diffuse energy) and sunshine recorder (total sunshine hours per day).

Because of sparseness of normal incidence pyrheliometer data, several investigators have used hemispherical pyranometer and/or sunshine recorder data for obtaining empirical relationships between direct and diffuse energy passing through a horizontal surface (ref. 1). One major assumption common to developing such empirical relationships of that one-half of the energy scattered by the atmosphere is returned to the Earth in the form of skylight and the remaining half is reflected back to space. A number of other assumptions and simplifications have been made. We will first list the problems connected with the currently accepted empirical relationships and measurements and point out how the situation can be improved by modeling:

(1) Mechanical restrictions of measuring instruments (e. g., field of view and occlusion of solar disk) preclude an accurate separation of direct and diffuse components.

(2) Insolation may be different at measurement and at collector sites.

(3) Common assumptions that one-half the scattered radiation returns to Earth as skylight and that it is isotropically distributed are not valid under many situations of interest.

(4) The effect of surface albedo on the radiation received by inclined collectors is usually neglected.

(5) The spectral response of measuring instruments is usually different from that of solar collectors.

(6) The ratio of diffuse to total radiation received at the surface depend on several variable parameters which are difficult or impractical to measure such as atmospheric composition, cloudiness, and reflectivity of the underlying surface.

(7) The meteorological insolation data base is of limited reliability.

ROLE OF BASIC RADIATIVE TRANSFER SIMULATION

IN SOLAR ENERGY EXPLOITATION

An alternate approach for obtaining a good understanding of various characteristics of the diffuse component of solar energy received at the surface is by numerical simulation of the transfer of solar radiation through realistic models of the terrestrial atmosphere by direct computation from the equation of radiative transfer.

We have recently developed and tested very efficient and accurate methods for obtaining direct numerical solutions to the radiative transfer equation for the Earth's atmosphere (refs. 2 and 3). These methods can be employed straightforwardly to remove the limitations listed previously and to provide additional design parameters not now available. In particular, with reference to the critical points listed previously, such modeling can offer the following improvements.

(1) In order to estimate the importance of circumsolar radiation on the operation of solar energy conversion systems, information is needed on the gradient of sky brightness from the edge of the solar disk out to about 5° at least, and further would be desirable. This quantity, while very difficult to measure, can be readily calculated.

(2) Calculations can be carried out for models with different sets of meteorological parameters characteristic of the different locations (e. g., Linke's turbidity factor and horizontal visibility). The model results can then be used to derive empirical relationships between energy passing through a tilted surface and some of the standard meteorological parameters.

(3) The models we have developed calculate both the intensity of the skylight and its spectral distribution and include the effects of surface albedo. Further development is needed only to make these models simple and cheaper to operate.

(4) As will be described presently, we have been able to include these variable parameters (atmospheric composition, cloudiness, and ground reflectivity) in our models and demonstrate their effects.

(5) The model calculations can be used to enhance the reliability and extend the scope of present methods of analyzing meteorological insolation data. As indicated previously, the differences in geographic location can also be accounted for.

In addition to these points, such an investigation can also provide the distribution of radiation at intermediate levels during scattered-cloud conditions. After combining such information with bi-directional reflectivity of scattered clouds, it would be possible to simulate the effect of diffuse radiation in the presence of scattered clouds.

REALISTIC RADIATION TRANSFER MODELS FOR SOLAR ENERGY SIMULATION

We have recently succeeded in applying the classical spherical harmonics expansion method to the direct solution of the radiative transfer equation. Since this has yielded much more efficient and economical solutions than heretofore, it is now feasible to perform model calculations that were not previously practical.

This spherical harmonics methods has been used to perform the most extensive investigation to-date of the effect of cloudiness on the transfer of solar energy through realistic models of the Earth's atmosphere (ref. 4). For this purpose, the solar spectrum in the 0.285 to 2.5 micrometers interval was subdivided into 83 subintervals of unequal widths for meaningful simulation of the absorption characteristics of carbon dioxide, water vapor, and oxygen (O_2 and O_3). Height distributions of water vapor and ozone as used in this particular investigation are shown in figure 1. They correspond to average, midlatitude summer conditions. Total amounts of ozone and water vapor

in a vertical column of 1 square meter cross section are 0.318 atm-cm, and 2.93 gm-cm⁻², respectively. Two height distributions of aerosol particles (viz. "Average" and "Heavy" with 19.7 and 82.3 million particles in a vertical column of 1 cm² cross-section, respectively) were used for this work. The size distribution of these aerosols is a modified gamma function commonly referred to in the atmospheric aerosol literature as Haze L, and it corresponds to typical distributions observed in the lower troposphere over large continental areas. The data discussed in this paragraph were used to develop eight models as listed in table I.

Results of the diffuse and direct energy emerging at the bottom of various atmospheric models (tables 2 and 3 of ref. 4) are re-analyzed and presented in figure 2 for ready reference. In this diagram, we have shown the variations (as a function of the solar zenith angle) of the fraction of the diffuse component in total solar energy passing through a horizontal surface at the bottom of the atmosphere. The results presented in figure 2 are for the case when the atmospheric model under investigation rests on a perfectly absorbing surface. Similar curves for the cases where the underlying surface isotropically reflects a fraction R of the total energy incident upon it (Lambert's law of reflection) can be obtained by making use of the data provided in table 6 and figure 13 of reference 4. In general, the value of this fraction can be expected to increase with R . However, this is a second-order effect for horizontal surfaces.

From the results presented in figure 2 we can see that the contribution due to the diffuse radiation increases rapidly with increase in the solar zenith angle for all models. It also increases with the dust content or turbidity of the atmosphere (model A or B, to C, to D). The presence of even a weak absorption by aerosol particles results in a small decrease in the contribution of the diffuse component (e. g., model D to D1). On the other hand, as would be expected, the presence of a stratus cloud layer of moderate thickness leads to a very large increase (models C1-ST and D1-ST) in the values of this ratio.

As mentioned earlier, results presented in figure 2 are for the solar energy integrated over the spectral region 0.28 to 2.5 micrometers. In reference 5 we have also shown that the ratio of diffuse to direct radiation is also strongly dependent on the wavelength of radiation. Thus, the contribution due to diffuse radiation is bound to be different for solar energy harvesting systems with different spectral responses and for illumination engineering applications.

REFERENCES

1. B. Y. H. Liu and R. C. Jordan, *Solar Energy* 4, 1 (1960). See also R. C. Jordan, ed., "Low Temperature Engineering Application of Solar Energy," Report published by American Society of Heating, Refrigerating and Air Conditioning Engineers, Inc., 345 E. 47th St., New York, N. Y. 20027 (1967).
2. J. V. Dave and J. Canosa, *J. Atmos. Sci.* 31, 1089 (1974).
3. J. V. Dave, "A Direct Solution of the Spherical Harmonics Approximation to Radiative Transfer Equation for an Arbitrary Solar Elevation, Part I: Theory; and Part II: Results," Reports published by IBM Scientific Center, Palo Alto, CA 94304, Nos. G320-3325 and G320-3327 (1974 and 1975).
4. J. V. Dave and N. Braslau, "Effect of Cloudiness on the Transfer of Solar Energy Through Realistic Model Atmospheres," Report published by IBM T. J. Watson Research Center, Yorktown Heights, N. Y., No. RC4869 (1974).
5. P. Halpern, J. V. Dave, and N. Braslau, *Science*, 186, 1204 (1974).

DISCUSSION

- Q: How many of the curves you have shown are analytical data and what correlation is there with experimental data? How sensitive is this to the shape of the aerosol, and do you worry if its cylindrical or spherical? Is your model predicted on what you can actually solve mathematically or from the real world model of the aerosols?
- A: I think, as everybody who has studied radiative transfer in great detail knows most of the work we deal with is for spherical particles. Since the original work was done by me, we deal with spherical particles. We have not dealt with nonspherical particles. I don't remember some of the other questions.
- Q: About 2 years ago people were coming up with cylindrical models; the question remains of how valid all these results were. Is there any correlation between the real world and some of the analytical models which are based on what you can solve mathematically?
- A: I think that's one of the reasons why I am here today. I am not aware of the detailed observations that are necessary to validate this type of model and I welcome certainly any information pertaining to that. I had not validated this simulation against observation simply because of time. Also, I am not aware of the detailed observations of the meteorological data that are necessary - for example, the vertical variations of the water vapor or the vertical variations of the aerosols, the size distribution, refractive index, etc. So I welcome that information. To answer

your question how realistic the model is, I think that in this case we try to be as realistic as possible in terms of the latest approaches. We have put in a very detailed spectral distribution in terms of breaking up the solar spectrum, we do consider multiple scattering, and we have done considerable work in varying the refractory index. Also, we have done other work on changing the size distribution and in putting in clouds.

Q: Can you indicate how sensitive your results are to these various parameters?

A: Yes. From what we have done it seems obvious that the clouds are the most sensitive parameter in this particular model. I think that has been borne out also by some of the observations that I have seen. For example, Dr. Peterson has presented in his observations that clouds apparently are the most sensitive to this particular model. The second most important factor, if a cloud is not there, is the imaginary portion of the refractory index; that is, how much energy is absorbed by the aerosol itself is the prime factor. So if you talk about a cloudless atmosphere then the aerosol parameter which is the most important is the imaginary portion of the refractory index or the absorptivity capacity of the aerosol itself. Going down from there it probably will have to do with the vertical distribution and the sizes but I think that the aerosol in general is the one we have to look out for.

COMMENT: Well, first I would like to offer some data on diffuse, direct, and total insolation and maybe we could get together and compare the model versus the measured values. We make fairly routine measurements at Waterton of diffuse, direct and total insolation. We tried to use some of these models, not your particular models, but models by Dr. Turner of Willow Run and Dr. Frazer of Goddard. We tried to use some of these models on Skylab and take out atmospheric effects and at the same time measure the atmospheric effects on the ground. One of the variables we had a real problem with was the ground albedo. In your curve the albedo was zero.

A: That's right.

Q: Since the ground albedo affects the parameters, then the question is what is the ground albedo?

A: I might just say that I unfortunately did not bring along the amount of output we have for different reflectivities. But, your point is very well taken that the ground albedo is a very important parameter and we did run cases where we do have albedo varying from 0.1 out to 0.8.

Q: It seems to me that a vital factor in any comparison which doesn't show in your last set of results is not the fraction but the actual amount of energy that's transmitted. For instance, the curve that you had as the highest will undoubtedly end up as the lowest on that basis and that's the way the comparison I think will have to be made.

A: Since I am a meteorologist and come from a little different discipline and I will have to convert to the quantities that are of interest here. That's one of the reasons why I am here.

TABLE I - ATMOSPHERIC MODELS

Model	Gaseous absorption	Aerosols		Stratus cloud layer	
		Height distribution	Refractive index		
A	No	No	-----	No	
B	Yes	No	-----	↓	
C	↓	Average	1.5 to 0.0i		
D		Heavy	1.5 to .0i		
C1		Average	1.5 to .01i		
D1		Heavy	1.5 to .01i		
C1-ST		Average	1.5 to .01i		Yes
D1-ST		Heavy	1.5 to .01i		Yes

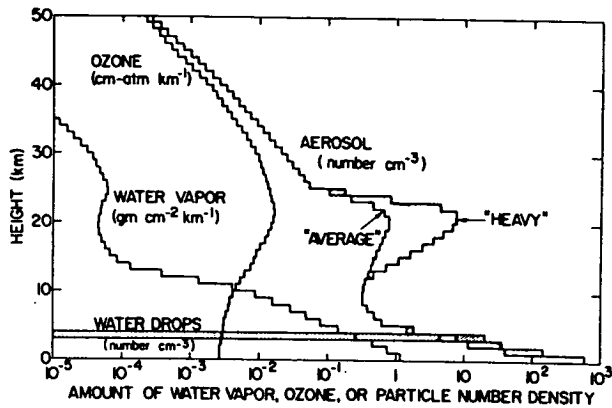


Figure 1. - Variations of water vapor concentration ($\text{gm cm}^{-2} \text{km}^{-1}$), ozone concentration (cm-atm km^{-1}), aerosol number density (number of particles per cc), and water-drops per cc) as function of height as used by Dave and Bralau (1974) in their work.

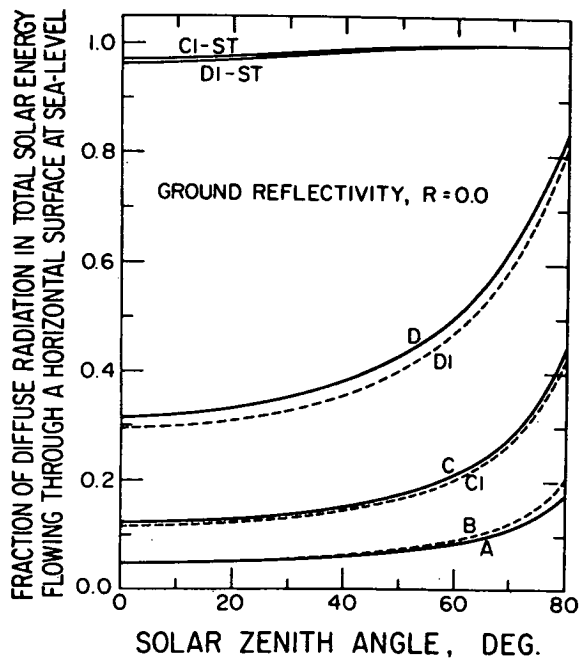


Figure 2. - Variations, as function of solar zenith angle, of the fraction of diffuse component in total solar energy passing through horizontal surface at sea level. Surface underlying atmosphere assumed to be perfect absorber. Results for atmospheric models described in table I.

LOW COST, LARGE AREA SOLAR SIMULATION

Vincent DeLeo

Spectrolab, Inc.

Spectrolab, Inc., has been the world's leading manufacturer of solar simulators for almost 15 years. Most of our people have devoted a major portion of their working life to designing and building solar simulators. Solar simulators are not a side line with us. They are a quality product, one in which we take great pride. We are specialists, and our products are acknowledged for their quality. We have profited from our early experience, both good and bad. We are proud to offer our system to you. It may be the finest system we have ever built.

Over the years, many major companies, including RCA and Honeywell, have built solar simulators, but for one reason or another have dropped out of the field. In the future, when you wish to modify the SPECTROSUN pulsed simulator to meet the constantly changing, more stringent test requirements, we will continue to be available to assist you.

The key to our pulsed system is the completely digital data acquisition and processing system that provides accurate, corrected data within seconds after the pulse. The data consists of up to 50 data points that are digitally printed out and drawn as a well-defined I-V curve after a single pulse. The data are extremely accurate and repeatable. The system is simple, versatile, and automated. It was designed to be a reliable testing tool. Its time-saving features reduce operating costs. One pulse is required to produce the entire I-V curve.

The performance of the illuminator is outstanding in the two most important parameters, spectral match and test plane uniformity of irradiance. The RAE in Farnborough, England, our first customer, estimates that the most pessimistic error in Skynet panel output, due to the difference in simulated and AM0 spectrum, will be less than 1.0 percent. The nonuniformity of irradiance produced by that system was ± 0.4 percent or better over a 2.5-meter diameter and less than ± 2.0 percent over a 5.0-meter diameter.

The data have been proven to be repeatable from pulse to pulse over many months of testing at RAE, BAC, NASA Goddard Space Flight Center, and under heavy use at Spectrolab. Data from one SPECTROSUN LAPSS correlates well with that from another. It is becoming the standard of the industry.

Since the spectral emission is rich in the ultraviolet region between 0.3 and 0.6 micron, the system is usable for testing the new, high efficiency solar cells, which have expanded response in this region.

The remaining significant consideration is safety. In systems such as these, unusual safety precautions must be taken. Ordinary interlocks, capacitor discharge circuits, and grounding may not be adequate. The stored capacitance of a pulsed system can be as much as 25 000 joules. Spectrolab has taken extreme precautionary methods to ensure test personnel safety.

In addition to providing normal interlocks, capacitor discharge circuits, and grounding, the energy storage capacitors are only charged at the initiation of the pulse. At that point, the pulse is automatically flashed within seconds or aborted by actuation of the abort circuit. Since only one pulse is necessary to complete the test, the hazardous condition exists for only a very short time.

The large area pulsed solar simulator system consists of two major subsystems, the pulse illuminator system and the data acquisition and processing system. A block diagram of the data acquisition and processing system is shown in figure 1.

The primary function of the pulse illuminator system is to irradiate the solar panel with simulated solar radiation. Its major components consist of a pulse forming network (PFN) assembly and an illuminator assembly. Within the PFN assembly is a high-voltage power supply and a sophisticated charge sensing device, which determines the exact point at which the energy in the PFN should be discharged. The illuminator assembly, or lamp housing, contains the two xenon flash lamps and the lamp igniter, as well as any auxiliary optics necessary to meet the desired performance levels (see fig. 2).

The other major subsystem of this simulator is the data acquisition and processing system (see fig. 3). This system, synchronized with the operation of the pulsed simulator, measures panel I-V performance characteristics, performs an analog to digital conversion on all data, stores the digital information, provides mathematical corrections, and prints uncorrected and/or corrected panel I-V characteristics. Major components of this system include a standard cell (provided by the user), an electronic load, digital data processing equipment, and a digital X-Y plotter.

The SPECTROSUN LAPSS is the finest system of its type ever made. This is true, whether you wish to consider the quality of illuminator irradiance, the ease of operation, or accuracy of the data produced.

DISCUSSION

Q: What's the cost of this low-cost system?

A: For a 15-foot-diameter beam you can do it for, let's say \$70 000. By comparison,

it would cost approximately a million dollars to do the same job for the same quality with a continuous system.

Q: You say you generate the I-V curve by shaping the pulse. Do you do this by shaping the intensity of the light pulse or by sweeping the load bank during the pulse?

A: By shaping the intensity of the light pulse a bank of capacitors.

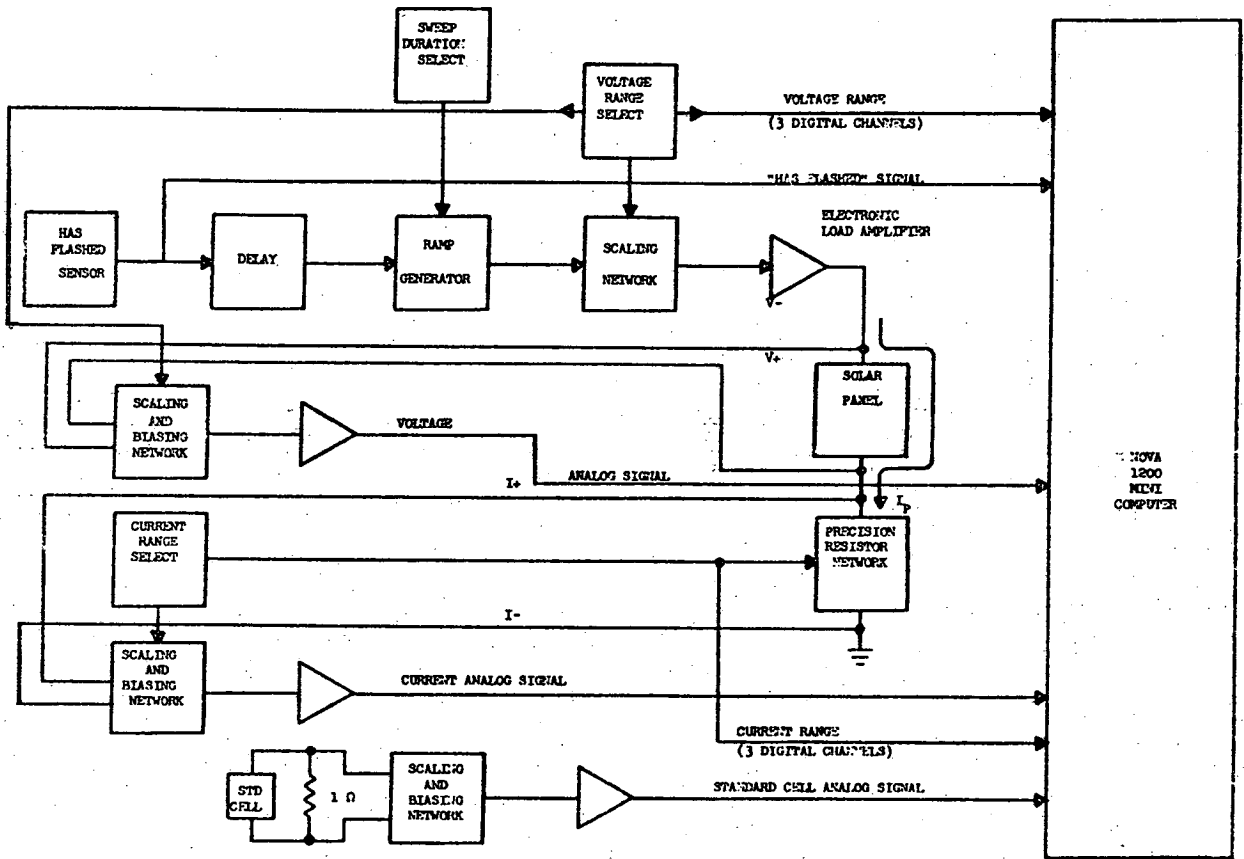
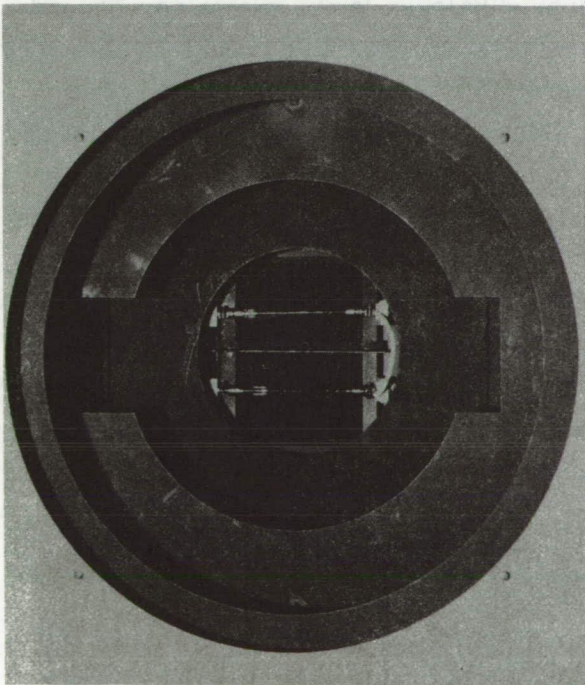
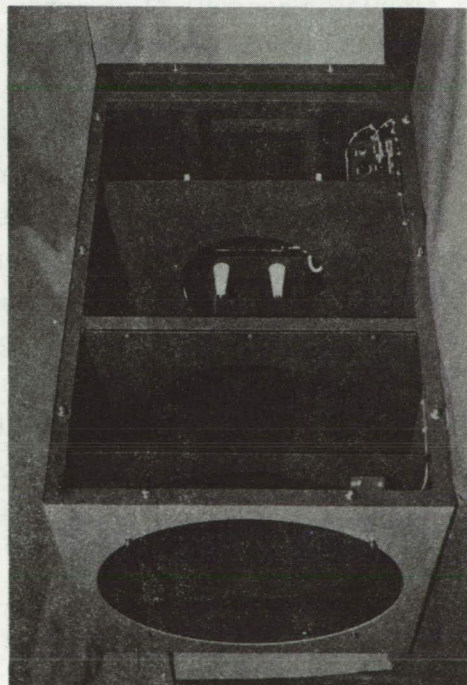


Figure 1. - Electronic load block diagram.



FRONT VIEW



SIDE VIEW

Figure 2. - Illuminator assembly.

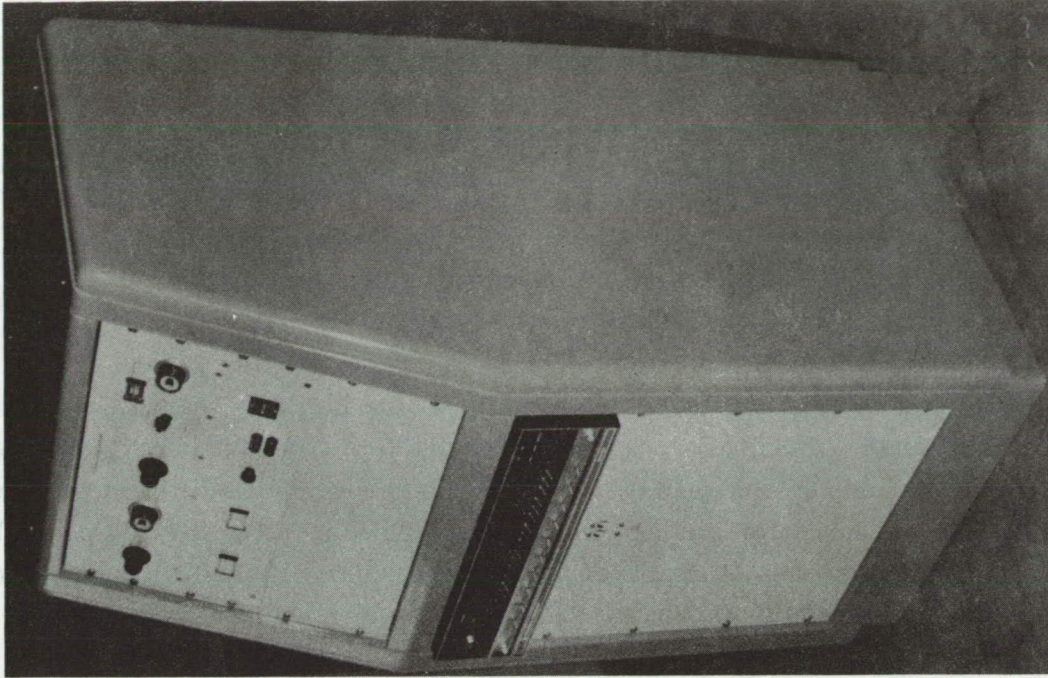


Figure 3. - Control console.

LOW COST, AM2 SIMULATOR

Henry Curtis

NASA Lewis Research Center
Cleveland, Ohio 44135

A low cost, AM2 solar simulator is in operation at the Lewis Research Center. It is used to test flat plate collectors for terrestrial utilization of solar energy. The design of the simulator and performance of a small prototype have already been reported (ref. 1). Although the simulator was designed to test flat collectors, it could possibly be modified for the continuous testing of large arrays of solar cells. This paper gives a brief description of the simulator and also presents its performance characteristics such as irradiance level, collimation angle, and spectral distribution of irradiance.

DESCRIPTION OF SIMULATOR

The simulator consists of an array of 143 quartz-halogen lamps with a corresponding array of 143 plastic Fresnel lenses. This provides an irradiated area 1.2 meters by 1.2 meters (4 ft by 4 ft) at a distance of 4.6 meters (15 ft) from the simulator. The lamps are General Electric model ELH rated at 300 watts - 120 volts. They consist of a quartz halogen bulb with tungsten filament set in an ellipsoidal reflector. The reflector has a dichoric coating which reflects the visible and transmits a large portion of the infrared. This reduces the infrared content of the output beam.

The lenses are plastic Fresnel lenses, grooved at 39.4 lines per centimeter (100 lines/in.). They are cut into hexagons, 15 centimeters (6 in.) across the flats. The lenses are purchased as squares but are easily cut. The combination of one lamp and one lens is the basic building block for the simulator. A simulator can be built to irradiate the desired test area by placing a number of lamp-lens combinations in an array.

Figure 1 shows a cutaway view of the simulator. The square front section is covered with the 143 hexagonal lenses. A plate holding the 143 lamps is 28 centimeters (11 in.) behind the lenses. The optical axis of each lamp is coincident with that of its respective lens. Forced air cooling of the lamp bases is provided by an exhaustor motor, with the direction of the cooling air indicated by the arrows in figure 1.

SIMULATOR PERFORMANCE

Figure 2 is a plot of average total irradiance as function of lamp voltage for the simulator. The irradiance ranges from 61 to 105 milliwatts per square centimeter as the voltage varies from 90 to 114 volts. The AM2 level of 75.7 milliwatts per square centimeter is at approximately 100 volts.

The distribution of total irradiance in the test plane is shown in figure 3. Since the area of the detector is such a small percentage of the area of the test plane (0.03 percent), we averaged four detector readings to obtain the average irradiance in larger area increments. The test plane is therefore divided into 64 equal squares each 15 centimeters (6 in.) on a side. The average irradiance in each square is given in milliwatts per square centimeter. The overall average irradiance during the distribution measurement was 76.2 milliwatts per square centimeter. In figure 3, the areas which are more than ± 10 percent from the average irradiance are marked. Note that only 5 percent of the total area is outside this number.

The spectral distribution of the simulator at 101 volts is given in figure 4. Also plotted in figure 4 is the AM2 spectral distribution. Both curves are normalized to a total irradiance of 75.7 milliwatts per square centimeter for comparison purposes. The simulator gives a fairly good match to the AM2 spectrum. The main reason for the good agreement is the reduction of the tungsten lamp's infrared output by the dichroic coating on the lamp reflector.

The simulator beam subtense angle as measured by the change in total irradiance with various aperture sizes is shown in figure 5. The irradiance drops to 95 percent of the maximum value at approximately 12° , thus defining the subtense angle. This implies that 95 percent of the incident irradiance is within a 12° cone centered on the normal to the test plane, or within $\pm 6^\circ$ of the normal.

REFERENCE

1. Yass, K.; and Curtis, H. B.: Low Cost, Air Mass 2 Solar Simulator. NASA TM X-3059, 1974.

DISCUSSION

Q: When you measured your spectral distribution, did you do this near the beginning of the lifetime of the lamps, and if so, did you check near the end of the lifetime of the lamps?

- A: It was very near the beginning of the lifetime of the lamps and 5 to 10 hours into it. That question has arisen in the past, and we do not measure the spectral distribution of the simulator per se over a period of time. However, we ran a couple lamps for 51 hours and measured the spectral distribution every 8 hours. I noticed no discernible change.
- Q: Was the choice of AM2 for your simulator predicated on what you could achieve or your assessment of what would be a more realistic choice?
- A: The choice of AM2 was chosen by the people who are in the business of testing flat plate collectors. We are in the instrumentation area, and the people in the solar collector business came to us. They said they would like a simulator to simulate AM2 conditions. The total irradiance does go well beyond 100 milliwatts per square centimeter.
- Q: Related to that, is this based on the fact that the integrated radiation under a curve has more time in the AM2 region?
- A: I really can't answer that.
- Q: There seems to be a very interesting tradeoff between the short wavelengths and the long wavelengths so you get the same efficiency for the solar cell. I think that must be dependent on the distribution of response in the silicon cell. I was wondering if you had done any sensitivity analysis to changes in distribution from the typical value you used?
- A: No, I have just used one spectral response for silicon solar cells which Henry gave me about 5 years ago and it's zero at 0.35 and goes up slowly from there. This probably does not include the newer cells which have a much better blue response.
- Q: Can you explain the variation in efficiency with voltage on the lamps? Is there an obvious reason for that?
- A: As far as the 5 percent, this is a calculated change; however, we measured the spectral distribution from 90 to 115 volts, and we get that much change. The spectral distribution does change that much. As you increase the voltage of a lamp from 90 to 115 volts you are running obviously at a higher temperature. Thus, in a blackbody consideration, you are pushing energy from the infrared into the visible and that's what's going on.
- Q: What is the cost of this system?
- A: The lamps were about \$5.40 a piece, the lenses about \$7.00, and the holders about \$0.57 (143 of those). The structure was built on one or two outside contracts which brought the total to about \$700.00 per square foot. Therefore, the cost is \$700.00 times 16 square feet. That does not include a couple of additional features such as an automatic shutoff which turns the lamps off slowly instead of immediately and a control device to change the tilt angle. If you add a few items like that, it

goes up to about \$900.00 per square foot. You could build it yourself. Instead of using aluminum, you could make it out of sheet metal, plywood, and 2 by 4's especially if you are making it small. The cost would then be considerably less. I was talking to one gentleman and he built a much smaller one very recently. I think he said eighteen lamps and his price was \$13.00 per lamp. The GSA price 2 years ago is a lot different from an individual buying a few lamps today. I haven't looked into that.

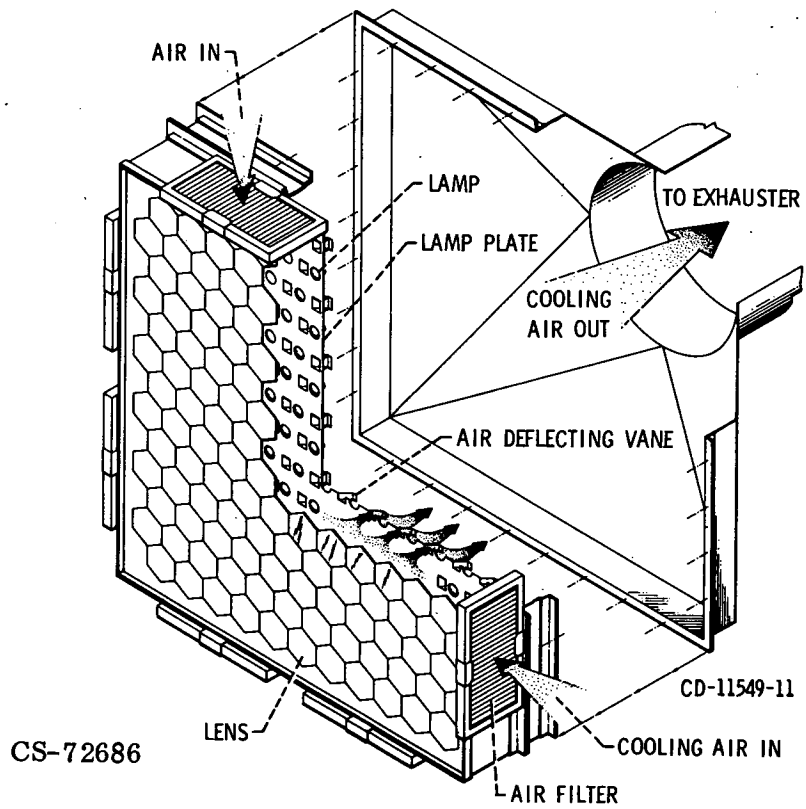


Figure 1 - Solar simulator cutaway view.

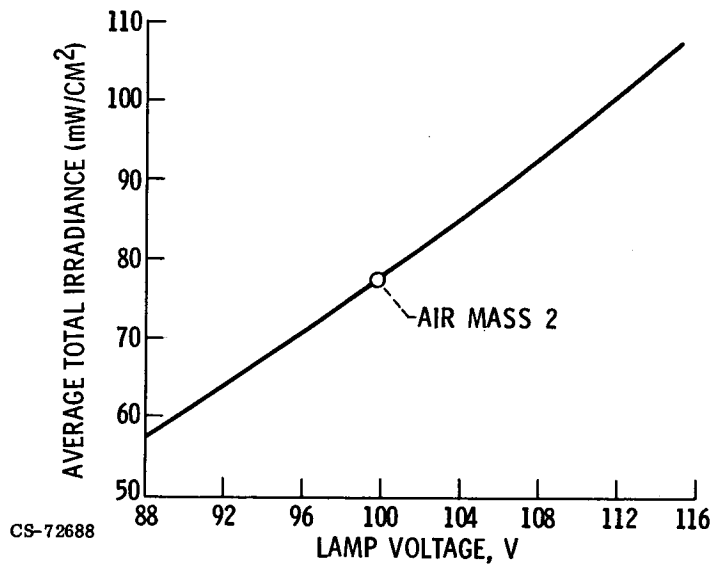


Figure 2 - Average total irradiance as function of lamp voltage.

			← 15 CM →					
	69.1	68.9	72.4	74.2	73.7	73.0	74.1	74.2
	73.4	74.0	78.5	82.3	82.1	79.2	78.3	77.8
	74.6	76.5	79.3	81.2	80.0	78.1	79.6	78.9
↑ 15 CM ↓	73.7	74.9	75.1	73.8	73.2	75.0	80.8	81.3
	72.5	71.3	69.2	67.9	69.8	74.3	80.4	83.3
	75.2	72.0	70.1	70.9	73.1	75.8	78.0	79.8
	75.3	71.9	72.4	76.5	81.2	81.3	79.0	79.0
	74.1	72.9	74.4	80.7	87.2	86.2	81.8	79.7

Figure 3 - Distribution of total irradiance. CS-72687

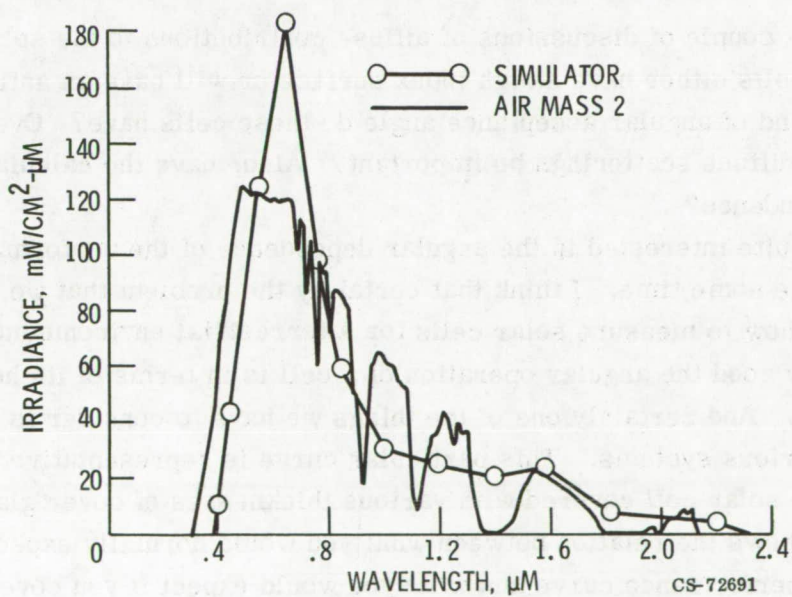


Figure 4 - Variation of spectral irradiance with wavelength. CS-72691

GENERAL DISCUSSION FOLLOWING SESSION II

- Q:** Your variations in efficiency with lamp voltage seem to be at variance with things that Henry Brandhorst was telling us, have you two had a chance to get together?
- A:** Yes, we've gotten together several time and well, it's different things I'm comparing it against three different measured spectral irradiances with a bank of lamps operating at different voltages. Ninety to one hundred and fourteen volts is a respectable difference, this difference causes a rather large change in the color temperature of the lamp and that pushes a lot of energy from the infrared into the visible. It's a calculated response against three different simulated measurements. It is not a measured response against the actual sunlight and that's the difference.

COMMENT: At the time this system was designed, we were unaware of any long-life xenon arc lamp solar simulator. We were fully aware of the systems that were available for zero air mass simulation, but, as was pointed out, the cost of those simulators run of the order of \$10 000.00 per square foot. The approach here was design something at a low cost that would be readily available.

- Q:** There were a couple of discussions of diffuse contributions to the solar insolation. Since solar cells either have a high index surface or will have an anti-reflection film, what kind of angular acceptance angle do these cells have? Over what kind of a range will diffuse scatterings be important? Also, have the calculations given the angular dependence?
- A:** We've been quite interested in the angular dependence of the performance of solar cells for quite some time. I think that certainly the problem that we will have in determining how to measure solar cells for a terrestrial environment will be determined by how good the angular operation of a cell is in terms of its hemispherical performance. And certainly one of the things we have to consider is how the device is used in various systems. This particular curve is representative of a conventional silicon solar cell covered with various thicknesses of cover glass. The very first curve shows the relation between what you would normally expect out of a cosine-type performance curve and what you would expect if you covered the cell and lost performance as a function of the transmission. The first thing shown is the transmission curve or what the cosine law would say and the second thing is what would happen to this cell if you had reflectance off the surface of the silicon. The second curve shows how the short-circuit current of solar cells performed relative to that corrected curve which takes into consideration the reflectance off

the surface of the solar cell. You can see from this that silicon solar cells are fairly good performers with angle of incidence. They follow the cosine law pretty well. We can therefore say that the solar cell will be able to use the diffuse component of solar radiation very well if it's put into an environment where it's able to see it.

Q: I think that it was brought out this morning that maybe the 0.942-micrometer water vapor band is important to solar cell performance. I was wondering if there are any plans to try and simulate that?

A: We have no immediate plans to simulate water absorption in our simulator.

AN ANALYSIS OF THE INFLUENCE OF CELL CHARACTERISTICS ON
THE SPECTRAL SENSITIVITY OF Cu_2S -CdS SOLAR CELLS*

Allen Rothwarf

Institute of Energy Conversion
University of Delaware
Newark, Delaware 19711

For Cu_2S -CdS solar cells, the photovoltaic response depends on the absorption coefficient α , the thickness of the Cu_2S layer d , the electron diffusion length L , the surface recombination velocity S , grain radius R , the drift field in Cu_2S F_1 , the interface recombination velocity S_p , the field in the CdS space charge region F_2 , and the mode of operation of the cell (front wall, back wall, and reflection modes).

For all modes of operation of the cell, the contribution to the current from carriers generated in the CdS can be neglected. For front wall cells the absorption coefficient for photons with energy above the band gap of CdS (2.4 eV) is greater than 10^5 per centimeter, and hence the photons are largely absorbed in the Cu_2S . For back wall cells, the CdS thickness is such that the carriers are created near the surface and recombine before reaching the junction. Thus, to determine the short circuit current one is primarily interested in the absorption and the recombination processes which occur in the Cu_2S .

We have calculated the expected light generated current density j_L as a function of α , d , L , S , R , F , S_p , and F_2 for the four modes of cell operation. The expressions are complex, and graphical results are given for some values of the parameters. To see where the dependence on these parameters arises consider figure 1 which shows the band diagram for the heterojunction and the several currents which can flow. One can write

$$j_{LO} = j_{LR} + j_L$$

where j_{LO} is the light generated current which crosses the junction, j_{LR} is the component which returns, and j_L the component which flows through the electrodes.

*Supported by the National Science Foundation, Research Applied to National Needs, under Grant AER72-03489, formerly GI-34872.

The j_{LO} component is a function of α , d , L , S , R , and F_1 . For

$$j_{LR} = qn_I S_I$$

n_I is the electron density at the interface and S_I is an effective interface recombination velocity which depends on the junction area and on the density and capture cross section of the interface states. For j_L we can write

$$j_L = qn_I v_D$$

where $v_D = \mu C d S F_2$ for μF_2 values well below the thermal velocity. The value of F_2 can depend on both the wave length and intensity of the light reaching the space charge region of the CdS.

The dependence of j_{LO} on grain size can be approximated by assuming a model in which the grains are cylinders of radius R , and all carriers which reach the grain boundary recombine there. For uniform generation the result is

$$j_{LO} = j_{LOO} \frac{1-d}{R} \frac{1-d}{3R}$$

where j_{LOO} is the value expected in a single crystal.

$$j_L = \frac{\frac{1-d}{R} \frac{1-d}{3R} \mu_{CdS} F_2 j_{LOO}(\alpha, d, L, S, F_1)}{S_I + \mu_{CdS} F_2} \quad (1)$$

where the dependence of j_{LOO} on the remaining variables is indicated. In equation (1) reflection losses, grid shading losses, and absorption in the cover plastic have been omitted.

We have calculated $j_{LOO}(\alpha, d, L, S, F_1)$ for the four modes of operation of the cell. In figure 2, the results for a front wall cell are illustrated. The ordinate is the ratio of the calculated value to the maximum value which would occur if all photons with sufficient energy were absorbed and all carriers created crossed the junction. The abscissa is the product of the absorption coefficient α and the thickness of the Cu_2S layer d . The curves are for different values of L/d . The upper curves are for $S = 0$ and the lower group for $S = \infty$. Figure 3 shows a similar set of curves for the back wall cell. In figure 4 is shown a comparison of the front wall, front wall reflection, back wall, and the back wall reflection modes for $S = 0$ and $L = d$. It is clear that the reflection modes give higher currents than the nonreflection modes and the back wall cells higher values than the front wall cells.

However, lest one conclude that a back wall cell is better than a front wall cell in all cases, it should be pointed out that the back wall cell gets no contribution from photons with energy greater than the band gap of CdS (2.4 eV). These photons represent roughly 20 percent of the AM1 spectrum, and because of the high α associated with such photons, an even greater proportion of the potential current.

The effect of the drift field in the $\text{Cu}_2\text{S F}_1$ is illustrated in figure 5 for a front wall cell. The field is in units of kT/qL . The field enhances the $S = \infty$ cases more than the $S = 0$ ones since the field serves two roles - one of keeping electrons away from the surface and the other of modifying the expression for the current and carrier densities.

Using the α as a function of λ results of Shiozawa et al. (ref. 2), we can convert the previous curves into spectral response as a function of wave length. Using the index of refraction as a function of wave length (ref. 2), one can also include the reflection losses and compare the result to experimental curves. Figure 6 shows $\eta_r j_{\text{LOO}}/j_{\text{L max}}$ for several cases. Here η_r is the calculated fraction of light reaching the Cu_2S assuming $n = 1.5$ for the cover plastic and epoxy. The experimental curve which is also shown is $j_{\text{L}}/q\Phi$, where Φ is the incident flux. The low values seen for the experimental curve indicate either experiment difficulties in aligning the optics and calibration or the effect of the low intensity of the monochromatic light, since the response to roughly AM1 white light indicates a value of $j_{\text{L}}/q\Phi$ greater than 0.4.

In table I we have the results of calculations of the expected j_{LOO} for AM1 and the tungsten-iodide AM1 simulator for several sets of parameters.

In table II the values used for the calculations are given. Our results indicate that the spectral response of the Cu_2S -CdS solar cell is sensitive to a large number of parameters. A solar simulator which does not closely match the solar spectrum can not be expected to give valid results for cells with significantly different parameters. As the results in table I illustrate, the values expected for j_{LOO} under AM1 can be larger or smaller than the corresponding values under the W-I simulator.

REFERENCES

1. Progress Reports NSF/RANN/SE/GI-34872/PR74/2, PR74/4.
2. L. R. Shiozawa; F. Augustine; G. A. Sullivan; J. M. Smith, III; and W. R. Cook, Jr.: ARL 69-0155, Oct. 1969.

DISCUSSION

[See DISCUSSION section following the next paper.]

TABLE I. - CALCULATED LIGHT GENERATED CURRENT

DENSITIES IN Cu_2S -CdS SOLAR CELLS

Mode	S	L, μm	D, μm	Losses	AM1 - j_{LOO} mA/cm^2	W-I simulator - j_{LOO} mA/cm^2
F	0	---	---	0	35.2	33.5
B		---	---	0	29.8	33.0
F		---	---	Reflection	29.6	28.5
B		---	---		26.0	28.9
F		---	0.3		19.0	15.9
B		---			19.2	16.0
FR		---			23.8	21.6
BR		---			24.7	23.4
F		0.3			12.9	11.3
FR		.3			16.7	16.3
B		.3			12.1	12.5
BR		.3			15.7	16.9
F		.5			16.4	13.9
FR		.5			20.5	18.9

TABLE II. - VALUES USED IN CALCULATIONS

λ , μm	$\bar{\alpha}$, 10^5cm^{-1}	n	Front wall, hr	Back wall, hr	AM1 ϕ , $10^{15}/\text{cm}^{-2}\text{-sec}$	W-I ϕ , $10^{15}/\text{cm}^{-2}\text{ sec}$
0.3 - 0.4	3.0	3.7	0.75	0.85	9	----
.4 - .5	1.5	3.6	.80	.86	25	3.6
.5 - .6	.8	3.5	.82	.86	38	20.7
.6 - .7	.45	3.3	.83	.87	39	44.8
.7 - .8	.30	3.1	.85	.87	38	48.3
.8 - .9	.23	2.9	.86	.88	30	48.3
.9 - 1.0	.10	2.7	.89	.89	27	31.1
1.0 - 1.05	.05	2.7	.90	.90	14	12.9

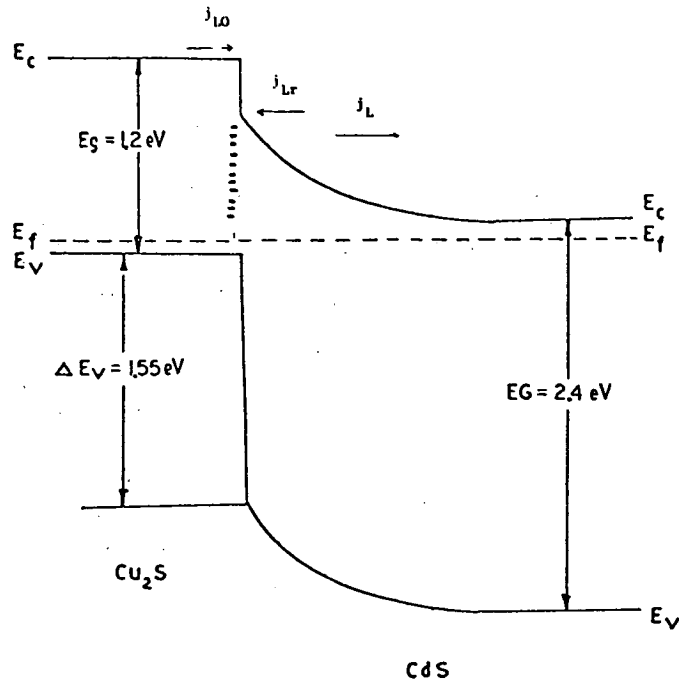


Figure 1. - Band diagram of Cu_2S - CdS solar cell with currents j_{L0} , j_{Lr} , and j_L indicated.

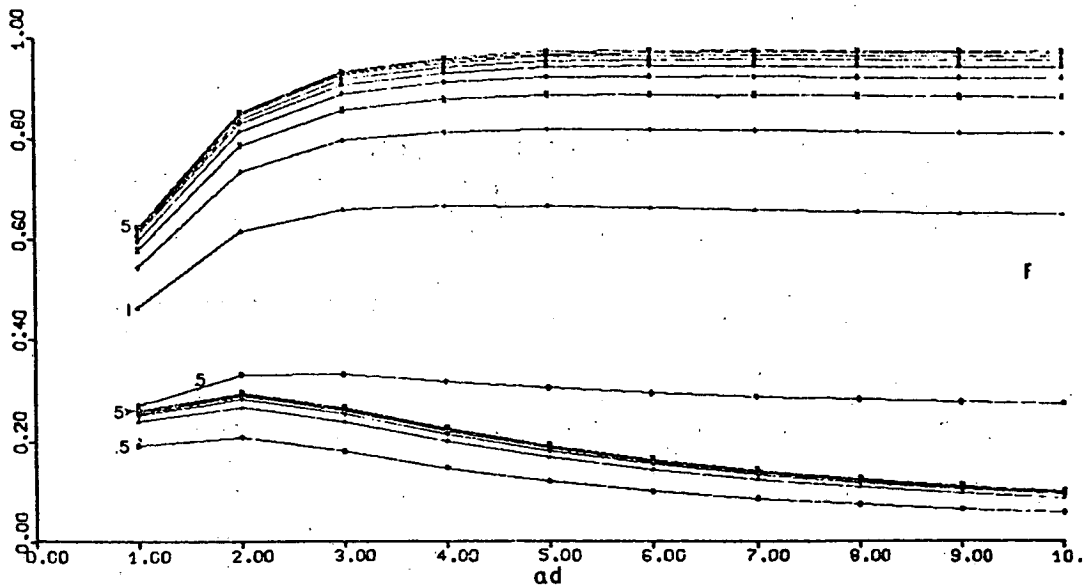


Figure 2. - Calculated values of j_{L0}/j_{Lmax} as function of ad for front wall mode of operation. Upper group of curves for $S=0$ with L/d values ranging from 0.5 to 5 in steps of 0.5. Lower group for $S=\infty$ case.

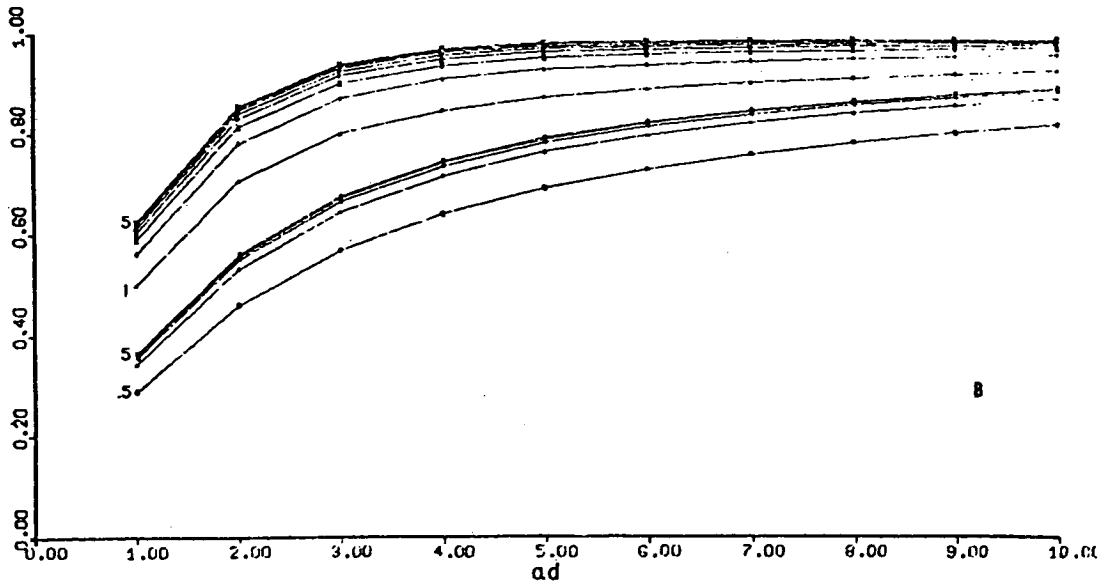


Figure 3. - Calculated values of j_{L00}/j_{Lmax} as function of αd for back wall mode of operation. Upper group of curves for $S=0$ with L/d values ranging from 1 to 5 in steps of 0.5. Lower group for $S=\infty$ case, starting with $L/d = 0.5$.

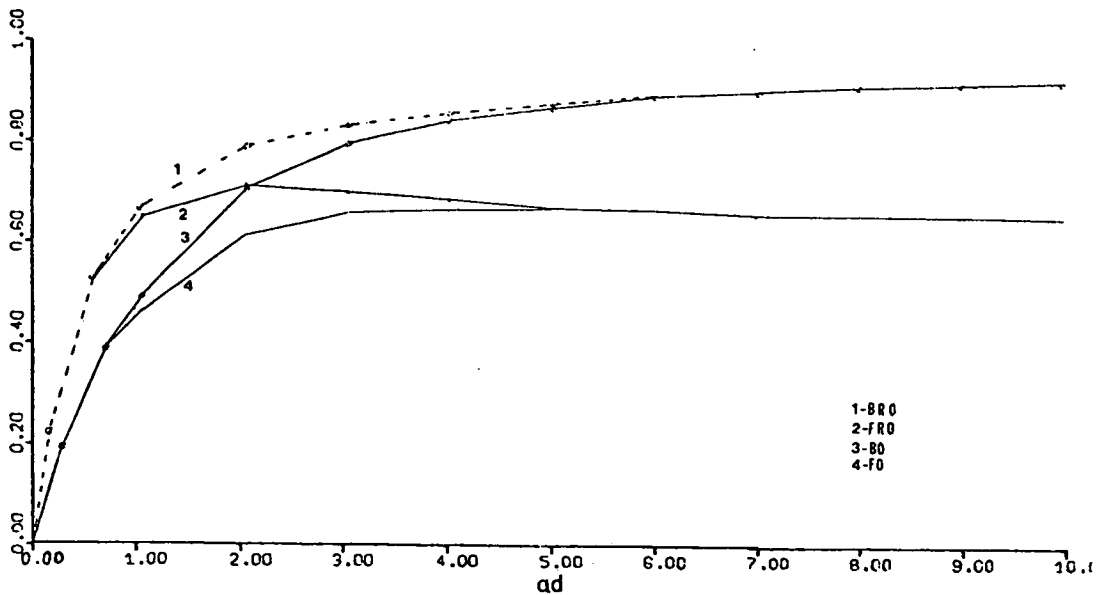


Figure 4. - Calculated values of j_{L00}/j_{Lmax} as function of αd with $S=0$ and $L=d$ for four modes of operation of the cell. Back wall reflection, 1; front wall reflection, 2; back wall, 3; front wall, 4.

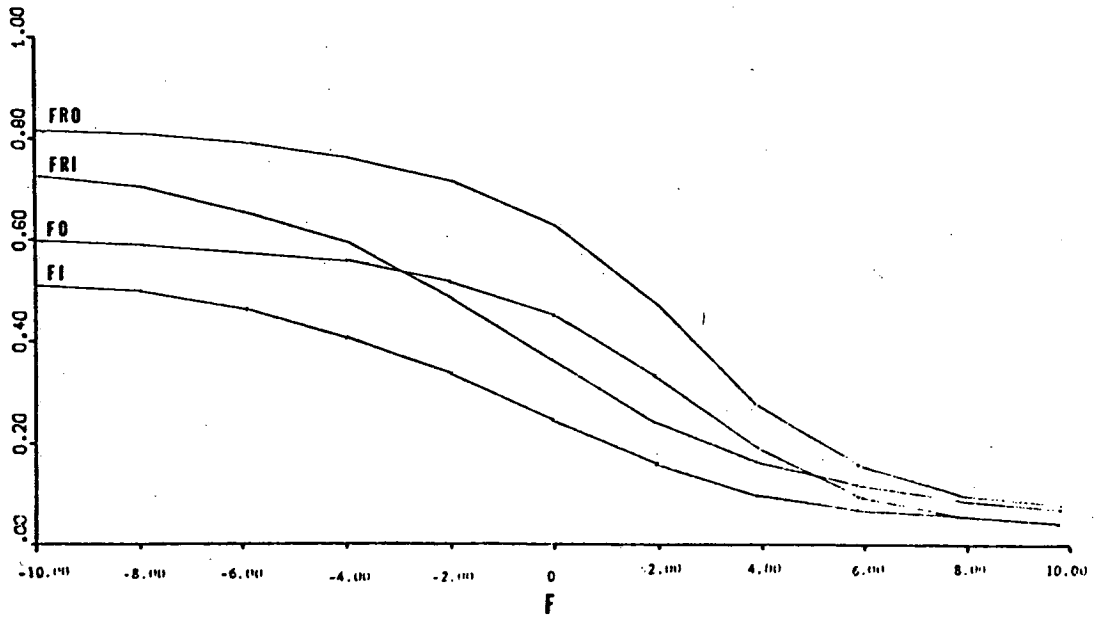


Figure 5. - Calculated values of j_{L00}/j_{Lmax} as function of drift field F_1 in Cu_2S with $\alpha L = 0.95$ and $\alpha d = 1.0$ for four cases: Front wall reflection, $S=0$, FRO; front wall reflection, $S=\infty$, FRI; front wall, $S=0$, FO; front wall, $S=\infty$, FI.

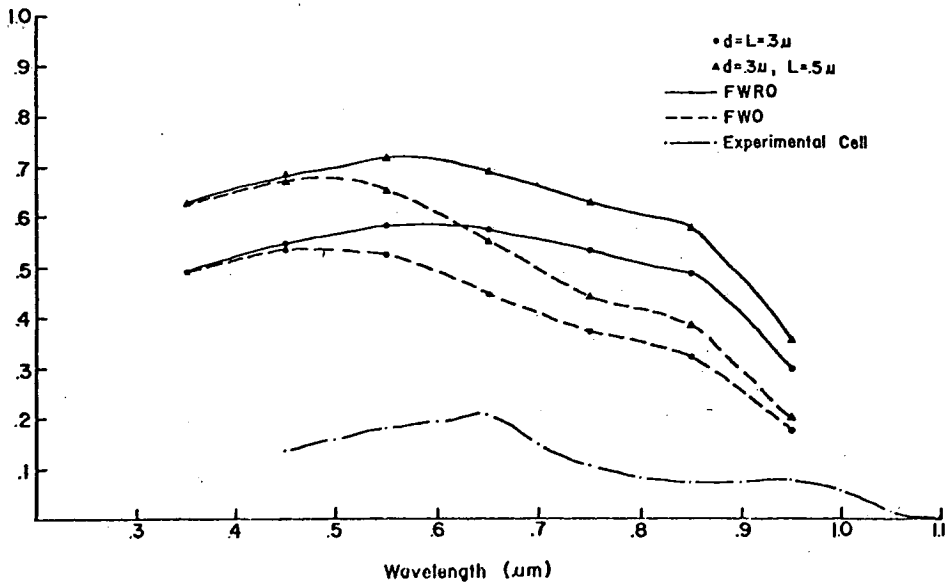


Figure 6. - Calculated spectral response for front wall (FWO) and front wall reflection (FWRO) cells with reflection losses and $S=0$. Experimental cell for front wall configuration with very low intensity light.

SPECTRAL EFFECTS IN CdS/Cu₂S SOLAR CELLS*

H. Hadley, Jr.

Institute of Energy Conversion
University of Delaware
Newark, Delaware 19711

Frontwall CdS/Cu₂S solar cells have a spectral response from a wavelength of about 1 micron to well into the blue region of the visible spectrum and are thus well suited to terrestrial application. However, the various parameters influencing the creation and collection of the light generated carriers (for instance the Cu₂S absorption constant and thickness) are not the same for all cells, giving rise to variations in the spectral distribution of the short circuit current.

For example, figure 1 shows the spectral distribution of I_{sc} corrected to a uniform intensity for the two cells 271B2 and 278C1. It is clear that there are significant differences in the blue sensitivity between these two cells. Investigation of a number of cells made at Delaware shows that this blue sensitivity variation is generally true, while the red region is relatively constant from cell to cell.

Thus, the spectral distribution of the illuminating source, especially in the blue region below the CdS band edge, is particularly important in determining the observed current output for a particular cell. AM1 terrestrial sunlight illumination appears as shown by the shaded region of figure 2. Also shown are the spectral outputs of the tungsten iodide (W-I), copper sulphate-water filtered simulated in use at Delaware and NASA-Lewis (solid curve) calibrated to AM1, and filtered high pressure xenon simulated in use at S. E. S., Inc. (dashed curve). It is important to note that the W-I simulator is deficient in the blue compared to AM1 sunlight, whereas the xenon is not. Also, the W-I simulator is deficient in the near IR around 0.950 micrometer due to the heavy water filtering (5.1 cm). The xenon simulator has considerable narrow line structure in this region, some of which is reduced with filtering.

A comparison of the short circuit currents for a number of CdS/Cu₂S cells under W-I and xenon AM1 simulation should show this variability in the blue sensitivity clearly. Figure 3 shows a histogram of the current ratios (Xe:W-I) for a number of recent Delaware cells. Clearly, there are significant variations in cell response under the different spectral illuminations.

*Supported by the National Science Foundation, Research Applied to National Needs, under Grant AER72-03489, formerly GI-34872.

Figure 4 shows the I-V characteristics for cell 278C1 under various conditions. This cell, as was shown, has a significant blue response to below 4500 Å. Curve 1 is the response under W-I AM1 simulation while curve 2 is for 100 milliwatts per square centimeter water-filtered xenon. Curves 3 and 4 are measurements under actual rooftop clear sky conditions in Delaware. Here the measured intensities of direct (collimated) and global radiation are below conventional AM1 intensities. Correcting these measurements (curves 3 and 4) to a uniform 100 milliwatts per square centimeter would produce the results shown in figure 5. Clearly, for this cell, the W-I simulation set with a standard CdS references provided by NASA-Lewis does not match the rooftop measurements nearly as well as the xenon simulation.

In summary, it is clear that for meaningful simulation of terrestrial sunlight it is necessary to have a source that matches as closely as possible the spectral distribution of sunlight. For CdS/Cu₂S, this is particularly critical in the blue region of the spectrum and xenon is seen to produce a better match to terrestrial conditions than the blue deficient W-I source.

ACKNOWLEDGEMENTS

The measurements of cell spectral response by Dr. G. Storti¹ are gratefully acknowledged. Measurements under xenon simulation were provided by S. E. S., Inc., Newark, Delaware, whose cooperation is also gratefully acknowledged.

DISCUSSION

- Q: There was a crossover in the IV characteristic in the next to last viewgraph. Is that legitimate?
- A: These are all plotted on the same scale here and of course the measurements were taken at different times. It is a legitimate crossover; it really exists. I can't explain it directly, other than to say there are resistive effects going on in some of these cells and it might be due to that.
- Q: Is this the same cell?
- A: These are four curves from the same cell under different conditions.
- Q: Are these linear with sunlight?
- A: Yes, they are. They are linear with intensity under the tungsten iodine simulation. I assume they are linear under sunlight, too. I haven't made those measurements. But they are linear over two orders of magnitude or more. I didn't go over two

¹Supported by the Office of Naval Research under Grant N00014-71-C-0169.

order of magnitude in intensity.

COMMENT: I think you just have a temperature effect. With the tungsten light you have an awful lot of absorption of infrared and you probably would find, if you could somehow get a thermocouple attached to the front of the cell, that that's just a thermal effect.

A: Well, the thermal effect may be present on the rooftop measurements, but the cell during the measurement under the tungsten iodine lamp was on a temperature controlled block maintained at 22° C.

COMMENT: I know what you're saying, but the temperature of the block and the temperature of the cell surface are two different things. Under tungsten light you have a lot of energy which must be transferred through the cell. So, if you put a thermocouple on the top of the cell, I think that you might see a temperature difference between the top cell surface and the control block.

Q: A point of clarification regarding the way you're measuring, or the way you're recommending cadmium sulfide solar cells be measured, in terms of giving them a figure of merit relative to their performance in a terrestrial environment. You suggested that the solar cell has a response that is different depending on the spectrum of the light which is incident on it and that the more blue the light the better it looks. You recommended that the light should be something like AM1 solar simulation. The question is, how often do you get an AM1 kind of an illumination on your specimen and does AM1 really represent a meaningful illumination to give you a value of how solar cells will perform in a terrestrial environment? Relatively, there are many other illumination spectrums which are going to be more meaningful in terms of the overall power output of the solar array. Why pick something like AM1?

A: AM1 was chosen as an example. It doesn't have to be AM1. We were talking about direct AM1; the global or total will have even more blue in it. We want to make sure that the blue response is not discounted in the simulator because the cells we are making have this blue response. If you're talking about back wall cells which are under development elsewhere, then if you use the tungsten iodine simulator you get a very good response because it's rich in the red. So, we are just saying that it doesn't have to be AM1, but you should have a good representation of the blue part of the spectrum in any simulator that you design.

Q: Does it follow that the more blue you put in the better the cell response? If so, you want to reflect not what makes the cell look best, but what gives you a figure of merit of how well the cell will perform in a normal kind of terrestrial environment.

A: Yes, I agree with that. The problem is that it would be hard to give such a figure of merit if you have a variability in the blue response.

COMMENT: You have made the point I wanted to make. As it turned out, because our simulator didn't have sufficient blue output, we didn't recognize that some of our processes enhanced the blue response while other processes did not. It was more or less accidental that we saw the enhancement by using another simulator with bluer output. Also, the French and Japanese reported to us that they had 6 and $6\frac{1}{2}$ percent efficient cells. However, they checked out in our simulator at $4\frac{1}{2}$ to 5 percent. So this is how the question was brought up and recognized. Now we can measure the spectral sensitivity and not only increase the red but also the blue sensitivity. As a matter of fact, there are some cells which increase in blue and decrease in red and vice versa. Therefore, different processes, possibly even more than two, are going on. Finally, it is a matter of not being blindfolded but working properly to obtain all the information. For that reason I think that it is important that we have a better simulator which at least has a blue component in it with some intensity.

COMMENT: This is a key point, but we don't want to dwell on it. John's point is also good - just because it makes a better cell, if you're not really getting the light through the package, if you are covering it with plastic that solarizes and cuts out that blue light, then you don't want a simulator that just makes your cell look better if that's really not what the cell is going to see eventually when it's used. The point here is that you really have to try to duplicate how it's going to be used.

- A: Absolutely. And I think the part of the blue we are looking at is not going into the ultraviolet but is the near blue range, and that is exactly where AM1 and AM1.5 and possibly AM2 will bring us. Possibly with some haze it even brings us into a more bluish range.
- Q: The question that John raised I'd like to expand to a broader issue than cadmium sulfide. AM1, if you look in terms of relative times of day, or whatever, is rather limited. One may not want to, for a real world simulation, design all the lamps for AM1. Perhaps, in a broader issue, shouldn't there be some other standard - one more closely related to the statistical real insolation that one sees and has to live with?
- Q: I think Dr. Böer eluded to the fact that some cells are red responsive and some are blue. Is this a variable in the process control of the cadmium sulfide cells and is the stability of the cadmium sulfide cell now controlled?
- A: Let me address the first part of the question. Yes, the variations in spectral distribution seem to be due to process differences. If we dip for a longer period of time and form a thicker copper sulfide layer and so on we can change the spectral distribution. As far as the stability of the cells go, maybe I should let Allen answer that.
- A: With stability, everytime you change a process, you introduce a possible new type of degradation. That means that everytime you change something, you have to test

those cells to see what their stability is and what their problems are. As Carl pointed out, we haven't been aware of the blue sensitive cells long enough to do a thorough study of their lifetime but they will be under test. We don't know that stability problems, if any, exist there.

COMMENT: I think that it should be reiterated that for all the testing that's been conducted, either at Delaware or now at Westinghouse, in general the copper sulfide cell, suitably protected from the atmosphere, shows high stability. At the moment, as Dr. Hadley indicated, some of the cells we are looking at are of very recent manufacture and we can't give accelerated test data. However, the initial indications are that those cells will also be quite stable when suitably protected. I would like to put one plug in for the simulation that we're talking about. The suggestion is not that we use an artificial blue-rich spectrum but that we use a simulation which reasonably matches natural sunlight. And I would ask the weather people who are here, is it not the case when you go from AM1 toward AM2 the overall spectral distribution is not changing significantly and therefore we would not expect similar testing at AM2 to give any change in actual efficiency for the cells that Dr. Hadley was talking about?

COMMENT: It seems here that coming back to what Dan Bernatowitz said yesterday, we really have two distinct problems. One is testing or comparing cells, and the other is really taking cells and designing systems. It looks like from the standpoint of systems because the spectral distribution may be quite different, at different areas because of diffuse components, that the spectral response to the cells is probably more useful than testing under simulators. In other words, if one has a spectral response curve, one can proceed, if the spectral characteristics of a given location are known, to the calculated system performance. Going back to the way the semi-conductor industry operated initially, they didn't define a standard test circuit for a transistor. What they did is get the characteristics of the device and then proceed to do designs from that standpoint. So I would like to argue to some extent for developing standards for doing the spectral sensitivity and using this as a basis for performance calculations rather than simulator testing.

COMMENT: It is worthwhile to consider, and for silicon there would be no great problem. However, for the cadmium sulfide cell there are intensity dependences which I eluded to which require spectral response testing with a biased white light of some sort to make sure that the charging at the interface, which is necessary to get the field to sweep the carriers away from the junction, won't give you an erroneous result. So it's worthwhile to consider but cadmium sulfide again may present a more complicated situation than silicon.

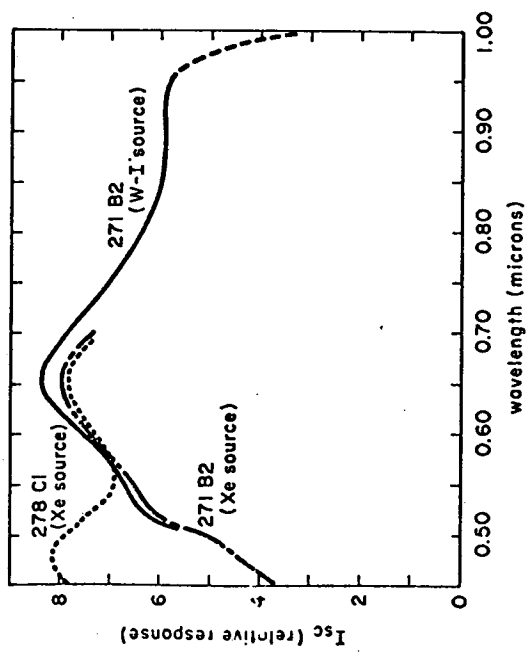


Figure 1.

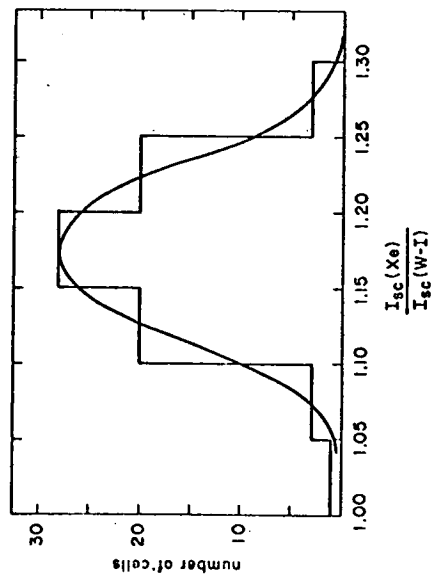


Figure 3.

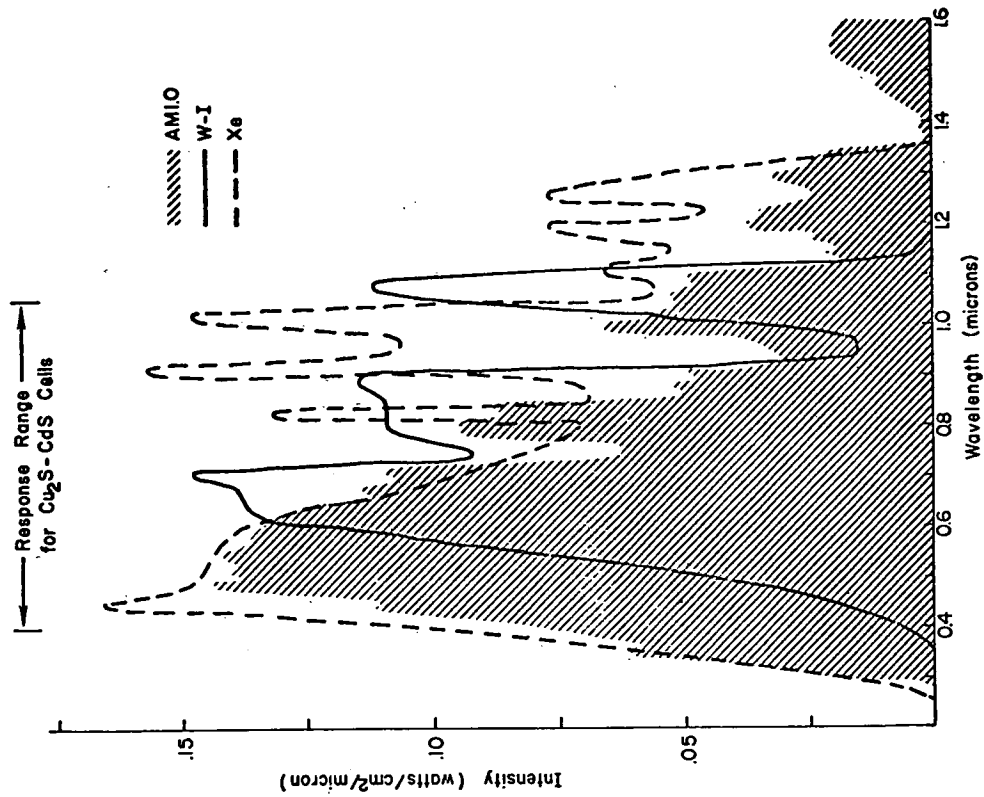


Figure 2.

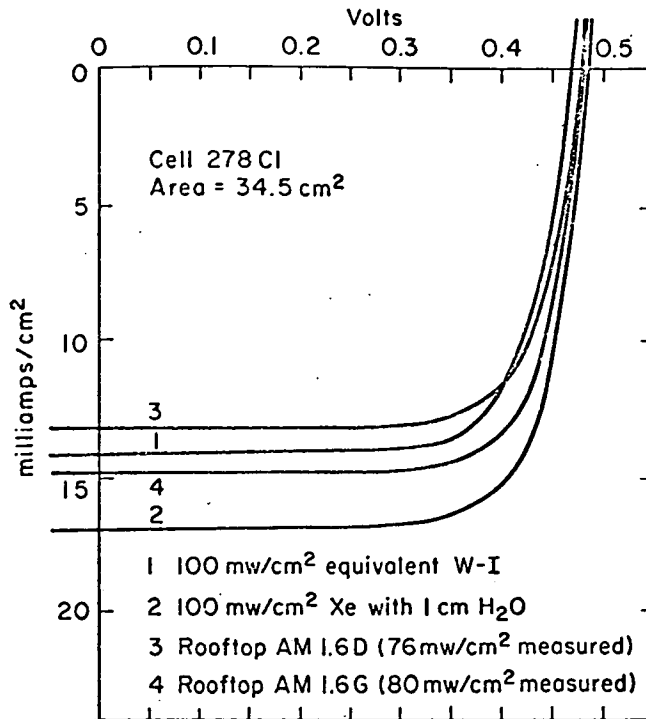


Figure 4.

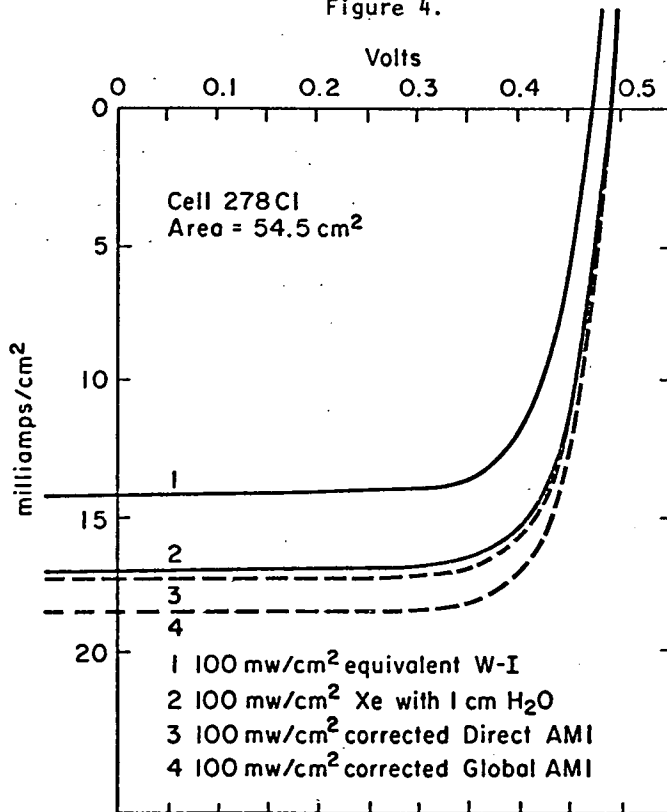


Figure 5.

PREDICTION OF TERRESTRIAL SOLAR CELL SHORT-CIRCUIT CURRENTS BY SPECTRAL ANALYSIS

Henry W. Brandhorst, Jr.

NASA Lewis Research Center
Cleveland, Ohio 44135

The key to predicting solar cell performance is determining the short-circuit current. This current depends on the intensity and spectral distribution of the light source and the spectral response of the solar cell. Thus, for the terrestrial case, measuring the cell current under natural sunlight is not continually available at test sites and laboratories. Furthermore, the intensity and spectral distribution of natural sunlight varies continuously. This variability makes predicting the solar cell short-circuit current difficult. Fortunately, the spectral distribution of unclouded sunlight may not vary greatly because solar cell current appears to be proportional to sunlight intensity. Therefore, errors in determining solar cell current in natural sunlight may only be a few percent.

However, since terrestrial sunlight is not always conveniently available, another means must be used for the routine measurement of solar cells. Unfortunately, no artificial light sources exist whose intensity and spectral distribution remain constant and duplicate terrestrial sunlight. These deviations in intensity and spectrum cause different errors in the current of cells whose spectral responses differ. Therefore, corrections developed for one type of cell are not applicable to others. Thus, an important part of any measurement method is how to correct for these errors - that is, how to provide an accurate calibration.

The most common method which uses an artificial light source controls the total input to the test solar cell by setting the light level with a calibrated solar cell whose spectral response reasonably duplicates that of the test cell. Then the output of the test cell is measured. This method is sensitive not only to the spectral distribution of the light source but also to the spectral response of the test cell. If the response of the test and calibrated cell are not identical, large errors in test cell current can be obtained. Figure 1 shows a spectral distribution of an artificial light source which simulates outer space sunlight. Figure 2 shows the spectral response of two cells. If the conventional cell in this figure were used to set the simulator, errors of the order of

10 percent in the current of the high blue response cell can be obtained.

It is the purpose herein to present an alternate approach to the predicting terrestrial solar cell short-circuit currents that may better correct for the errors caused by variations in cell spectral responses. This technique, pioneered by Gummel and Smits (ref. 1) and further used by Mandelkorn (ref. 2), uses spectral response measurements on the solar cells themselves. These spectral response measurements multiplied by the solar spectrum and then integrated yield the short-circuit current of the solar cell. The Gummel and Smits method is unique in that a detailed description of the solar spectrum is not required for an accurate short-circuit current prediction provided a sufficiently wide range of spectral responses were used to calibrate the technique. This technique has been in use at the Lewis Research Center for about 10 years (ref. 2) and has shown an accuracy of the order of 2 percent on predicting outer space short-circuit currents. Initial results on applying the technique to predicting terrestrial solar cell short-circuit currents will be presented.

METHOD

The method as described by Gummel and Smits requires the simultaneous measurement of a test cell and a monitor cell under a sequence of eight narrow bandpass interference filters. The ratios of test to monitor cell short circuit are obtained, and the integrated short-circuit current of the test cell is obtained by

$$I_{sc} = E_i R_i w_i$$

where R is the test to monitor cell short-circuit current and w_i is an appropriate weighting factor for each filter. The weighting factors were obtained by Gummel and Smits by measuring the short-circuit currents of a set of solar cells on a clear day near noon at high altitude. This set of solar cells was carefully selected to encompass the widest practical range of silicon solar cell responses available, and it included radiation damaged cells. It is important to note that so long as the set of cells used in such measurements has a sufficiently wide spread in spectral responses the weighting factors can be determined without prior information on quantum efficiencies or on the spectral composition of sunlight as long as the spectrum did not change during measurement. Because the objective of this earlier work was the prediction of outer space currents, the terrestrial weighting factors obtained were also modified for the difference in intensity between terrestrial sunlight and outer space sunlight at each wavelength interval. However, neither the terrestrial nor the outer space filter factors were reported. When the Lewis Research Center built up their simulator, only the filter factors for outer space were obtained.

Therefore, it was necessary to determine a set of terrestrial filter factors. These were obtained by reversing the Gummel and Smits technique and by multiplying the outer space weighting factors by the ratio of the terrestrial intensity to the outer space intensity at each given wavelength. A calculated AM1 spectrum was used. The spectrum used was essentially that described by Thekaekara except that the Johnson AM0 curve was used. It is obvious that errors can occur in this reversal approach due to a lack of knowledge of the spectrum used by Gummel and Smits. An absolute terrestrial calibration was not made because cells with a sufficiently wide range of spectral response were not readily available.

EQUIPMENT

The equipment used is shown in figure 3. A light beam from a tungsten-iodine 3400 K light bulb is directed sequentially through eight narrow bandpass monochromatic interference filters. Filter wavelengths are 0.4, 0.45, 0.5, 0.6, 0.7, 0.8, 0.9, and 0.95 micrometers, and they have a full width at half maximum of the order of 200 Å. The monochromatic light beam simultaneously illuminates a test cell and a monitor cell mounted beside each other. No bias lights are included. These measurements on cadmium sulfide cells were not made. The short-circuit currents of the test and monitor cells are digitally measured, and the ratios of test to monitor cell currents are taken mathematically. These ratios could also be obtained electronically if desired. These measurements, when properly calibrated, also yield the spectral response of the test solar cell.

EXPERIMENTAL PROCEDURE

A group of 31 silicon solar cells was selected for comparing the short-circuit current determined by the filter wheel technique and by natural sunlight measurements. The outer space short-circuit current of these cells had been obtained previously by the airplane technique. Five different types of cells were measured: (1) uncoated conventional cells (UC), (2) uncoated velvet-surface (low reflectivity chemically etched texturized surfaces) cells (UV), (3) silicon oxide coated conventional cells (C), (4) silicon oxide coated terrestrial (deeper junction) cell (T), and (5) Ta₂O₅ coated Helios (high blue response) cells. The short-circuit currents of these cells were measured in clear, normally incident sunlight using a 10 to 1 collimating tube. All temperatures were controlled to 25⁰±2⁰ C. Solar intensity was measured using a normal incidence pyrheliometer; intensities ranged from 85 to 95 milliwatts per square centimeter. Because it was shown in reference 3 that solar cell short-circuit current is proportional to intensity

under collimated conditions, all cell currents were adjusted to an arbitrary intensity of 100 milliwatts per square centimeter, which corresponds to the intensity obtained at AM1. Therefore, these data will be referred to as AM1 currents although the true air mass measured during these measurements was about 1.7.

This group of cells was then measured in the filter wheel simulator shown in figure 3; the ratio of the short-circuit current of these cells to the monitor cell was obtained. These ratios were multiplied by the set of weighting factors derived from the Gummel and Smits data and the Lewis filter wheel simulator. Integration yielded the predicted terrestrial solar cell short-circuit currents.

RESULTS AND DISCUSSION

Table I shows the averages of the measured AM0 to AM1 (100 mW/cm^2) current ratios. The AM0 values were from airplane calibration, and the AM1 values were from the terrestrial sunlight measurements.

A variation in this ratio is due to the differences in the spectral response among the cells. The responses of the conventional (C), terrestrial (T), and uncoated velvet (UV) cells were all similar and indeed these ratios varied only from 1.14 to 1.16. Also shown is the average percent error in the predicted AM1 currents using the filter wheel simulator. The percent error was obtained as follows:

$$\text{Percent error} = \frac{I_{sc1, \text{predicted}} - I_{sc1, \text{measured}}}{I_{sc1, \text{measured}}} \times 100$$

Thus, a negative error indicates that the predicted current was less than the measured current. It can be seen that the error is less than 2 percent for all groups with the exception of the uncoated conventional cell. This degree of accuracy is similar to that obtained in predicting outer space currents.

Figure 4 shows graphically all the data from which the averages in table I were obtained. A distinct relationship appears to exist between the AM0 and AM1 current ratios and the average percent error in the predicted terrestrial short-circuit currents. The lack of perfect agreement is caused by the differing spectral responses of the cells and errors in the filter weighting factors. However, the errors obtained for most cells are as low as those obtained by using calibrated cells and artificial light sources. With a more careful derivation of the weighting factors or an absolute calibration using a widely divergent set of solar cells it is possible that accuracies of the order of ± 2 percent for all types of cells can be achieved.

Finally, the filter wheel approach appears to require a single reference spectrum to be successful. However, it is possible that this requirement may not be restrictive for terrestrial solar cell predictions. Based on previously stated data (VARIATION OF SOLAR CELL EFFICIENCY WITH AIR MASS, p. 51), it appears that under collimated conditions solar cell current is directly proportional to intensity. Thus, the slight changes that occur in the terrestrial solar spectrum do not appear to greatly affect the current of the cells. Therefore, the requirement of constant reference spectrum for the filter wheel technique may be fulfilled and a high degree of accuracy can be achieved.

CONCLUSIONS

The accuracies (± 2 percent) shown in predicting the currents for four of the groups of cells measured in this study indicate that careful consideration should be given to using the filter wheel technique for the independent prediction of terrestrial solar cell short-circuit currents. With further study and calibration it is possible that accuracies of the order of 2 percent for all types of cells may be achievable. However, before cadmium sulfide cells can be measured, a provision for bias lights must be incorporated into the equipment.

REFERENCES

1. Gummel, H. K.; and Smits, F. M.: Evaluation of Solar Cells by means of Spectral Analysis. Bell System Tech. J., vol. 43, no. 3, 1964, p. 1103.
2. Mandelkorn, J.; Broder, J. D.; and Ulman, R. P.: Filter Wheel Solar Simulator. NASA TN D-2562, 1965.

DISCUSSION

- Q: I can see where this would work for short-circuit current. But when you want to get a complete current-voltage curve and the actual operating power, how do you do that?
- A: Once you've obtained the short-circuit current, it makes little difference (and I use little very advisedly) what light source you use to get the I-V curve. Now with CdS, if you use a red light source, you will get a wrong value. But say you use a blue-rich light source like the bulbs Henry Curtis talked about yesterday. Then, even with cadmium sulfide, once you adjust the intensity to read the true short-circuit

current, the I-V curve you obtain will overlay what you might measure in a xenon simulator or anything else like that.

Q: Would it be possible to modify this so one could obtain the spectral sensitivity at various angles of incidence in order to determine the effects of diffuse radiation?

A: Yes. It's just the way you mount the cells, and I think that is fairly straightforward. However, you must be a little bit careful how you do it.

Q: Isn't it true that we're either looking at the source and the calibration of the source when thinking in terms of a simulator or we're thinking of a detector (when thinking in terms of the spectral response measurements of the detector) and the calibration of the detector. So, if we forget for a moment the cadmium sulfide cell and all its associated difficulties, which say the spectral response measurements are not the way to go, then the following are some questions we need to ask ourselves: How well can we duplicate the spectral distribution in an average AM1 or AM2 condition? How long do those lamps last as a function of time? How well can they be calibrated as a function of time as opposed to the detector? I guess the point I'm trying to make is that it seems to me that it's a choice between the source, with its calibration and reliability, as opposed to the detector, with its calibration and reliability. As one man put it yesterday, where do you want to put the responsibility - on the source or on the detector? I think this is a question that has to be answered here.

A: The one nice thing about this system is that your light source doesn't make any difference. For your detector you have an option; solar cells were chosen because they all have the same speed of response and the bandpass covers the range that you're interested in.

Q: When you consider the filter part of your source you have a problem, or you could have, because the filter is part of it and the stability is important.

A: Yes.

TABLE I. - USE OF FILTER WHEEL SOLAR SIMULATOR TO PREDICT
 TERRESTRIAL SHORT-CIRCUIT CURRENTS

Silicon solar cell type	Number of cells	Measured average of AM0/AM1 I_{sc} ratio	Average percent error, AM1 filter wheel prediction
Uncoated conventional (UC)	4	1.08	-4.19
Uncoated velvet (UV)	5	1.14	-1.44
Conventional (C)	11	1.15	+ .5
Terrestrial (T)	2	1.16	- .72
Helios (H)	9	1.18	+1.16

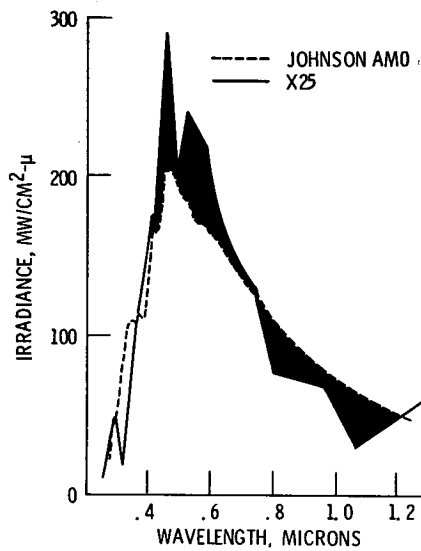


Figure 1. - Comparison of solar spectra.

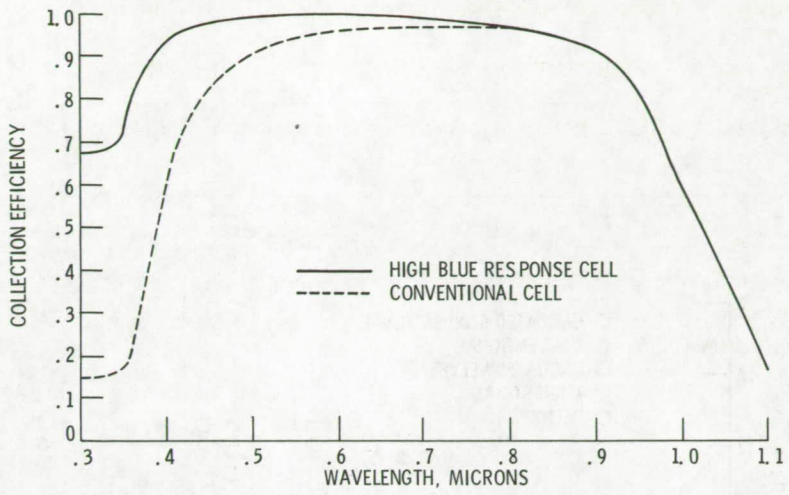


Figure 2 - Comparison of solar cell spectral responses.

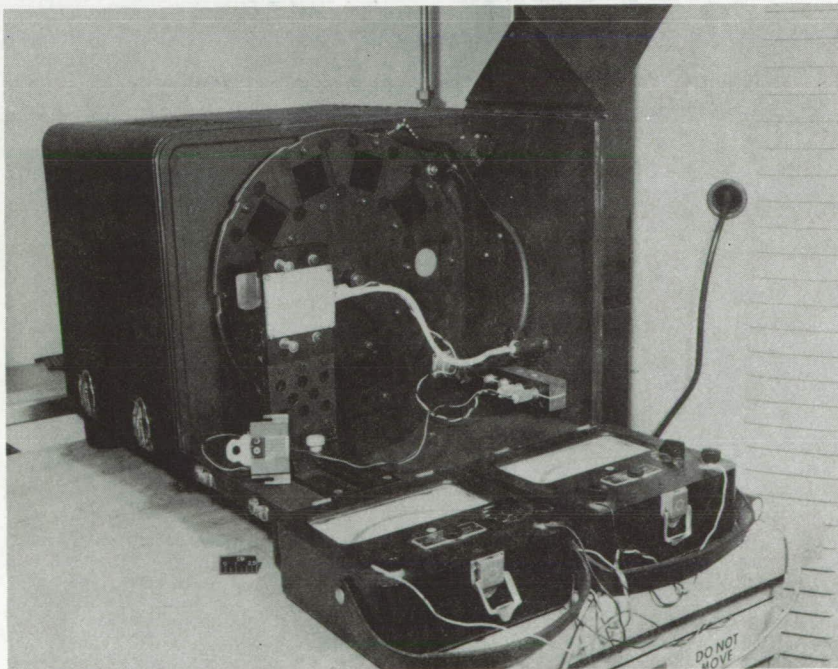


Figure 3 - Filter wheel solar simulator.

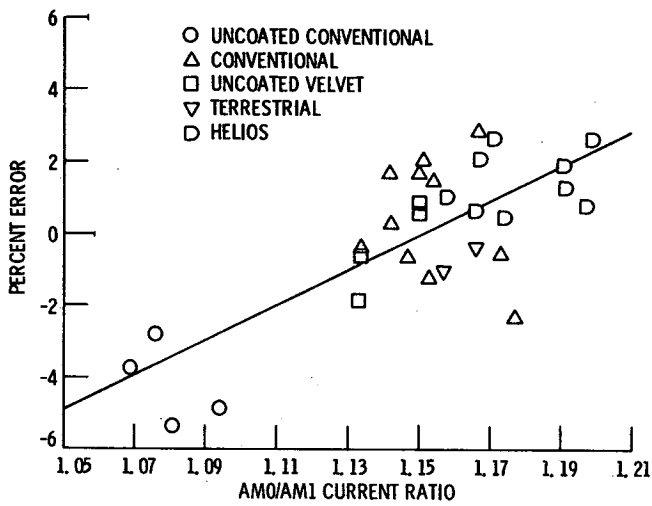


Figure 4 - Dependence of filter wheel prediction error on AMO/AMI current ratio.

TERRESTRIAL SOLAR CELL MEASUREMENTS

Engene L. Ralph

Spectrolab, Inc.
Slymar, California

Solar cell measurements can be made very reliably and close correlation from one laboratory to another can be achieved if proper control of the light source and of the cell temperature is maintained and if a properly calibrated standard solar cell is used to determine the intensity of the light source.

Historically, the first accurate measurements of solar cells were made in natural sunlight on the Earth's surface. Performance characteristics were able to be measured to within ± 5 percent accuracy using a thermopile (pyrheliometer or pyranometer) radiation intensity standard. The inconvenience, cost of measurements, and limited volume restrictions made indoor artificial light sources necessary.

The first standardization work of any consequence was done by the joint meeting of the West Coast Subcommittee of the AIEE Solid State Device Committee and the Semiconductor Photodiode Task Group of the IRE Solid State Devices Committee at Los Angeles, California, on December 17, 1959 (ref. 1). This work defined a standard cell package and defined the procedures to be used in measuring solar cells against a pyrheliometer intensity standard.

Subsequently a task force made up of representatives from various solar cell manufacturers prepared a JEDEC format for the Electronic Industrial Association (EIA) that included solar cell test procedures, calibration techniques, and standardization criteria (ref. 2). From that time on most of the emphasis has been on improving solar cell measurements for determining space sunlight (AM0) performance.

MEASUREMENT TECHNIQUES

There are basically two approaches for making accurate solar cell measurements:

- (1) Use of a light source of any spectral distribution set at the proper intensity using a calibrated standard cell that is essentially identical to the cells being tested
- (2) Use of natural sunlight at an intensity near 100 milliwatts per square centimeter or an artificial light source that essentially has the same spectral distribution as natural sunlight

With artificial light sources the procedure is to set the intensity using the I_{sc} of a calibrated standard cell, then test other cells in the light source at a controlled temperature. In the case of a natural sunlight test or an artificial light source test where the intensity is not controllable, the standard cell I_{sc} is measured at the same time as the test cell so that the data can be extrapolated to the standard test conditions using the equation

$$I_{sc} \text{ (Expol)} = \frac{I_{sc} \text{ (Std. cal.)}}{I_{sc} \text{ (Std. meas.)}} \cdot I_{sc} \text{ (Meas.)}$$

In all of these tests care must be taken to control other test conditions such as collimation angle, intensity uniformity of the light beam, fluctuation or drift, accuracy of read-out system, spectral uniformity, and test fixture design.

CALIBRATION OF STANDARD CELLS

Standard solar cells to be used in the previous measurements should be encapsulated to protect them from damage so that they can provide a stable reference. They should be prepared in accordance with the requirements of JEDEC Publication No. 58. Normally the calibration is performed in natural sunlight preferably under ideal conditions at a high altitude site such as Table Mountain, California. Typical requirements at Spectrolab for calibrating cells are the following: three calibration points are obtained on at least two different days; minimum intensity, 97 milliwatts per square centimeter; maximum sky radiation, 13 percent; intensity stable to ± 0.4 percent in 30-second period; no clouds within 15° half-angle cone of line to Sun; cell temperature, $28^\circ \pm 2^\circ$ C. Calibrations done under these restrictions are reproducible to within a standard error of 2 percent as shown by figure 1. Extrapolation to a standard test condition intensity of 100 milliwatts per square centimeter is performed using the slope of the curve in figure 1 which is 0.7 percent current increase per milliwatts per square centimeter.

PERFORMANCE TESTING

Once a light source has been set up and calibrated using a standard cell then all manufacturers solar cells or solar cell arrays can be tested and compared accurately. It is recommended that the EIA Format JS4-RDF4 be used and followed in rating all terrestrial solar cell systems, with standard test conditions being 100 milliwatts per square centimeter equivalent AM1, sunlight intensity, and a cell test temperature of $28^\circ \pm 2^\circ$ C.

Additional performance data would be provided at typical operating temperatures and sunlight intensities at the option of the suppliers and depending on the application.

REFERENCES

1. Lockheed Missiles and Space Division: Solar Cell Measurement Standardization. Rep. LMSD-288184, Feb. 1960.
2. Electronic Industries Association: Performance Test Procedure for Solar Cells and Calibration Procedure for Solar Cell Standards for Space Vehicle Service. JEDEC Pub. No. 58, July 1966.

DISCUSSION

Q: Why doesn't your regression intercept zero?

A: Because we're really at a high altitude and we're going through a spectral change. If you noticed Henry's number on his extrapolation to AM0 was roughly a 118 factor instead of a 135 factor. The ratio of AM0 to AM1 is 135 to 100. However, you only get an extrapolation to AM0 of 118 or an increase of 18 percent instead of 35 percent. What's happening is as you go closer and closer to the AM0 spectrum the curve is bending and you don't linearly extrapolate according to a regression that would go through the origin - it's a curve. So, we're on that portion of the curve, as you're going through an AM1 region, and, as has come out several times in our discussions, we're at a critical point in our spectrum change that is going to effect the solar cell responses.

Q: Could it also be that the cell is nonlinear if you went down toward zero?

A: No. As you're going down toward zero, you're pretty much following that curve right on down linearly. But we're right at the curve. Those data points are from 95 to about 105 milliwatts. If you went from 95 on down, it's a completely different set of curves and a different slope.

Q: Do the specifications on sunlight, which you have in those standards, allow a reasonable latitude for measurements in other parts of the country?

A: Those conditions are pretty hard to meet. I think Martin would probably be able to do it in their test facilities. However, this is a high altitude test so most places would not be able to meet those requirements. The variability is very small and that's why that site was used as conditions were similar each time. Most places in the country do not have conditions so similar day in and day out. I don't know if anyone else wants to comment on whether those conditions can be met. I know JPL

did some work in their backyard in Pasadena, and I think they did get good correlations trying to do it at their elevation as compared to Table Mountain.

COMMENT: We've tried several different things. But if we tried to compare the pyrheliometer measurements obtained in our backyard with the pyrheliometer measurements obtained at Table Mountain we would find significant deviations in terms of the performance we would predict for the various solar cells. We have used, however, an AM0 extrapolation technique such as that which you get by plotting the log of the short-circuit current against the air mass. But measuring under conditions at JPL and then trying to extrapolate to what we would get at Table Mountain would give us a different kind of number. In other words, at a lower elevation it just doesn't repeat that well.

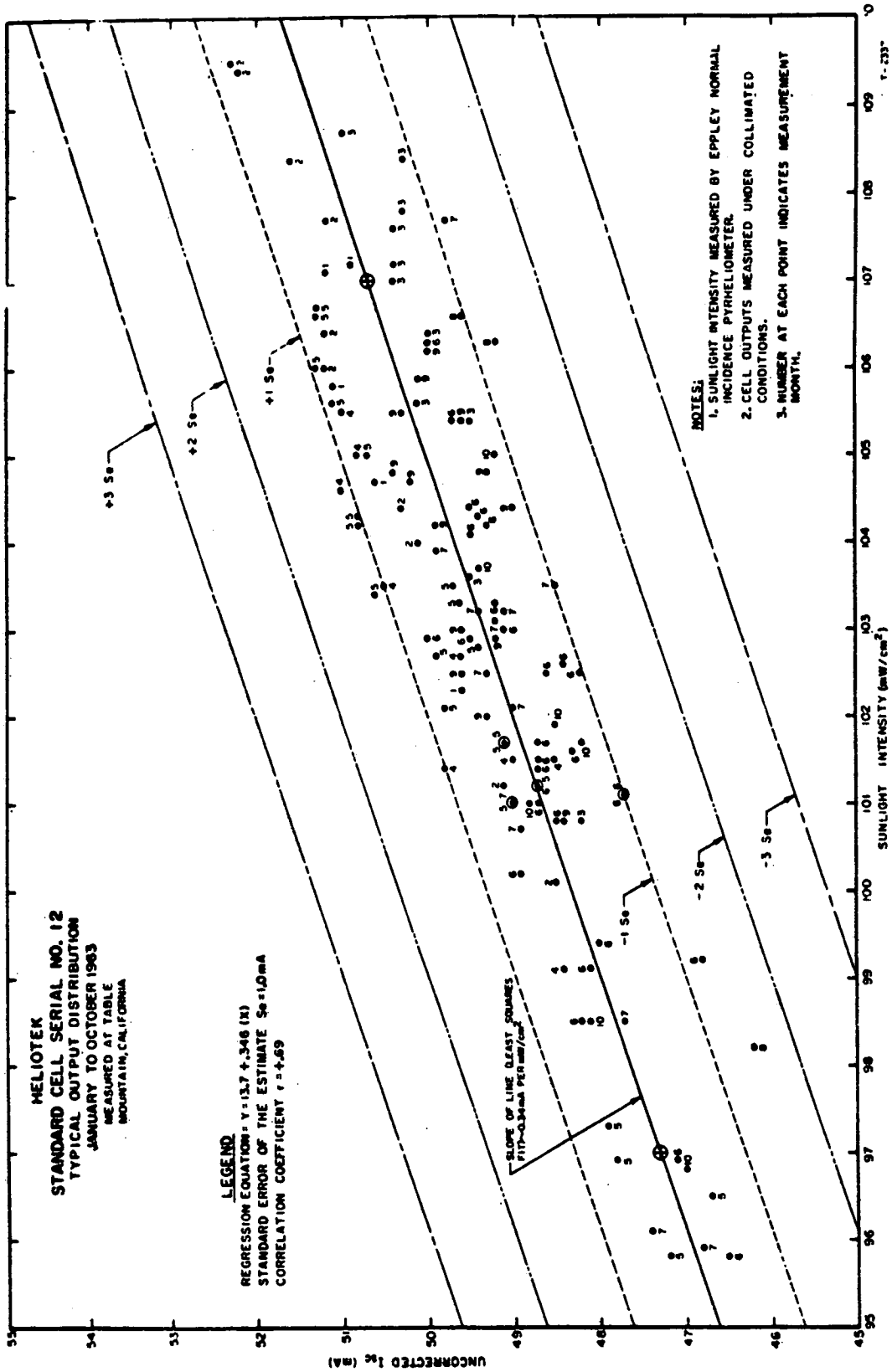


Figure 1.

SOLAR CELL MEASUREMENT TECHNIQUES USED AT

NASA LEWIS RESEARCH CENTER

Russell E. Hart

NASA Lewis Research Center

Cleveland, Ohio 44135

Obtaining accurate values of the outerspace short-circuit current and performance of solar cells has been a difficult problem for years. Attempts to simulate the outerspace sunlight spectrum in the laboratory have not resulted in a perfect spectral match. Thus, the problem of setting the intensity of the simulator becomes paramount. Because of the imperfect spectral match and because of the temporal variation of the source, adjusting the light level with a slowly responding thermopile leads to large inaccuracies. In fact, errors of the order of 10 to 20 percent can easily result from this approach. A more accurate means of adjusting the simulator light level is to use a calibrated solar cell whose spectral response closely matches those of the test cells. Thus deviations in the source spectrum will be compensated for. Methods were developed for obtaining the outerspace output of solar cells using either balloons or high altitude airplanes so that a supply of calibrated cells is readily available. Of course, precautions must be taken in the circuitry used to measure cells to prevent extraneous effects, such as contact resistance, from adversely affecting the measurements. Finally, to complete the solar cell evaluation, a means for obtaining cell spectral response must be available. The objective of this paper is to describe the techniques in use at the Lewis Research Center to obtain accurate measurement of the outer space performance of solar cells.

EXPERIMENTAL TECHNIQUES.

Several techniques are used at NASA Lewis Research Center to evaluate solar cells for space use. These techniques are applicable to establishing standard testing procedures for terrestrial conditions.

Calibrated Solar Cells

As observed before, it is important to have calibrated solar cells of the same type as the cell being tested in solar simulators. To calibrate cells for AM0 conditions a F-106 aircraft is being used as shown in figure 1. An opening was cut just behind the radome on the left side of the aircraft. A 6-inch-diameter, 22-inch-long collimating tube containing the solar cells is mounted behind the opening. The angle of the tube is adjustable for the solar declination angle at the time of each flight. Cells are mounted on a temperature controlled plate at the base of the collimating tube. Although ambient temperatures of about -55°C are encountered, cell temperature is controlled to $25^{\circ}\pm 3^{\circ}\text{C}$. The airplane is flown to 50 000 feet and then descends at a rate of 2000 feet per minute to an altitude of 25 000 feet. During this descent, on an east to west track, solar cell short-circuit current and atmospheric pressure are recorded on a data acquisition system. Air mass is calculated from the atmospheric pressure and the declination angle. A langley plot of the logarithm of the short-circuit current against air mass is made to obtain the outer space short-circuit current. Figure 2 shows the plot of a typical (2 cm by 2 cm) silicon cell without an AR coating. The change in slope at an air mass of 0.5 is caused by dust accumulation at the tropopause. The position of this break is variable. The data above the tropopause are extrapolated to AM0 to obtain the outer space short-circuit current. This current is then corrected slightly for the Earth-Sun distance and ozone absorption in the Chappuia band. Data such as these can be taken for any kind of solar cell. Flights occur all year except during the summer months when the tropopause is too high.

Light Source

With the use of a calibrated standard cell with the same spectral response as the cell being tested, almost any light source can be used to evaluate the unknown cells. Because identical spectral responses are rarely obtained, the cells should be measured in a simulator whose spectrum matches sunlight as closely as possible. The artificial AM0 light source currently used at Lewis is a Spectrosun X-25L solar simulator with close AM0 filtering.

In practice, a standard cell whose spectral response closely approximates the test cell response is used to set the intensity of the solar simulator. The test cell is then placed in the collimated beam and the current-voltage (I-V) characteristic obtained. From the I-V plots, short-circuit current I_{sc} , open-circuit voltage V_{oc} , maximum power P_{max} , curve power factor FF, and efficiency are obtained. Over the years this system has obtained solar cell outer space short-circuit currents with an average error of less than 2 to 3 percent.

Electrical Circuit

A four-wire system such as shown in figure 3 must be used to ensure accurate data. The four-wire method eliminates the effect of wire and contact resistances. Because current does not flow in the voltage leads, the true cell voltage is measured by the X-Y plotter. Next to errors in the short-circuit current, wire and contact resistances are the most common source of error in device measurements. In the load circuit shown, the bucking voltage applied to the cell is controlled by the ten turn potentiometer. Load voltages up to ± 2 volts can be obtained. The 4- and 2-volt batteries used are obtained by cutting one of the straps in a standard 6-volt automobile battery.

Spectral Responses

At Lewis spectral responses are measured using 18 narrow bandpass interference filters ranging in wavelength from 0.35 to 1.2 micrometer. During cell measurement these filters are shifted over the samples sequentially. The light source is a 1000-watt tungsten-iodine bulb whose voltage is carefully regulated. The light intensity through the filters is measured with a thermopile and requires the removal of the test plane. The thermopile is removed, the test plane and cell are replaced, and measurements are made under each filter. The cell current under each filter and the corresponding intensity are used to obtain the spectral response values. Reproducibility of these measurements is ± 5 percent. This measured cell can then be used as a monitor cell against which an unknown cell can be measured without using the thermopile. A simple ratio of both cell currents, corrected for active area differences, multiplied by the spectral response of the known cell yields the spectral response of the unknown cell. This system is easy to use and reproducible. Figure 4 is a typical spectral response obtained in this manner. The test cell is a 10 ohm-centimeter cell with no antireflection coating. It is clear that the monitor cell spectral response must be accurately measured. Therefore, further improvements in absolute spectral response measurements are desirable.

Alternate Light Source

The last system in use is a tungsten lamp light source using ELH lamps made by the General Electric Company. The spectrum of this light source is similar to AM2 sunlight. A dichroic coating on the reflector reflects the visible part of the spectrum toward the test plane while most of the infrared radiation from the bulb is transmitted through the reflector. This has a side benefit of making the control of the sample temperature easier. A light source using these lamps has been used to measure over 4000

silicon cells of the same type. Samples of 50 cells were remeasured in the solar simulator, and the results reproduced to ± 2 percent on all parameters. Thus, it appears that this light source can be a useful tool for measuring cells of similar spectral responses, so long as a standard cell of the same spectral response is available.

CONCLUSIONS

In order to make accurate measurements of the outer space performance of solar cells, a well-defined testing procedure has been evolved. This procedure uses calibrated solar cells whose spectral response closely matches those of the test cells to set the intensity of an artificial light source. The spectrum of this light source reasonably approximates the spectral distribution of outer space sunlight. Electrical measurement circuitry uses a basic four-wire system. Over the years this system has obtained the outer space performance of solar cells with an error of less than 3 percent. As supplementary information, cell spectral responses are measured using 18 narrow bandpass monochromatic interference filters. These measurements permit selection of an appropriate calibrated solar cell to be used in adjusting the light source intensity.

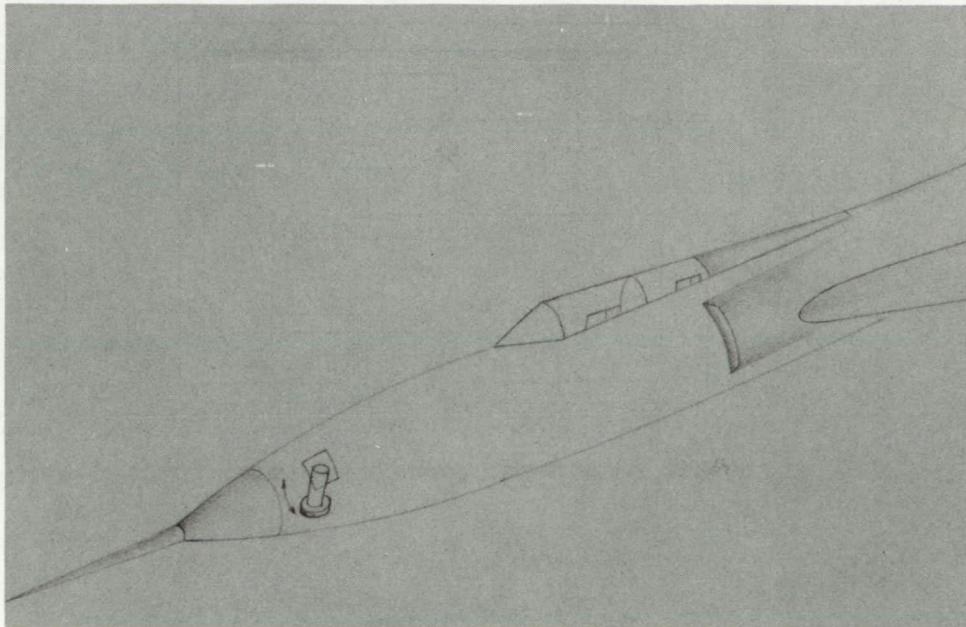


Figure 1. - Collimating tube location in F-106 aircraft.

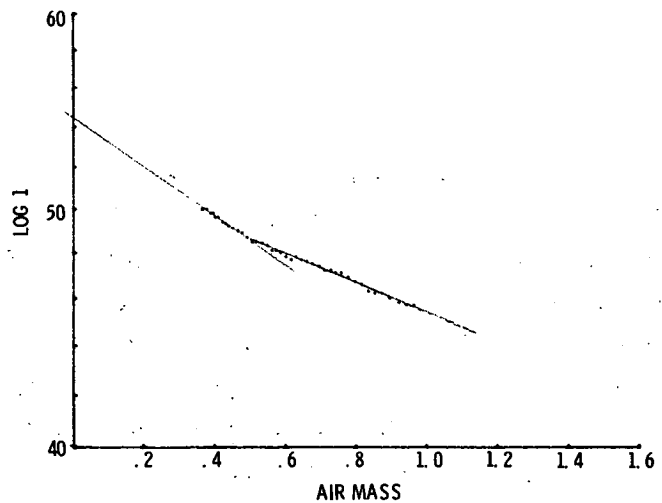


Figure 2 - Langley plot of uncoated silicon cell.

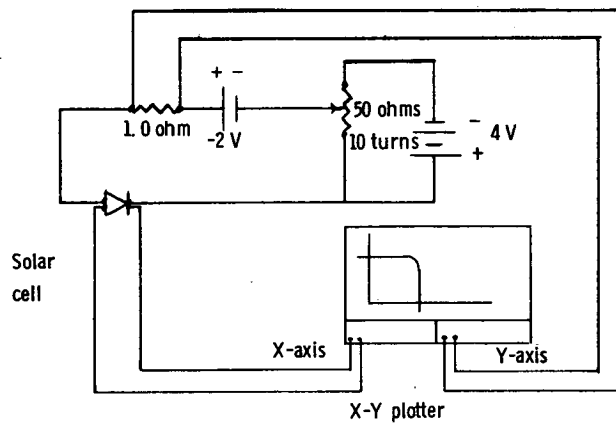


Figure 3 - Circuit diagram of current-voltage curve plotter.

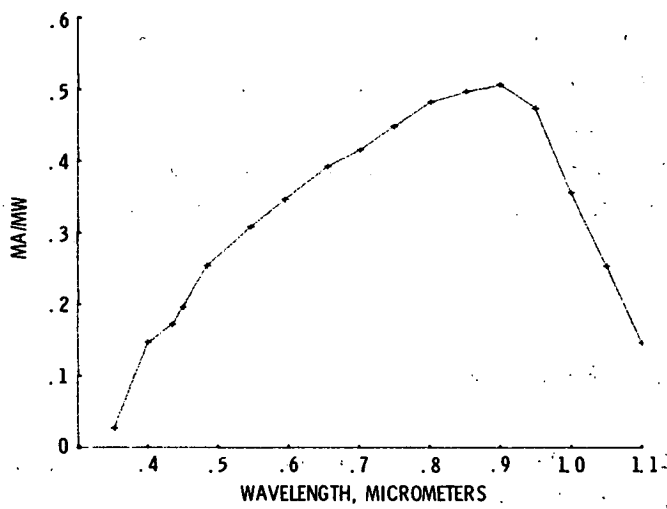


Figure 4 - Uncoated silicon cell spectral response.

A STANDARD FOR SOLAR CELL TESTING AND REPORTING*

John D. Meakin

Institute of Energy Conversion
University of Delaware
Newark, Delaware 19711

Solar cells are rapidly becoming a realistic source of electricity for terrestrial applications. In order that meaningful comparisons can be made between different types of cells and between cells from different producers, it is essential that standardized solar simulation and cell testing be established. The production of a reproducible and reliable simulated solar spectrum is discussed elsewhere. Herein we attempt to lay the groundwork for the meaningful and reliable testing and reporting of Solar Cell performance.

APPLICATION OF TEST RESULTS

There are two general classes of use for solar cell performance figures. The first includes all practical or deployment oriented uses where the total power output per unit area of array is the critical parameter. The second use is related to the basic photovoltaic aspects of solar cells, where the user of the data is concerned with such factors as photon to carrier conversion efficiency within the device.

For the practical application of cells, it is felt that, in principal at least, all cells could be configured to give 100 percent packing density. Accordingly, the cell area used for computing practical efficiency should be the full light intercepting area of the cell excluding only those main current carrying leads which would be either hidden behind the cell itself or could be overlapped by an adjacent cell. The reported performance figure could then be used to compute the potential array output for packing densities less than 100 percent.

For the fundamental analysis of cell performance the actual illuminated area of the cell is of interest; therefore, photon efficiency will be computed using the total cell area minus the area covered by opaque grids or other current collecting devices.

*Supported by the National Science Foundation, Research Applied to National Needs, under Grant AER72-03489, formerly GI-34872.

CELL TESTING

It is felt unnecessary to spell out in great detail the specific electrical techniques for taking current and voltage measurements. Obvious precautions must be taken to obtain meaningful current measurements near the short-circuit condition or voltage measurements near open circuit, especially with cells showing low fill factors. A four-point probe arrangement must be used.

There is both fundamental and practical interest in recording dark I-V curves. In some cells the dark behavior is influenced both by recent exposure to light and by low light intensities. If dark I-V curves are reported, they should be taken at zero illumination and after a sufficient time in the dark so that all transient effects have ceased. If this condition is not met, then the reported curves should be annotated to show the actual "dark" conditions.

Cells may be strongly influenced by the temperature at which the test is performed. Accordingly, the cell temperature must be controlled by holding the cell against a suitable metal block and the actual temperature during testing recorded.

ILLUMINATION

It is not the purpose of this paper to present a definition of a standard illumination such as AM1. However, it is proposed that for natural and simulated illumination the flux be given as an Air Mass Equivalent, e. g. , AM1.2. For simulated illumination the type of source should also be stated.

DEFINITIONS

Physical Parameters

Cell area - practical. - The practical cell area is the full light intercepting area excluding only tabs or leads which are behind the cell or would be covered by adjacent cells.

Cell area - illuminated. - The illuminated cell area is the practical cell area minus the total area of opaque grids or current collecting devices.

Temperature. - The test temperature is that of a metal block held in good thermal contact with the nonilluminated face of the cell.

Electrical Parameters

Short-circuit current. - This is the current flowing through the cell at zero potential drop.

Open-circuit voltage. - This is the potential drop across the cell at zero current flow.

Current density. - This is defined as the total current flow through the cell divided by the practical area. It should be recorded in milliamperes per square centimeter.

Maximum power output. - This is the maximum product of the cell current and voltage. It should be recorded in watts.

Maximum power output density. - This is the maximum power output divided by the practical cell area. It should be recorded in milliwatts per square centimeter.

Open-circuit voltage. - This is the cell voltage at zero current flow and should be recorded in volts.

Fill factor. - This is the ratio of the maximum power output to the product of the short circuit current and open circuit voltage. It may be expressed as a decimal fraction or a percentage.

Input Power Density

Natural insolation. - This is the total incident radiant flux per unit area. It should be expressed in milliwatts per square centimeter and as an AM equivalent.

Simulated insolation. - This should be given as the equivalent natural incident radiant flux (i. e., AM1.0). If available, the actual total flux in milliwatts per square centimeter should be reported.

Practical efficiency. - This is defined as the ratio of the maximum output power density and the input power density. It may be referred to as the efficiency and given as a decimal fraction or percentage.

Photon efficiency. - This is defined as the practical efficiency divided by the ratios of illuminated area to practical area. It must be referred to as the photon efficiency and may be given as a decimal fraction or percentage.

PRESENTATION OF DATA

All measured and deduced parameters should be presented with appropriate error limits based on the measuring accuracy and precision. A suggested report format is as follows:

Cell Test Results

CdS cell	283A2
Cell area, cm^2	54.5 \pm 0.2
Test temperature, $^{\circ}\text{C}$	21 \pm 1
Illumination, W-I, water filter, AM1, mW/cm^2	59
Open-circuit voltage, V	0.47 \pm 0.01
Short-circuit current, mA/cm^2	17.5 \pm 0.2
Fill factor, percent	72.7 \pm 2
Efficiency, percent	5.1 \pm 0.1
Photon efficiency, percent	5.9 \pm 0.1

DISCUSSION

COMMENT: Everybody here has been talking about measuring cells by means of short-circuit current. When we talk about useful engineering information for systems people, I think the one thing we really have to consider doing is measuring power. I suggest maybe the maximum power point or total power under the I-V curve would be a significant improvement in the measurement of solar cell output.

A: Most of those people, especially those with an eye to the application of cells, think very routinely in terms of efficiency which, of course, is always peaked to the maximum power point of the cell. One point which has been reached, which I think should be reiterated is a lot of the aspects of the silicon cell do not carry over into the CdS. One point which I did mean to mention is that if people are to publish I-V curves, especially light and dark I-V curves, then it is necessary, especially with CdS cells, to give the conditions under which these are taken. If you take dark I-V curve first, you can get quite a different dark I-V curve than if you take a light I-V curve and then immediately within the last half minute take a dark I-V curve. So again I think a general plea should be made that when we describe experimental results we should follow the traditional rules that you make it possible for anybody to read those results and go away and reproduce them by following your recipe and instructions.

GENERAL DISCUSSION FOLLOWING SESSION III

COMMENT: We have discussed the last couple of days many things that relate to array measurements as opposed to cell measurements. One of the points I want to raise right now, that we must have agreement on, is that we are going to focus solely in this meeting on cell measurements and not array and systems problems because that is where we are now. I'll propose that and open the floor for discussion on that subject.

COMMENT: What you said is the first thing I'd like to take issue with. The point of making cell measurements is eventually to apply them, and it seems to me the first thing you have to decide is what's significant. For example, is water vapor significant? Cell measurements with or without a water absorption column may be very significant. So, in order to make significant cell measurements, you have to bear in mind what the systems are going to be. Dr. Redfield brought up the point that if you're going to have an economical system you must decide on the optimum thickness of a silicon solar cell. You don't want to waste a lot of very valuable silicon in building a cell that's too thick if you're not going to use the full spectrum of the cell. So I think this is an integral part of this discussion. I agree, you can talk about cell measurements and you can talk about systems measurements and you can conceive, for example, of taking cell measurements as a series of spectral points. But you have to keep in mind what the end purpose is. Otherwise, you may be doing useless refinements.

COMMENT: I think, compared to the air column on top of the cells, the few thousandths of an inch of water vapor which you may have captured in encapsulation, or even the few yards in the longest simulator I've ever seen, makes very little difference in terms of additional adsorption whether you have 100 percent relative humidity or if you have 0 percent relative humidity.

Q: What do you mean you are not going to consider systems?

A: The problem that we have facing us immediately is that there are people in the ERDA and NSF programs making and evaluating devices and trying to find out whether one approach has a performance advantage over some other approach. At the present time we have no agreement on a standard testing procedure, a standard light source, or a standard spectrum. We must in this meeting reach agreement on those so that one of the recommendations of this workshop will be standardized test procedures against which all experimenters can evaluate their cells. This does not have to be the best of all possible systems because we have many unanswered questions which necessitate more research before we come up with an ultimate system.

This would merely be an interim system that would take us through this next year until we can meet again. The questions we're going to raise today will need to be answered and then we can come back and have a second look at a more permanent system. At that point, some of the array problems or measurements of the arrays in the field are a reasonable consideration.

COMMENT: I think our meeting should begin to address the problems associated with the so-called systems measurements. I don't want to detract from what you've said, because I think it's very important. But, we also have a real time problem in understanding the systematic applications of the technology that we have. I think that it may be possible in the course of the various workshops to broaden the discussion from perhaps what you have suggested to something which may have a greater significance to the community in terms of getting the data we need for all types of cells.

COMMENT: It seems to me from the number of ideas that have been passing around that this is the kind of thing that is needed in order to characterize cells, but not the arrays yet, in all the important parameters. A standard spectrum has to be chosen taking into account the nonlinear effects of things such as cadmium sulfide. A monochromatic beam has to be available. The angle of incidence from the normal has to be variable. We have to be able to measure the power in the monochromatic beam. The electronics may never be done this way, but this will give you an idea what has to be done. You measure the current and convert it to a voltage. You measure a change in current that corresponds to turning on and off a beam. You measure the total current, the current which corresponds to having the standard spectrum on the cell. You do the same thing for voltage across the load. You now have all the electrical parameters as a function of incident radiation. For a fairly monochromatic beam, it's possible to measure this response function at the standard distribution for various angles of incidence. You get the actual response for the different angles of incidence, and this allows you to go from your standard distribution to the particular distribution you expect in your particular local environment. It seems to me that almost every question is fairly well addressed by this system, except for arrays. We don't have enough power in a monochromatic beam spread over the larger rays to do a measurement of this nature.

RESULTS OF SESSION I WORKING GROUP - SOLAR INTENSITY AND SPECTRUM CONDITIONS FOR TERRESTRIAL PHOTOVOLTAICS

John R. Hickey, Chairman

Twenty-one of the participants at the workshop were included in working group I. The working group met for approximately 5 hours on March 20, 1975. The main function of the discussion of this working group was to establish a representative terrestrial solar radiation environment. In addition, the group discussed a number of related topics concerning the calculation and measurement of the terrestrial solar energy for use in support of the photovoltaic program.

Since the charge to the subgroup by the workshop chairman was to concentrate on a 1-year interim period, the subgroup chairman attempted to limit discussion to this. A set of recommendations and comments were developed from the discussions and were presented to the general workshop attendees on March 21, 1975. It is obvious that followup work by a smaller committee will be required in the near future to come up with a refined set of recommendations. This report is essentially an attempt by the working group I chairman to elaborate on the meeting.

CHAIRMAN'S REMARKS

1. It had been established in a previous session that the wavelength scale of interest was essentially that from 0.35 to 1.4 micrometers.

2. There was a need for additional people in this working group who were more familiar with the present state of terrestrial solar measurements. Roland Hulstrom had to leave before the working group session, and Mr. Goldberg of the Smithsonian Radiation Biology Laboratory and Dr. K. Hansen of NOAA could not attend the meeting.

3. The necessary interaction with other disciplines employing solar radiation data such as meteorology, atmospheric physics, other solar radiation utilization programs, radiation biology, agriculture, hydrology, etc. will be necessary.

4. The fate of the recommendations made at the November 1973 NSF/NOAA workshop related to the NOAA measurement system and network should be more clearly understood. Mike Riches of NOAA explained much of this both in the working group and at the general sessions.

5. There seemed to be a general feeling that the 1-year interim period put too many constraints on the discussion, even for the topic of general measurement.

CONDUCT OF WORKING GROUP

The discussion began with a request for a recommendation on which solar curve to employ. The basic result was that no acceptable measured terrestrial curve could be employed. A number of curves including Moon's and Gate's work were reviewed. It was the opinion of many that an extraterrestrial solar curve should be employed in conjunction with a model atmosphere. Which extraterrestrial curve and which model then became the questions. It was recommended that a curve derived from Thekaekara's curve (NASA SP-8005) be considered. Since curves were published in the NSF Workshop proceedings it was felt that the basic data types and programs must be available there. A number of persons thought the use of other curves and models might be more appropriate, but that the curve which would be derived by Thekaekara might be the easiest to get for the interim period.

Attempts were made to ascertain which air mass (solar zenith angle) would be most representative. For the continental United States and on a year round basis it was felt that AM2 would suffice for the interim period.

The fact that the curve should be representative of Sun plus sky radiation rather than only direct beam was discussed at some length. For blue sensitive cells it was felt that Sun plus sky was more representative of the true situation. It was noted that the curve should be representative of some mounting configuration angle such as the latitude or latitude plus 10° rather than either the direct or the global (horizontal) beam. No conclusions were made with regard to these matters. It is doubtful that any present atmospheric model would calculate these fluxes directly.

Regarding atmospheric models, Dr. Halpern, of IBM, was consulted by the group on what their (Dave, et al.) model could do. He explained that they were very committed and that to perform such an analysis in the near future would be difficult. He suggested that Dr. Baxter Armstrong be contacted soon if the committee wished to pursue this matter in the future.

The chairman expressed the feeling that the output of the cells was a function of the integral of the product of the relative spectral response of the cell with the relative spectral distribution of the incident light. This, of course, is a simple case omitting temperature, angular dependence, and other effects. If the relative spectral response of a cell is chosen, it can be convolved with many possible solar curves to ascertain the sensitivity of the integral to the shape of the solar curve. This can be done using numerical integration techniques without having to worry about actual measurements. The method has been proven in filter factor analysis commonly used in filter radiometry. It

was also mentioned that when this method is applied to calculating cell efficiencies by a technique of dividing by the total incident radiation as measured by a conventional pyranometer or pyrheliometer the limits of the integral in the numerator are essentially those of the cell response while the integral in the denominator has limits of the entire terrestrial solar spectrum.

It must be pointed out, and it was a number of times during the workshop, that clouds are the biggest modifier of solar radiation reaching the ground. Also, auxiliary weather data would probably be required at sites where solar radiation is to be measured.

Mike Riches, of NOAA, explained a number of times the NOAA position regarding the network and other special solar monitoring stations. It is the chairman's opinion that NOAA should prepare a short report on this topic, which comes down to a cost analysis versus data utilization and necessity.

Since some of the participants were knowledgeable concerning the recommendations of the NSF workshop, the workshop proceedings were referred to a number of times. This prompted the other attendees to request that they be supplied with copies of the proceedings so they would be prepared for future discussions.

It was a general opinion that good spectral response data should be obtained for the various photovoltaic devices. It was felt that high accuracy absolute spectral response determinations are fundamental to this field. The high accuracy methods described by Jon Geist were referred to. It was generally accepted that support of this type of fundamental radiometry should be supported by agencies sponsoring the photovoltaic workshop.

The matter of units was discussed briefly. It was generally accepted that SI units be employed in reporting results in this discipline. As far as the solar radiation quantities are concerned, the group preferred units of watt-meters, micrometers, etc., such that solar spectral curves would be expressed in $\text{Wm}^{-2}\text{-}\mu\text{m}^{-1}$ or in $\text{Wcm}^{-2}\text{-}\mu\text{m}^{-1}$ (Later in the general session there was a request that the solar radiation also be expressed in photon flux.)

CONCLUDING REMARKS

It should be obvious that the discussion did not proceed in the orderly fashion as delineated previously. The discussions varied from one topic to another and many topics overlapped or had a direct bearing on each other. This is not meant to be a complete recap of the working group, but a group of thoughts which were easily separated in the mind of the chairman.

From such an attempt to classify the recommendations arising from the workshop, the initial set of recommendations presented on March 21, 1975, were prepared. These

recommendations, in a somewhat modified and corrected form, are here restated:

1. The terrestrial solar curve to be used to assess photovoltaic response should be one computed using an accepted extraterrestrial solar spectral irradiance curve, which is corrected to a terrestrial curve using a model atmosphere.

(a) For the 1-year interim period, a direct beam curve for AM2 should be employed. This should be requested from Dr. M. Thekaekara of NASA/GSFC. A tabulation over the wavelength range of 0.35 to 1.4 micrometers should be requested. The working group felt that this should be used for the interim period only while a more representative terrestrial curve is developed.

(b) After the interim period a more representative curve should be developed from a suitable extraterrestrial curve and model and the IBM group should be requested by the organizing committee to develop such a curve using their 83 unit spectral interval model. The letter of request should be submitted in the near future.

(c) In the interim period the suitability of the curve should be assessed by a comparison with available spectral data, specifically that being obtained by the Smithsonian Institution. The extraterrestrial curve should be compared with new satellite data from NIMBUS F.

2. The pertinent recommendations of working group 2 of the NSF/NOAA workshop should be endorsed regarding the monitoring network and specifically.

(a) The spectral distribution in 0.1 micrometer bandwidths at 10-minute intervals at 5 stations should be measured and the auxiliary weather data such as cloud cover should be reported for these stations. A subcommittee should be formed to decide whether direct or global data are necessary.

(b) NOAA should record high resolution high accuracy spectral radiation measurements at Boulder.

(c) A high quality mobile station should be operated as part of the NOAA program.

3. The members of this workshop should be supplied with copies of the NSF/NOAA workshop report.

4. The Report of the Workshop on Accurate Radiometry for Solar Conversion should be brought to the attention of this organizing committee.

5. The high accuracy spectral radiometric analysis techniques described by Jon Geist should be supported by this photovoltaic group.

6. SI units should be employed in all reporting of solar data and solar spectral data related to this program.

RESULTS OF SESSION II WORKING GROUP - TERRESTRIAL SUNLIGHT SIMULATION

Henry Curtis, Chairman

The topics for discussion in session II (as listed by the letter of invitation to the Workshop) were

Irradiance and spectral irradiance standards

Measurement techniques for lamp sources and solar simulator systems

Lamp sources and simulator systems which accurately and reproducibly simulate terrestrial sunlight at low cost

There were approximately 15 attendees at session II with the bulk of the discussion concerning the choice of the source for terrestrial sunlight simulation. The main recommendations of session II are as follows:

1. A tungsten filament quartz-halogen lamp with same sort of dichoric filtering should be the source for terrestrial solar simulation. The major considerations in this choice were low cost, interim period of use, and availability. Of these the low cost was the most important. There were strong reservations concerning tungsten lamps by people with cells with significant response in the blue region (0.4 to 0.5 μm). It was the general consensus that if a particular cell suffered by comparisons made using a tungsten source further qualifying data could be given. There are also problems involved in suggesting a standard source when there is little operational experience with such sources.

2. All lamps should be operated at a constant voltage with total irradiance measured using a black total detector. For testing purposes, the irradiance level should be set using a standard cell (with a spectral response close to the cell being tested) supplied by the same central testing lab. To obtain the desired irradiance level, either add lamps or vary the distance, but keep voltage constant.

3. At the present time, the only standard of spectral irradiance is the tungsten filament, quartz halogen lamp with reflector available from the NBS. Any measurements of spectral irradiance of a source, made using a monochromator, should be related to this standard. An alternate method to measure spectral irradiance is with a set of standard filtered cells supplied by a central testing lab.

4. Work should continue toward measuring the absolute spectral response of cells. Then the cell efficiency could be calculated using the standard solar curve from session I.

RESULTS OF SESSION III WORKING GROUP - METHODOLOGY FOR
MEASUREMENT AND CALIBRATION OF SOLAR CELLS

Eugene L. Ralph, Chairman

Although this working group had initial difficulty understanding the workshop objectives and guidelines, these difficulties were resolved and some unanimous conclusions were formulated. The key factor in resolving these questions was the realization that an agreement on acceptable measurement methods was needed immediately that could be used over the next year to make accurate comparative measurements of many different types of cells at various laboratories across the country. With these guidelines and time periods in mind, the following conclusions and recommendations were unanimously agreed on:

1. It was concluded that a set of recommended data parameters be adapted as minimum standard measurements and standard test conditions for comparing different types of cells and for reporting performance data. Of course, additional data can always be provided, but it was concluded that the following list represents the minimum data that provides sufficient information to intelligently compare cells:

Light intensity, mW/cm^2 (sunlight equivalent)	100
Cell temperature, $^{\circ}\text{C}$	28 \pm 2
Cell efficiency, mW/cm^2	$\frac{I_{\text{mp}} \bar{V}_{\text{mp}}}{A} \div 100$
Total cell area including electrodes, A	
Short-circuit current, I_{sc} at V, mV	<20
Open-circuit voltage, V_{oc} with meter, $\text{k}\Omega/\text{V}$	>10
Light beam axis perpendicular to cell	

2. It was realized that the acceptable test method was dependent on whether the measurement was for research or scientific testing, production testing, or large systems testing. Consequently, a listing (following table) of proposed testing methods were evaluated in respect to these various categories to see which test methods were acceptable to everyone. If both a no and a yes appear, it indicates that at least one person objected and at least one agreed to this test method for some reason. A no indicates that everyone objected to this method. A yes indicates that everyone would accept the results of this test method. Since the ground rules were to consider test methods for only

this coming year and time was short, no ratings were made for the systems tests.

The following table summarizes the results:

Test method	R&D tests	Production tests
Filter wheel	No/Yes	No
Tungsten ^a	No	No/Yes
Xenon (filtered; pyrhelimeter)	No/Yes	No/Yes
Xenon ^a (filtered)	Yes	Yes
Tungsten ^a (ELH)	No/Yes	No/Yes
(SR biased × SD) ^b	No/Yes	No
Sunlight (pyrhelimeter)	Yes	No/Yes
Sunlight simulator ^c	No/Yes	No/Yes

^aStandard solar cell set to equivalent of 100 mW/cm² of sunlight.

^bSpectral response under biased light times sunlight spectral distribution; absolute calibration.

^cAbsolute calibration.

From this table it is clear that the only test that everyone felt was satisfactory for production testing of a wide range of cell types was a filtered xenon light source set up with a standard cell of the type being tested. This test method was also found acceptable for R&D or scientific measurements. Measurements in sunlight against a calibrated pyranometer or other thermopile detector were found to be acceptable and accurate for R&D tests but not satisfactory for production due to the limited test times.

3. It was agreed that standard solar cells must be properly packaged and protected and calibrated by a recognized testing laboratory. The test method should be to test in sunlight against a calibrated thermopile detector. A standard must be similar to the type cell that is to be tested in the artificial sunlight sources. That is, it should be similar material, similar spectral response, and have been manufactured using essentially the same fabrication processes.

4. Group III had the following general recommendations:

(a) The minimum specifications for sunlight conditions during calibration of standard solar cells still need to be defined and a committee should do this very soon. This committee should specify cloud conditions, sky radiation, H₂O content, intensity, etc.

(b) A central laboratory should be designated responsible for calibrating standards and setting up testing standards.

(c) A program should be started now to determine the influence and sensitivity of various parameters which may or may not be important such as air mass, scattered light, H₂O vapor, seasonal changes, intensity effects, angle of incidence effects, and degradation of light sources effects.

(d) Preparation should begin now for the large scale systems testing requirements that will soon be needed.

(e) The degree of accuracy needed in all these tests should be determined so that excessive efforts for high accuracy are not expended if the accuracy isn't needed for the applications.

UNIFIED RECOMMENDATIONS OF THE WORKSHOP

Henry Brandhorst, Coordinator

Differences among the recommendations made by each of the Workshop sessions were resolved during the Workshop by a meeting of the chairmen. These unified recommendations were presented to and discussed by the Workshop as a whole. The agreed upon recommendations of the whole Workshop for the interim period of 1 year are as follows.

Solar cell measurements: It was agreed that measurements of solar cell performance in natural sunlight are the most acceptable. The details of the measuring procedure to be used will be made available later. For laboratory measurements, a broadband spectrum filtered artificial light source was recommended. The light source will most likely be a xenon arc lamp because this source contains the ultraviolet light needed for accurate assessment of cell performance. Furthermore, many of these simulators are readily available. The intensity of this light source is to be set with a calibrated solar cell of the same spectral response as the cell to be tested insofar as possible. The experience of the space program has shown that using this procedure results in reliable measurements under artificial light sources.

Performance measurement: Several measurement conditions were specified by the Workshop so as to put terrestrial solar cell measurements on a common basis. A cell temperature of $28^{\circ} \pm 2^{\circ}$ C was specified as was a 100 milliwatt per square centimeter intensity for the solar simulator. This intensity value was chosen for tradition, ease of efficiency calculation, and from a desire to use as high an intensity as reasonable to test cell operation. For the purpose of efficiency calculations, total cell area is to be used. Short-circuit current is to be measured at a less than or equal to a 20-millivolt load, and the impedance of the voltmeter used to obtain open-circuit voltage is to be greater than 10^4 ohms per volt.

Supporting measurement techniques: The Workshop recommended that an absolute spectral response measurement technique which is applicable to all types of solar cells be developed in a timely fashion.

Program support: It was agreed that for theoretical calculations, a standard AM2 solar spectral distribution curve should be used. AM2 was chosen because it is more representative of the spectral distribution viewed by a solar cell year round than an AM1 distribution.

Finally, it was recommended that a centralized national laboratory be established to perform reference photovoltaic measurements, issue calibrated solar cells, and perform the R&D necessary to support the measurements program. It is anticipated that the NASA-Lewis Research Center will fill that role for the ERDA.

Page intentionally left blank

Page intentionally left blank

APPENDIX - SUPPLEMENTAL PAPERS

Page intentionally left blank

Page intentionally left blank

SPECTRAL DISTRIBUTION OF DIRECT AND DIFFUSE SOLAR ENERGY

RECEIVED AT SEA LEVEL OF A MODEL ATMOSPHERE*

J. V. Dave and P. Halpern

IBM Corporation Scientific Center
Palo Alto, California 94304

and

N. Braslau

IBM Thomas J. Watson Research Center
Yorktown Heights, New York 10598

Knowledge of the spectral characteristics of the direct and diffuse solar energy received by surfaces near the ground is required in the photovoltaic harvesting of solar energy, and in other fields such as biophysics and illumination engineering. These characteristics depend on optical properties of various atmospheric constituents and of the underlying ground, on the position of the Sun, and orientation as well as geometric shape of the surface. Experimental determination of these multi-parameter dependent characteristics has been classified as one of the major tasks in the field of atmospheric radiation. Thus, it is customary to restrict such experimental investigations to a few selected cases only (e.g., McCree and Keener, 1974).

Recently, Dave and Braslau (1974) have performed extensive calculations of the transfer of solar energy through one-dimensional, but otherwise realistic, models of the terrestrial atmosphere. For this purpose, they divided the solar spectrum (0.28 to 2.5 μm) into 83 spectral intervals of unequal width for simulating the absorption bands of carbon dioxide, oxygen, ozone, and water vapor. Computations of the direct as well as diffuse spectral energy passing at levels with height h kilometers above the ground, and with the parameter h given by $h = 0(1)50$ kilometers, were carried out after including all orders of scattering and appropriate absorption by molecules, aerosols, and water drops. Models used by them vary from a model with no gaseous absorption and no aerosols or water drops at one extreme to several models with climatic cloud cover and high concentrations of aerosols at the other. This study of Dave and Braslau culminated in a

*Palo Alto Scientific Center Report 320-3332.

voluminous set of data which can be used to obtain values of the direct and diffuse components of solar energy in 83 different spectral intervals, 51 levels of the atmosphere separated by 1-kilometer intervals, 8 different atmospheric models, 9 different positions of the Sun, and any reasonable Lambert reflectivity of the underlying surface.

As the existence of such data became known, several scientists from different disciplines inquired about the possibility of obtaining a part of the whole of these data in graphic as well as tabular form. We hope that some of their needs will be met by this report in which we have discussed spectral characteristics of the direct and diffuse solar energy passing through a horizontal surface at the bottom of one model atmosphere. This model atmosphere corresponds to an average mid-latitude summer case but without any clouds, resting on a perfectly absorbing ground, and illuminated by the Sun at 60° from the local zenith.

ATMOSPHERIC MODEL

The atmospheric model for which results are discussed in this report is referred to as Model C1 by Dave and Braslau (1974). A vertical column of unit cross section of this model contains 0.318 atm-cm of ozone, and 2.925 gm-cm^{-2} of water vapor whose height distributions correspond to those encountered under average mid-latitude, summer conditions (McClatchey et al., 1970). This unit column also contains 19.7×10^6 particles in 1-square-centimeter column with its height distribution having a strong maximum near the ground. Further information about the height distributions of these three constituents can be found in figure 6 of the original report. A constant mass-mixing ratio was assumed for the other two absorbing constituents (viz. carbon dioxide and oxygen).

The size-distribution function of aerosol particles (assumed spherical) at any given level is represented by a modified gamma function with a mode radius of 0.07 micrometer and referred to as "Haze L" by Deirmendjian (1969). This is a typical aerosol size distribution observed in the lower parts of the atmosphere over continents. The aerosol substance is assumed to be made of a material with a refractive index of 1.5 to 0.01i (i. e., the aerosols absorb a small fraction of the energy incident on them) independent of the wavelength. Spectral dependence of the scattering and absorption optical thicknesses of this aerosol column can be found in another paper of Braslau and Dave (1973 b).

LIMITATIONS

The model of the atmosphere used in our investigation is a one-dimensional, or a plane-parallel, model. That is, the atmosphere is assumed to be homogeneous and of

infinite extent in horizontal directions. Any nonhomogeneity due to changes in the absorption and/or scattering properties of a unit volume is confined to the vertical direction only. The basic equation of the atmospheric radiative transfer for a plane-parallel atmosphere is solved, for a given spectral region, by using the method of a direct numerical solution of the spherical harmonics approximation to the transfer equation (Dave and Canosa, 1974). In this way, appropriate absorption and all orders of scattering are included automatically.

This or any other method for solving the basic transfer equation for the scattering as well as absorption phenomena is strictly valid only for the case of monochromatic incident radiation. It is permissible to treat a part of the electromagnetic spectrum as monochromatic when the absorbing and/or scattering properties of atmospheric constituents vary gradually and by small amount with wavelength over the region under consideration, and, furthermore, the Bouger-Langley law is valid. Over the spectral region of interest the absorption coefficients of ozone, water vapor, carbon dioxide, and ozone vary rapidly and by large amounts. Furthermore, because of the band structure and overlapping of lines, the Bouger-Langley law is not applicable in the case of water vapor and carbon dioxide absorption unless the absorption is fairly weak. In order to meet the restrictions of monochromaticity in the strictest sense, one would have to divide the solar spectrum into several thousand intervals. In spite of this, we feel that the spectral division used by us provides reliable data of high practical value for about 69 of the 83 spectral intervals. The spectral regions for which the calculated diffuse solar energy data can be in some doubt are those having strong absorption by carbon dioxide and water vapor. Further information on this aspect can be found in sections 3d to 3f of Braslau and Dave (1973 a), and in the fourth paragraph of the Introduction in Dave and Braslau (1974).

RESULTS

Three quantities (expressed in the units $\text{mW-cm}^{-2}-\mu\text{m}^{-1}$) pertinent to our discussion are defined as follows:

- $F_{o\lambda}$ direct solar energy received by a horizontal flat surface at the top of the atmospheric model
- $F_{s\lambda}$ direct solar energy received by a horizontal flat surface at the bottom (viz. sea-level) of the atmospheric model
- $F_{d\lambda}$ diffuse skylight energy received by a horizontal flat surface at the bottom of the atmospheric model

Strictly speaking, these quantities represent power per unit wavelength interval. The work energy is used in the customary sense.

Values of $F_{o\lambda}$, $F_{s\lambda}$, and $F_{d\lambda}$ are plotted as functions of wavelength in micrometers in figures 1 and 2 for the spectral regions 0.305 to 1.05 and 1.05 to 2.5 micrometers, respectively. These values are for the model C1 (Dave and Braslau, 1974) resting on a perfectly absorbing ground and illuminated by the Sun at 60° from the local zenith. Numerical values of these quantities are given in table I.

Values of $F_{o\lambda}$ quoted here are based on those reported in the Handbook of Geophysics (Howard et al., 1961). The reader interested in obtaining values of $F_{o\lambda}$, $F_{s\lambda}$, and $F_{d\lambda}$ corresponding to the most recent solar irradiance (P_λ) data (Thekaekara, 1973) can do so in the manner now described.

Consider, for example, that Thekaekara (1973) gives a value of $105.9 \text{ mW-cm}^{-2}\text{-}\mu\text{m}^{-1}$ at $\lambda = 0.33$ micrometer. Thus, the most recent value of $F_{o\lambda}$ for our model is $52.95 \text{ mW-cm}^{-2}\text{-}\mu\text{m}^{-1}$ (note that a factor of $\cos \theta_o = \cos 60^\circ = 0.5$ is used to obtain the normal component of the direct solar energy), while the value used by us in table I is $55.50 \text{ mW-cm}^{-2}\text{-}\mu\text{m}^{-1}$. Hence, our numerical results for $\lambda = 0.33$ micrometer will have to be multiplied by a factor of $52.95/55.50$, or 0.954 . Accordingly, values of $F_{o\lambda}$, $F_{s\lambda}$, and $F_{d\lambda}$ corresponding to $\lambda = 0.33$ micrometer and the most recent solar irradiance data are 52.95 , 7.72 , and $17.05 \text{ mW-cm}^{-2}\text{-}\mu\text{m}^{-1}$, respectively.

The presence of the intervening atmosphere results in the introduction of several additional absorption features in the spectrum of the direct and diffuse solar energy emerging at the bottom of the model atmosphere. The atmospheric gases responsible for a given feature can be identified with the help of the results presented in figures 7 and 8 of Braslau and Dave (1973 a). Another important feature of the results presented in figure 1 is that the diffuse solar energy received by a horizontal flat surface is greater than the direct energy received by it for wavelengths smaller than 0.375 micrometer. This is due to much higher scattering efficiency of molecules and aerosols at the shorter wavelengths. Consequently, we find small but significant displacements among the maxima of the three spectral distribution curves. The $F_{o\lambda}$ as a function of λ curve shows a maximum around 0.46 micrometer, but that of $F_{s\lambda}$ as a function of λ shows a broad maximum in the spectral region 0.47 to 0.60 micrometer, and that of $F_{d\lambda}$ as a function of λ shows a maximum in the range 0.41 to 0.46 micrometer.

In table II, we have given values of the ratio ($F_{d\lambda}/F_{s\lambda}$) of the diffuse to direct solar energy received by a horizontal surface located at the bottom of two different model atmospheres for nine different zenith angles (θ_o) of the Sun and $\lambda = 0.535$ micrometer. One of the models is the model C1 described earlier; the other model referred to as D1 contains 82.3×10^6 particles in its vertical column of 1 square centimeter cross section. This 4.2-fold increase in the aerosol content is arrived at after increasing the aerosol content of the 0 to 5 and 12 to 25 kilometer regions of model C1 (see fig. 6 of Dave and Braslau, 1974). The ratio $F_{d\lambda}/F_{s\lambda}$ increases rapidly with an increase in the zenith

distance of the Sun. For model C1, the diffuse component is about one-seventh the direct component for the case of overhead Sun, but about 1.2 as much as the direct one for the Sun at 80° from the local zenith. Values of these ratios increase with an increase in the aerosol content, but not linearly. A 4.2-fold increase in the aerosol content results in the increase in the value of $F_{d\lambda}/F_{s\lambda}$ by a factor of about 3.3 for $\theta_0 = 0^\circ$ and by a factor of about 7.4 for $\theta_0 = 80^\circ$.

CONCLUSION

In the preceding sections we have presented representative results of an extensive simulation study to show the spectral dependence of the diffuse component in the total solar energy rate received by a horizontal surface at the bottom of the atmosphere. These results can be used for inferring general trends and for preliminary planning in a variety of solar energy applications. Desirability of providing such simulation data for other zenith angles of the Sun and atmospheric models can be determined after assessing the degree of interest of the scientific community. There is no basic difficulty in generating such simulation data for any one-dimensional model of the terrestrial atmosphere and for cases where a much finer division of the solar spectrum is used. To this effect, it should be pointed out that capability now also exists for determining the gradients of sky brightness as a function of wavelength and zenith angle of the Sun (Dave, 1975 a and b).

REFERENCES

1. Braslau, N.; and Dave, J. V.: Effect of Aerosols on the Transfer of Solar Energy Through Realistic Model Atmospheres. Part I: Non-Absorbing Aerosols. *J. Appl. Meteor.*, vol. 12, 1973, pp. 601-615.
2. Braslau, N.; and Dave, J. V.: Effect of Aerosols on the Transfer of Solar Energy Through Realistic Model Atmospheres. Part II: Partly-Absorbing Aerosols. *J. Appl. Meteor.*, vol. 12, 1973, pp. 616-619.
3. Dave, J. V.: A Direct Solution of the Spherical Harmonics Approximation to the Radiative Transfer Equation for an Arbitrary Solar Elevation. Part I: Theory. *J. Atmos. Sci.*, vol. 32, 1975, pp. 790-798.
4. Dave, J. V.: A Direct Solution of the Spherical Harmonics Approximation to the Radiative Transfer Equation for an Arbitrary Solar Elevation. Part II: Results. *J. Atmos. Sci.*, vol. 32, to be published in July 1975 issue.

5. Dave, J. V.; and Braslau, N.: Effect of Cloudiness on the Transfer of Solar Energy Through Realistic Model Atmospheres. *J. Appl. Meteor.*, vol. 14, 1975, pp. 388-395. (Also IBM Watson Research Center, Yorktown Heights, N. Y. Report No. RC 4869, 1974.)
6. Dave, J. V.; and Canosa, J.: A Direct Solution of the Radiative Transfer Equation: Application to Atmospheric Models with Arbitrary Vertical Nonhomogeneities. *J. Atmos. Sci.*, vol. 31, 1974, pp. 1089-1101.
7. Deirmendjian, D.: *Electromagnetic Scattering on Spherical Polydispersions*. American Elsevier, New York, 1969.
8. Howard, J. N.; King, J. I. F.; and Gast, P. R.: Thermal Radiation. Ch. 16 in *Handbook of Geophysics*, rev. ed., MacMillan, New York, 1961.
9. McClatchey, R. A.; Fenn, R. W.; Selby, J. E. A.; Garing, J. S.; and Volz, F. E.: Optical Properties of the Atmosphere. Rep. No. AFCRL-70-0527, Air Force Cambridge Research Laboratories, 1970.
10. McCree, K. J.; and Keener, M. E.: Effect of Atmospheric Turbidity on the Photosynthetic Rates of Leaves. *Agricult. Meteor.*, vol. 13, 1974, pp. 349-357.
11. Thekaekara, M. P.: Solar Energy Outside the Earth's Atmosphere. *Solar Energy*, vol. 14, 1973, pp. 109-127.

TABLE I - SPECTRAL DISTRIBUTION OF DIRECT SOLAR ENERGY (F_{D}) RECEIVED BY A HORIZONTAL SURFACE AT TOP AND DIRECT (F_{D}) AND DIFFUSE (F_{D}) SOLAR ENERGY RECEIVED BY IT AT BOTTOM OF A MODEL ATMOSPHERE

[Zenith angle of the sun, 60° ; Lambert reflectivity, 0; size distribution of aerosol, Haze I; refractive index, 1.5 to 0.01; atmospheric model, C1 (see Dave and Braisau, 1974).]

Center wavelength, μm	Bandwidth, μm	F_{D} , $\text{mW-cm}^{-2}\text{-}\mu\text{m}^{-1}$	F_{D} , $\text{mW-cm}^{-2}\text{-}\mu\text{m}^{-1}$	F_{D} , $\text{mW-cm}^{-2}\text{-}\mu\text{m}^{-1}$	Center wavelength, μm	Bandwidth, μm	F_{D} , $\text{mW-cm}^{-2}\text{-}\mu\text{m}^{-1}$	F_{D} , $\text{mW-cm}^{-2}\text{-}\mu\text{m}^{-1}$	F_{D} , $\text{mW-cm}^{-2}\text{-}\mu\text{m}^{-1}$
.2975	0.0050	30.20	0.0004	0.0021	0.9935	0.0130	37.76	30.79	4.45
.3025		30.00	.032	.128	1.0490	.0980	33.90	28.57	3.94
.3075		35.00	.348	1.19	1.1015	.0070	33.90	27.89	3.63
.3125		39.00	1.38	4.30	1.1085	.0070	26.42	16.90	2.12
.3175		40.50	2.80	7.93	1.1320	.0400	26.46	4.39	.518
.3225		46.50	4.78	12.28	1.1610	.0180	26.47	14.16	1.66
.3300	.0100	55.50	8.09	17.87	1.1800	.0200	26.45	21.74	2.63
.3400		57.00	10.86	19.74	1.2350	.0900	21.73	18.78	2.18
.3500		58.60	13.52	20.50	1.2900	.0200	21.15	17.20	1.87
.3600		60.00	16.01	20.56	1.3200	.0400	17.02	6.89	.687
.3750	.0200	62.87	20.01	20.62	1.3500	.0200	17.05	.0680	.0082
.3950		67.67	25.89	20.76	1.3950	.0700	15.65	.0020	.0003
.4150		95.55	42.07	27.34	1.4425	.0250	13.80	.3652	.0342
.4350		93.25	45.78	24.87	1.4625	.0150	13.83	2.39	.2064
.4550		108.0	57.69	26.91	1.4770	.0140	13.85	1.54	.1316
.4750		107.1	60.98	24.95	1.4970	.0260	12.92	5.20	.4369
.4950		100.7	60.14	21.98	1.5200	.0200	11.38	9.43	.8245
.5150		96.75	59.71	19.80	1.5390	.0180	11.30	10.04	.8740
.5350		98.50	62.09	18.91	1.5580	.0200	11.32	10.14	.8680
.5550		96.47	61.84	17.48	1.5780	.0200	11.32	9.87	.8250
.5750		95.40	61.78	16.38	1.5920	.0080	11.31	10.16	.8424
.5950		93.40	61.77	15.46	1.6100	.0280	9.63	8.41	.6822
.6150		88.27	59.61	14.19	1.6300	.0120	9.38	8.73	.6758
.6350		84.67	59.15	13.48	1.6460	.0200	9.35	8.40	.6608
.6550		82.00	58.99	12.92	1.6780	.0440	9.34	8.10	.6135
.6780	.0260	76.51	58.13	12.22	1.7400	.0800	7.78	5.21	.3595
.7035	.0250	74.28	55.48	11.14	1.8000	.0400	7.13	.284	.0019
.7250	.0180	70.88	46.51	8.18	1.8600	.0800	6.51	.0002	.0000
.7400	.0120	68.50	51.92	9.87	1.9200	.0400	5.49	.0007	.0000
.7525	.0130	67.69	52.82	9.93	1.9600	.0400	5.49	.652	.0352
.7625	.0070	65.42	28.54	5.01	1.9850	.0100	5.50	2.88	.1547
.7680	.0040	64.75	45.80	8.32	2.0050	.0300	4.93	1.44	.0759
.7770	.0140	62.46	49.41	9.01	2.0350	.0300	4.67	2.97	.1563
.7985	.0250	60.42	47.32	8.39	2.0650	.0300	4.67	2.35	.1182
.8250	.0320	56.71	39.88	6.70	2.1000	.0400	4.31	3.58	.1810
.8455	.0090	53.55	42.76	7.20	2.1480	.0560	3.97	3.45	.1675
.8675	.0350	51.10	41.47	6.84	2.1980	.0440	3.72	3.09	.1423
.8890	.0080	49.12	39.53	6.35	2.2700	.1000	3.32	2.98	.1300
.9100	.0340	46.23	29.92	4.55	2.3600	.0800	2.94	2.03	.0791
.9470	.0400	42.51	11.33	1.60	2.4500	.1000	2.55	.492	.0170
.9770	.0200	39.70	26.73	3.81					

TABLE II. - RATIO OF DIFFUSE TO
 DIRECT SOLAR ENERGY RECEIVED
 BY HORIZONTAL SURFACE
 LOCATED AT BOTTOM
 OF ATMOSPHERIC
 MODELS C1 AND D1^a

[Wavelength, 0.535 μm ; Lambert
 reflectivity, 0.]

Solar zenith angle, deg	Ratio of diffuse to direct solar energy, $F_{d\lambda}/F_{s\lambda}$	
	For model C1	For model D1
0	0.147	0.481
15	.152	.500
30	.170	.566
40	.193	.651
50	.232	.804
60	.304	1.112
70	.471	1.969
75	.670	3.308
80	1.196	8.852

^aDave and Braslau, 1974.

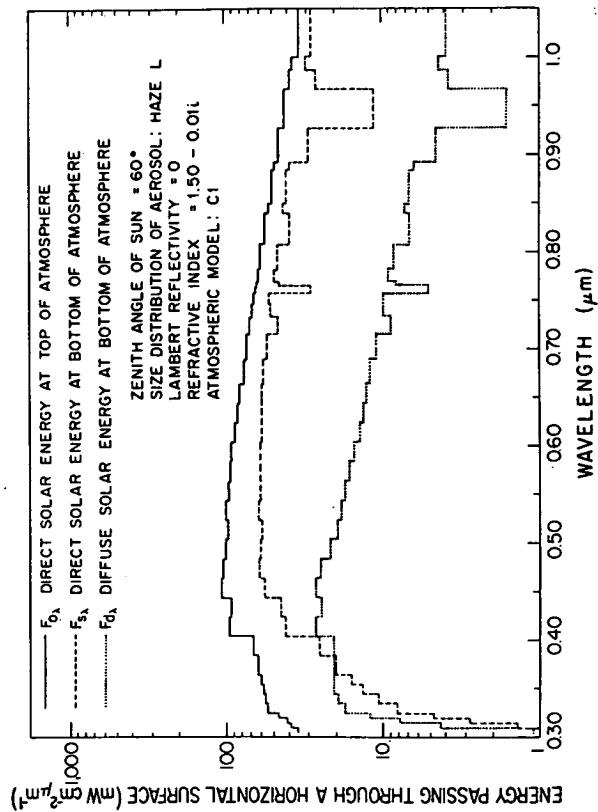


Figure 1. - Computed spectral distributions of the 0.305 to 1.05 μm region of the direct solar energy (solid curve) incident on a horizontal flat surface located at the top, and the direct (broken curve) as well as diffuse (dotted curve) solar energy received by it when located at the bottom of a model atmosphere.

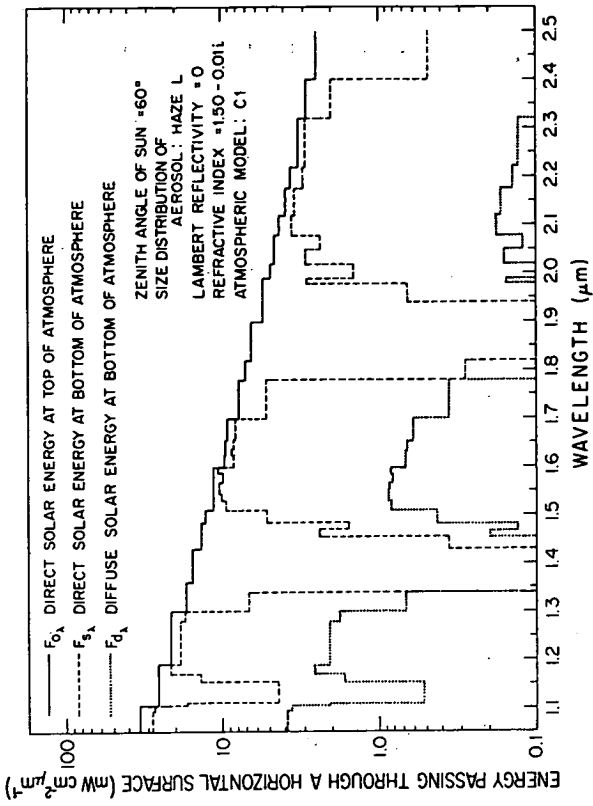


Figure 2. - Computed spectral distribution of the 1.05 to 2.5 μm region of the direct solar energy (solid curve) incident on a horizontal flat surface located at the top, and the direct (broken curve) as well as diffuse (dotted curve) solar energy received by it when located at the bottom of a model atmosphere.

Stationary Silicon Solar Cell Converter Calculations^a

Werner Luft

International Rectifier Corporation El Segundo, California

The power output from a silicon solar cell converter depends on its geographical location. The article shows how the required amount of silicon solar cells for a given power output is determined for any place on the globe; the optimum angle to which a stationary converter should be tilted; and how the required storage device capacity for continuous operation is calculated.

INTRODUCTION

There are many places on earth where conventional electrical power is not readily available. If electrical communication equipment such as receivers, transmitters, or relay links are to be operated in such places, special means for power supply must be devised. One of the most suitable of the unconventional sources is the silicon solar cell converter.

The silicon solar cell converter can not only provide electrical power anywhere a reasonable amount of sunshine is available, but it can also operate for long periods without attendance. This second advantage is of especial importance for microwave or radio relay links. However, when continuous power output is required day and night through the whole year, the converter must be complemented with storage devices.

It is the intent of this article to show how the required amount of silicon solar cells for a given power output can be determined for any place on earth; the angle such a stationary converter should be tilted to, and the capacity required by the storage device to insure continuous operation throughout the year.

NOMENCLATURE

A	Collector area, m^2
φ	Declination of the sun, degrees
Λ	Geographical latitude, degrees
κ	Time angle from solar noon, degrees
Θ	Sunrise hour angle (true solar time), degrees
m_h	Relative optical air mass
m	Optical air mass
p	Atmospheric pressure, millibars (1 mb = 10^3 dyne/cm ²)
G	Total insolation on a surface perpendicular to the sunrays, wm^{-2}

F_λ	Spectral correction factor for silicon solar cells
ϕ	Angle with x -axis of normal to horizontal surface element, degrees
ξ_s	Angle of south-facing flat collector with horizontal surface, degrees
Γ	Angle with x -axis of normal to tilted collector surface, degrees
λ	Angle between actual latitude and optimum latitude for given declination and collector angle ξ , degrees
P	Power, watts
I	Current output, amperes
V	Voltage output, volts
F_T	Temperature correction factor of output voltage for silicon solar cells
Q	Charge, ampere-hours

Subscripts

N	North
S	South
Opt	Optimum
Max	Maximum

Equations and Definitions

$$\zeta = (\pi/2) - \Lambda_N = (\pi/2) + \Lambda_S \quad [1]$$

$$m = 10^{-3} p m_h \quad [2]$$

$$\Lambda_{N \text{ Opt}} = \varphi_N + \xi_S; \quad \Lambda_{S \text{ Opt}} = \varphi_S + \xi_N \quad [3]$$

$$\Lambda_{\text{Opt}} - \Lambda = \lambda \quad [4]$$

$$\cos \phi = \cos \zeta \sin \varphi + \sin \zeta \cos \varphi \cos \kappa \quad [5]$$

$$\cos \phi_{\text{max}} = \cos \zeta \sin \varphi + \sin \zeta \cos \varphi \quad [6]$$

$$\cos \Theta = \tan \varphi / \tan \zeta \quad [7]$$

$$\cos \Gamma = \cos (\zeta + \xi) \sin \varphi + \sin (\zeta + \xi) \cos \varphi \cos \kappa \quad [8]$$

$$\cos \Gamma_{\text{max}} = \cos (\zeta + \xi) \sin \varphi + \sin (\zeta + \xi) \cos \varphi \quad [9]$$

Insolation on clear days

The amount of solar energy received on an area of the earth's surface varies over the day and over the year. The daily variations are caused by the spinning of the earth and the yearly variations by the change in solar declination.¹⁻⁶

^aReprinted from Solar Energy, vol. VI, no. 1, January 1962.

The power input on a horizontal collector of area A is given at any moment by the equation:

$$P_{in} = AG \cos \phi \quad [10]$$

and for a collector facing south and making an angle of ξ with the horizontal by the equation:

$$P_{in} = AG \cos \Gamma \quad [11]$$

Figure 1 shows the geometry and nomenclature used for the angles.

Since the power input is proportional to $\cos \phi$ or $\cos \Gamma$ it is necessary to determine these quantities. Both ϕ and Γ can be expressed in terms of ζ , the declination φ and the time angle κ as shown in Eqs. [5] and [8].

The relation of ζ to a latitude is given by Eq. [1] and the solar declination φ is given in Fig. 2 for each month throughout the year for the Northern and Southern Hemispheres.⁷

Both $\cos \phi$ and $\cos \Gamma$ will reach their maximum at solar noon, i.e., for $\kappa = 0$. In Fig. 3 $\cos \phi_{max}$ is shown as

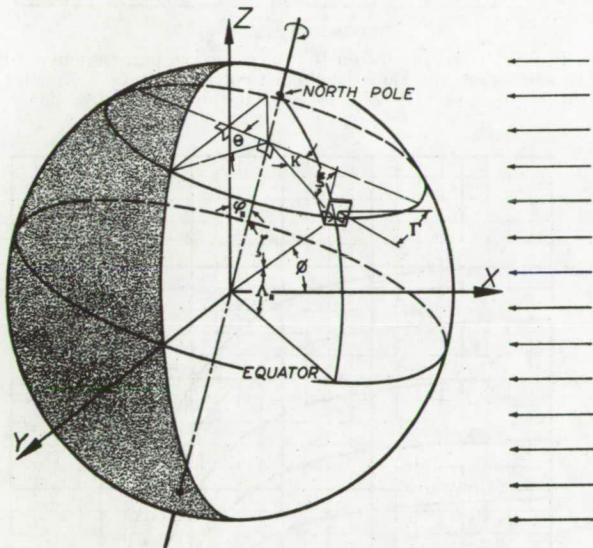


FIG. 1—Geometry and nomenclature.

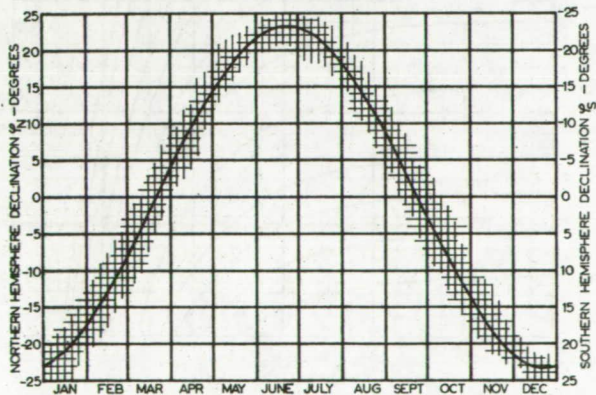


FIG. 2—Solar declination as a function of date for Northern and Southern Hemisphere.

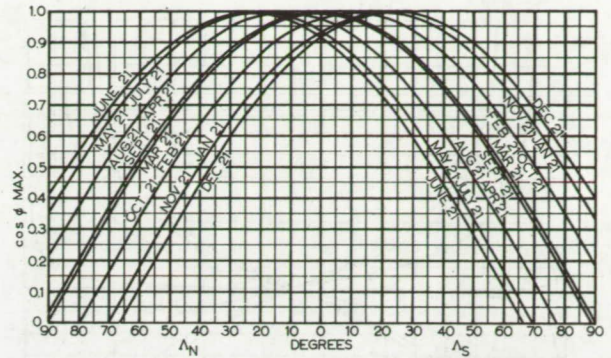


FIG. 3— $\cos \phi_{max}$ as a function of latitude for Northern and Southern Hemisphere with the 21st of each month as parameter.

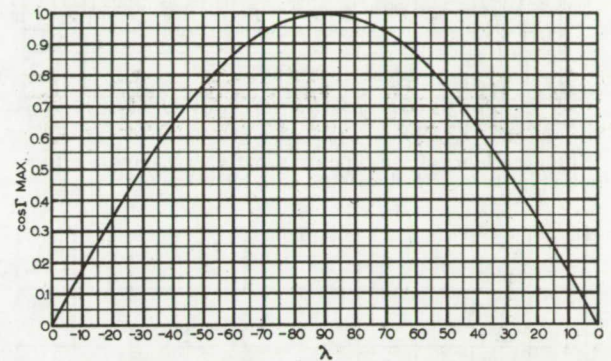


FIG. 4— $\cos \Gamma_{max}$ as function of λ .

a function of latitude for each month. This figure together with Fig. 4 which gives the number of sunshine hours on a clear day throughout the year permits a fast determination of the relative magnitude of the insolation on a horizontal surface at any part of the globe.

$\cos \Gamma_{max}$ cannot conveniently be represented in the same way since this would require one graph for each angle ξ . Therefore, $\cos \Gamma_{max}$ is shown in Fig. 5 as a function of λ which is defined by Eqs. [3] and [4].

The insolation intensity G is not constant, but varies with the length of path in the atmosphere through which the sunrays must pass, i.e., the optical air mass. The relative optical air mass (m_h) is a function of $\cos \phi$ which is shown in Fig. 6. The optical air mass (m) is a function of height above sea level and thus atmospheric pressure, and can be determined from the relative optical air mass using Eq. [2].

SILICON SOLAR CELL CHARACTERISTICS

The output from a silicon solar cell depends not only on the input power intensity, but also on the spectral distribution of such input. The relative response of silicon cells to solar radiation increases with increasing air mass. For calculational purposes it is convenient to use a solar input which has been corrected for spectral variations. This enables us to work with the nominal

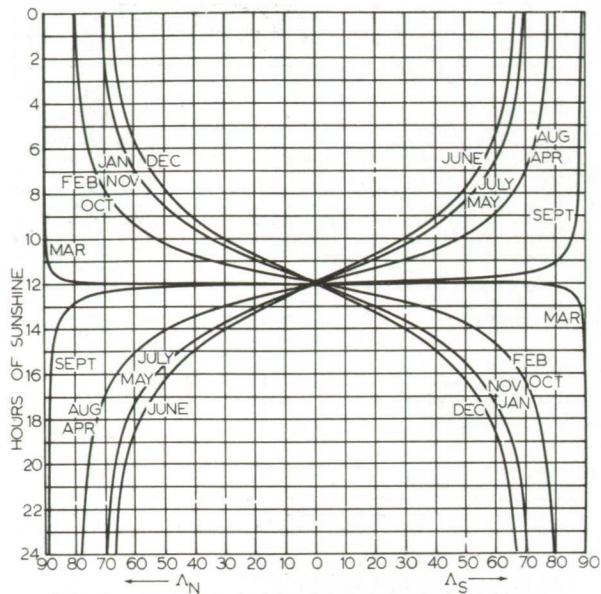


FIG. 5—Hours of sunshine per day for clear days as a function of latitude with the 21st of each month as parameter.

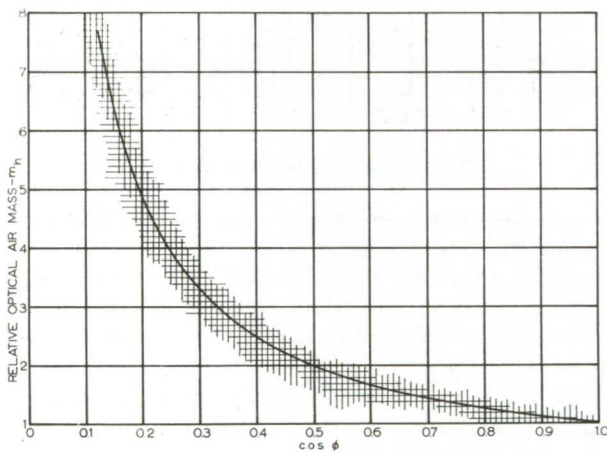


FIG. 6—Relative optical air mass versus $\cos \phi$.

efficiency of silicon cells which refers to optical air mass one. In Fig. 7 which shows the insolation as a function of air mass the corrected insolation is given by the curve $F_{\lambda}G$.*

The typical output characteristics of a silicon solar cell having a nominal efficiency of 10% and an active area of 1 cm^2 operating at a cell temperature of 30 C are given in Fig. 8 for several values of $F_{\lambda}G$. The effect of increased area per cell is the same as for parallel connection of cell, viz., a proportional increase of output current. An increase in voltage is obtained through series connection of cells or cell groups in parallel. The voltage is proportional to the number of cells in series.

* The correction factor is based on the following atmospheric conditions: Precipitable water = 20 mm , Dust: 300 particles per cm^2 , Ozone 2.8 mm .⁸

Increased temperature decreases the output voltage by approximately 0.54% per degree centigrade. It is therefore of importance to keep the solar cell temperature as low as possible. To achieve this, the collector is best placed on top of a hill to allow maximum cooling by the wind. Under no circumstances should the cells be placed under glass leaving an air layer between the glass and the cells, since such an arrangement acts as

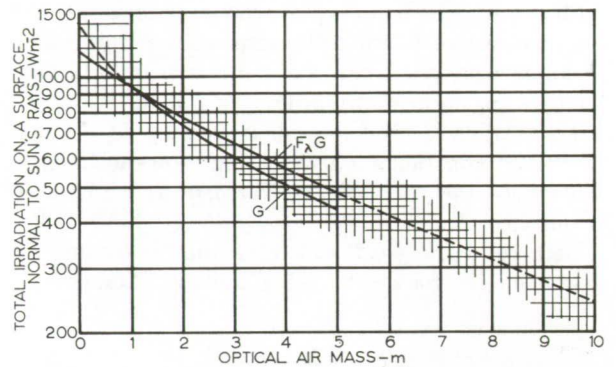


FIG. 7—Total insolation (G) on a surface perpendicular to the sun's rays and same insolation corrected for silicon solar cell relative spectral response as function of optical air mass.

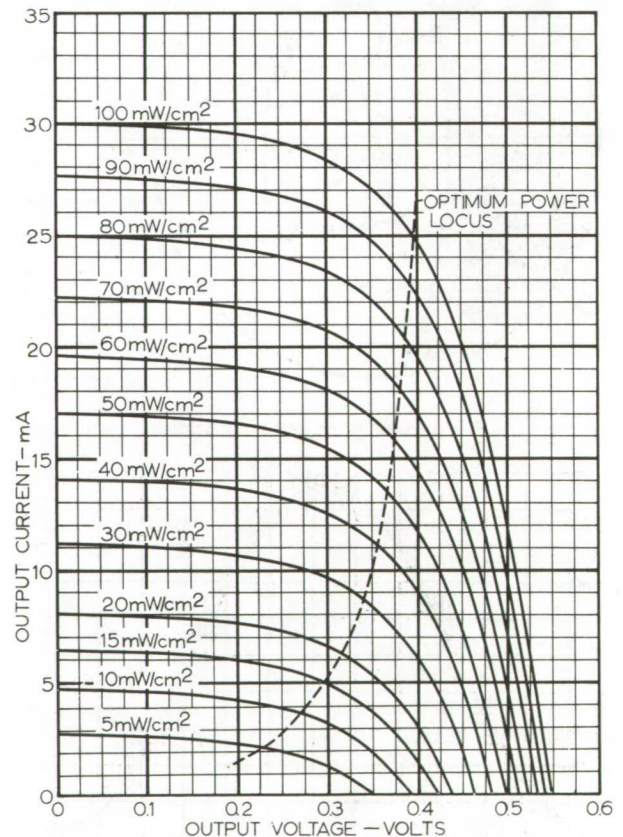


FIG. 8—Typical output characteristics for silicon solar cells of 10% efficiency at optical air mass one having an active area of 1 cm^2 as function of $F_{\lambda}G$. Cell temperature 30 C .

a heat trap. Also, care should be taken to allow maximum cooling at the back of the converter. This cooling is achieved by causing the air to flow in direct contact with the back of the cell modules which are usually the basic building blocks of the converter.

It is necessary to avoid shadows falling over any part of the converter while operating, since this may drastically reduce the power output.⁹

voltage by V_{corr} which gives the number of cells to be connected in series.

Example

Determine the number of solar cells required to supply 500 mw at 20 v average output over any time of the year at Holsteinsborg, Greenland ($\Lambda_N = 66^\circ 56'$, sea level), the following additional data being known.

1954 to 1958	J	F	M	A	M	J	J	A	S	O	N	D
Temperature												
Max. °C.....	5	9	9	10	19	18	20	19	14	11	6	4
Min. °C.....	-30	-32	-24	-19	-11	-4	-3	-1	-3	-12	-21	-26
Clouds %.....	51	45	46	47	48	50	45	55	56	57	58	51

To obtain the maximum power output, the converter must be tilted to the correct angle ξ . This angle will depend on the time at which maximum power output is desired. For intermittent load, optimum output may be needed when the average amount of sunshine is least, whereas, for continuous load throughout a year, the yearly output over the full year should be optimized. At any particular time, the optimum angle, ξ_{opt} , is given by the difference between the latitude and the declination. When optimum power output over the full year is required, several trial and error calculations may have to be made,

CALCULATIONS FOR A CONVERTER OF GIVEN OUTPUT

1. Determine φ , $\cos \phi_{max}$ and the sunshine hours per day for each month of the year.
2. Determine ζ and ξ_{opt} .
3. Calculate $\cos \phi$ and $\cos \Gamma$ from sunrise to sunset for each month and tabulate the hourly averages for $\cos \phi$ and $\cos \Gamma$.
4. Tabulate m_h for each average value of $\cos \phi$, as well as m if the location is not at sea level, and $F_\lambda G$.
5. Tabulate the product of $F_\lambda G$ and $\cos \Gamma$ for corresponding values.
6. Determine an optimum voltage (V_{opt}) per cell which corresponds to the input energy ($F_\lambda G \cos \Gamma$) and tabulate the output current from one cm^2 active cell area for each value of $F_\lambda G \cos \Gamma$ at that voltage.
7. Tabulate the products of current and time (Q) and sum up the products over the day.
8. Plot the obtained charge vs. date and integrate. Divide the required output by the average output to determine the active cell area required for clear days. Divide this area by the percent clear sky to obtain the total active area in parallel.
9. Determine the cell temperature from data of the ambient temperature and correct V_{opt} for the actual temperature. Divide the required charging or operating

We tabulate first φ , $\cos \phi_{max}$, hours of sunshine for clear days for the 21st of each month as shown in Table 1. Inspection of Table 1 reveals that the solar input is negligible for December and small for November and January. The first month for which attempts should be made to supply the full required power is February or March. If we choose March the storage system must be increased. The ultimate choice will depend upon the relative cost for solar cells and storage batteries. Since solar cells present the higher cost item we have chosen March as first month for full power output. The optimum angle of the collector for March 21 ($\varphi_N = -0.11$) is:

$$\xi_{opt} = \Lambda_N - \varphi_N = 67 \text{ degrees.}$$

We now calculate $\cos \phi$ and $\cos \Gamma$ from sunrise to sunset. The results are plotted in Figs. 9 and 10. From these figures the average values of $\cos \phi$ and $\cos \Gamma$ over one hour periods are tabulated as shown in Table 2.

From Fig. 6 we determine the relative optimal air mass and from Fig. 7 the corresponding values of $F_\lambda G$

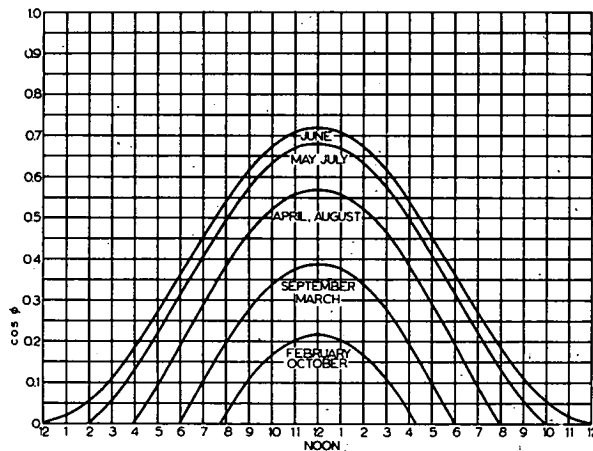


Fig. 9—Daily variation of $\cos \phi$ for Holsteinsborg (67° north) for several months of the year.

TABLE 1

	J 21	F 21	M 21	A 21	M 21	J 21	J 21	A 21	S 21	O 21	N 21	D 21
Declination ϕ_n , Degrees	-20.09	-10.87	-0.11	+11.56	+20	+23.44	+20.65	+12.42	+1.05	-10.32	-19.72	-23.44
$\cos \phi_{\max}$	0.05	0.218	0.39	0.57	0.68	0.725	0.69	0.58	0.41	0.22	0.06	0
Sunshine on clear day, hrs	4.3	8.4	12	16	20	24	20	16	12.3	8.5	4.5	0

TABLE 2

Month	Time	$\cos \phi$	$\cos \Gamma$	m_A	$F_{\lambda G}$ Wm^{-2}	$F_{\lambda G} \cos \Gamma$ Wm^{-2}	Output per cm^2 active area @ $30^\circ C$					
							V	ma	ma-hr			
Feb. -10.5	12	0.215	0.970	4.55	510	495	0.35	14	28			
	13	.189	.910	5.15	470	428						
	14	.138	.765	6.9	370	283						
	15	.067	.590	14	150	88						
										1.5	3	
									71			
March 0	12	.387	.988	2.57	690	681	.35	19	38			
	13	.360	.925	2.75	670	620						
	14	.310	.790	3.20	630	498						
	15	.288	.605	3.42	600	363						
	16	.150	.385	6.4	390	150						
	17	.050	.130	15	130	17						
										0	7	
							0	0				
									128			
April +12	12	.570	.965	1.75	810	781	.37	20.8	41.6			
	13	.545	.902	1.82	790	713						
	14	.496	.765	2.0	770	589						
	15	.425	.590	2.35	740	437						
	16	.338	.370	2.92	660	244						
	17	.240	.130	4.1	550	71.5						
	18	.140	0	—	—	—						
	19	.043								0	0	
												146.6
May +20	12	.680	.925	1.48	850	786	.37	21	42			
	13	.655	.865	1.54	840	726						
	14	.606	.742	1.65	820	608						
	15	.538	.570	1.85	790	450						
	16	.452	.360	2.2	750	270						
	17	.360	.130	2.75	680	88.5						
	18	.268	0	—	—	—						
	19	.177								0.6	1.2	
	20	.093										
	21	.025										
												152.0
June +23.4	12	.720	.906	1.40	865	784	.37	20.9	41.8			
	13	.696	.847	1.45	850	720						
	14	.647	.725	1.55	840	609						
	15	.583	.555	1.71	815	442						
	16	.500	.355	1.98	770	274						
	17	.410	.130	2.42	720	93.6						
	18	.316	0	—	—	—						
	19	.225								0.7	1.4	
	20	.145										
	21	.079										
	22	.033										
	23	.010										
												151.2

for each value of $\cos \phi$ which is entered in Table 2. Then the product $F_{\lambda G} \cos \Gamma$ is tabulated.

From Fig. 8 a voltage of 0.35 v per cell will cause the cell to operate in the vicinity of the optimum power locus illustrated by the dashed line. Now tabulate the output currents at 0.35 v per cell in Table 2. The cur-

rent is multiplied by the time for which the cell gives such output (which is twice as much as indicated in the hour column) to obtain the charge. The charge per day is added up. For March this makes 128 ma-hrs/day average. The output per cm^2 active cell area for every month is then tabulated in a similar manner. Plotting

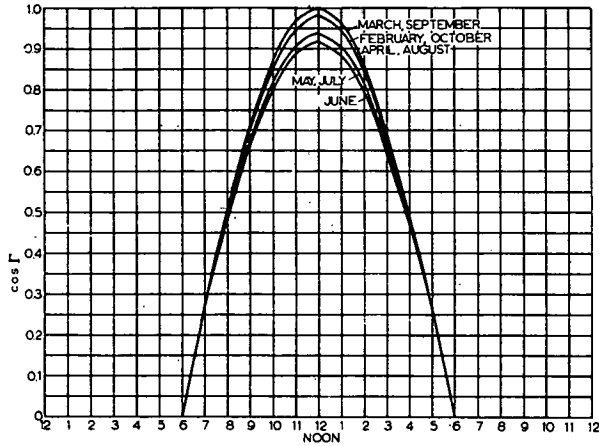


FIG. 10—Daily variation of $\cos \Gamma$ for collector having $\xi = 67^\circ$ in Holsteinborg for several months of the year.

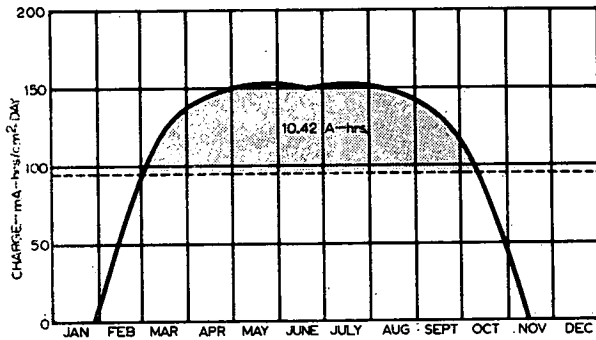


FIG. 11—Daily charge per cm^2 active cell area vs date for converter having $\xi = 67^\circ$ in Holsteinborg over the full year. Sectioned area: required storage capacity for system.

the data allows us to draw a curve as shown in Fig. 11. Integrating the area under this curve graphically determines the average output per cm^2 of active cell area per day. In this case, the average is $95 \text{ ma-hrs/day-cm}^2$.

The output required from the converter is $24 \times 500/20 = 600 \text{ ma-hrs/day}$. Consequently, $600/95 = 6.32 \text{ cm}^2$ of active cell area in parallel is required. This corresponds closely to four cells of standard $1 \times 2 \text{ cm}$ size.

The voltage per cell is 0.35 v at $+30 \text{ C}$. The maximum ambient temperature is only $+9 \text{ C}$ for March, but we may assume that the cell temperature during windless periods is 20 C above the ambient. The temperature coefficient of the voltage is approximately $0.54 \%/C$. The actual voltage per cell is therefore 0.352 v .

The number of cells which are required in series is $20/0.352 = 57$ and the total number of cells is $4 \times 57 = 228$. Since the sky is clouded for about 50% of the day the actual number of cells required is $228/0.50 = 456$. To this number of cells there must be added a sufficient number of cells to compensate for the blocking diode which should be used to avoid discharge through the converter under periods of no illumination.⁹

The required storage capacity of the battery is equal to the sectioned area in Fig. 11, which is 10.42 amp-hr . Depending on the discharge deemed advisable, the actual required storage capacity of the batteries is obtained. For instance, assuming maximum discharge to 70% of rated capacity, then the batteries must have a capacity of $10.42/0.30 = 35 \text{ amp-hr}$ at 20 v .

REFERENCES

1. Hand, I. F., "Insolation on Cloudless Days at the Time of Solstices and Equinoxes," *Heating and Ventilating*, **11**, 97-100 (Feb. 1954).
2. Jordan, R. C. and Threlkeld, J. L., "Solar Energy Availability for Heating in the United States," *Heating, Piping & Air Conditioning*, **25**, 111-122 (Dec. 1953).
3. Hand, I. F., "Distribution of Solar Energy over the United States," *Heating and Ventilating*, **10**, 73-75 (July, 1953).
4. Threlkeld, J. L. and Jordan, R. C., "Direct Solar Radiation Available on Clear Days," *Heating, Piping and Air Conditioning*, **29** (12), 135-145 (Dec. 1957).
5. Fritz, S., "Solar Radiation During Cloudless Days," *Heating and Ventilating*, **46**, 67-74 (Jan. 1949).
6. Fritz, S. and MacDonald, T. H., "Average Solar Radiation in the United States," *Heating and Ventilating*, **46** (7), 61-64 (July, 1949).
7. IGY Instruction Manual, Part VI, Radiation Instruments and Measurements, Pergamon Press, New York, 1958.
8. Moon, P., "Proposed Standard Solar Radiation Curves for Engineering Use," *J. Franklin Inst.*, **230**, 583-617 (Nov. 1940).
9. Luft, W., "Partial Shading of Silicon Solar Cell Converter Panels," 1961.

ATTENDEES

Evelyn Anagnostou
NASA Lewis Research Center
21000 Brookpark Road
Cleveland, Ohio 44135

Robert Backner
Solar Systems, Inc.
8124 N. Central Park
Skokie, Ill. 60076

Cosmo Baraona
NASA Lewis Research Center
21000 Brookpark Road
Cleveland, Ohio 44135

Joan B. Berkowitz
Arthur D. Little, Inc.
Acorn Park
Cambridge, Mass. 02140

Daniel Bernatowicz
NASA Lewis Research Center
21000 Brookpark Road
Cleveland, Ohio 44135

William Bifano
NASA Lewis Research Center
21000 Brookpark Road
Cleveland, Ohio 44135

Karl W. Boer
University of Delaware
Institute of Energy Conversion
Newark, Del. 19711

Eldon C. Boes
Sandia Laboratory
Albuquerque, N. Mex. 87115

Henry Brandhorst
NASA Lewis Research Center
21000 Brookpark Road
Cleveland, Ohio 44135

Jacob Broder
NASA Lewis Research Center
21000 Brookpark Road
Cleveland, Ohio 44135

C. Thomas Brown
Georgia Institute of Technology
Atlanta, Ga. 30332

Donald Buchele
NASA Lewis Research Center
21000 Brookpark Road
Cleveland, Ohio 44135

John A. Castle
Spectrolab
12500 Gladstone Avenue
Sylmar, Calif. 91342

T. L. Chu
Electronic Sciences Center
Southern Methodist University
Dallas, Tex. 75275

Henry Curtis
NASA Lewis Research Center
21000 Brookpark Road
Cleveland, Ohio 44135

Vincent DeLeo
Spectrolab
12484 Gladstone Avenue
Sylmar, Calif. 91342

Edgar DeMeo
Department of Engineering
Brown University
Providence, R. I. 02912

John C. C. Fan
Lincoln Laboratories
Massachusetts Institute of Technology
Lexington, Mass. 02173

Erwin Fischer-Colbrie
Lawrence Livermore Lab
L156
Livermore, Calif. 94550

Edwin C. Flowers
Division of Meteorology
EPA National Environmental
Research Center
Research Triangle Park, N. C. 27711

Americo Forestieri
NASA Lewis Research Center
21000 Brookpark Road
Cleveland, Ohio 44135

Robert Fornay
Jet Propulsion Laboratory
4800 Oak Grove Drive
Pasadena, Calif. 91103

Michael Godlewski
NASA Lewis Research Center
21000 Brookpark Road
Cleveland, Ohio 44135

Jon Geist
Room A223 MET
National Bureau of Standards
Washington, D. C. 20234

John V. Goldsmith
Jet Propulsion Laboratory
4800 Oak Grove Drive
Pasadena, Calif. 91103

Edwin Greeneich
Westinghouse Research Laboratories
Beulah Road
Pittsburgh, Pa. 15235

Francis Guistairno
D. H. Baldwin Company
1820 Mills Avenue
El Paso, Tex. 79900

R. O. Grubel
General Electric Company
21800 Tungsten Road
Euclid, Ohio 44117

Gregory Haas
Mitre Corporation
McLean, Va. 22101

Henry Hadley
University of Delaware
Institute of Energy Conversion
Newark, Del. 19711

Jack Hall
Rockwell International
3370 Miraloma Avenue
Anaheim, Calif. 92803

Paul Halpern
IBM
2670 Hanover Street
Palo Alto, Calif. 94304

James W. Harrison, Jr.
Research Triangle Institute
P. O. Box 12194
Research Triangle Park, N. C. 27709

Russell Hart
NASA Lewis Research Center
21000 Brookpark Road
Cleveland, Ohio 44135

Eric Hearn
IBM
E. Fishkill
Hopewell Junction, N. Y. 12533

John Hickey
Eppley Laboratories
12 Sheffield Avenue
Newport, R. I. 02840

Dale Hill
Mail Zone T-1-H
Monsanto Company
800 N. Lindberg Blvd.
St. Louis, Mo. 63166

William E. Hornt
Boeing Aerospace Company
Seattle, Wash. 98124

Roland L. Huistrom
Martin Marietta Aerospace
P. O. Box 179, MS 1610
Denver, Colo. 80201

James A. Hutchby
NASA Langley Research Center
Hampton, Va. 23365

Allen K. Kan
Aerospace Corporation
P. O. Box 92957
Los Angeles, Calif. 90009

Lawrence Kazmerski
Electrical Engineering Department
University of Maine
Orona, Maine 04473

J. M. Kendall
Jet Propulsion Laboratory
4800 Oak Grove Drive
Pasadena, Calif. 91103

Gordon Kent
Syracuse University
Syracuse, N. Y. 13210

Alan R. Kirkpatrick
Simulation Physics
41 B Street
Burlington, Mass. 01108

Thomas Klucher
NASA Lewis Research Center
21000 Brookpark Road
Cleveland, Ohio 44135

William Kurth
Tyco Labs., Inc.
Bear Hill Waltham, Mass. 02154

John Lamneck
NASA Lewis Research Center
21000 Brookpark Road
Cleveland, Ohio 44135

Curtis Lampkin
D. H. Baldwin Company
1820 Mills Avenue
El Paso, Tex. 79900

Sheng S. Li
College of Engineering
The University of Florida
Gainesville, Fla. 32601

Shing-Ging Liu
RCA Laboratories
201 Washington Road
Princeton, N. J. 08540

Lt. Commander Lloyd R. Lomer
U.S. Coast Guard COMOT
(G-DET-2)
400 7th Street, S. W.
Washington, D. C. 20590

W. Luft
TRW
One Space Park
Redondo Beach, Calif. 90278

Albert R. Lunde
Boeing Aerospace Company
Thermal Radiation Laboratory
Seattle, Wash. 98124

Hal Macomber
JPL/Caltech
4800 Oak Grove Drive
Pasadena, Calif. 91103

Leonard M. Magid
Energy Research and Development
Administration
1800 G Street, N.W.
Washington, D. C. 20545

Stanley Marsik
NASA Lewis Research Center
21000 Brookpark Road
Cleveland, Ohio 44135

George Mazaris
NASA Lewis Research Center
21000 Brookpark Road
Cleveland, Ohio 44135

Jim McCormick
Dow Corning Corporation
12334 Geddes Road
Hemlock, Mich. 48626

John D. Meakin
Institute of Energy Conversion
University of Delaware
Newark, Del. 19711

Louis Melamed
U.S. Coast Guard R&D
Avery Point
Groton, Conn. 06106

John Minnucci
Simulation Physics
41 B Street
Burlington, Mass. 01108

Tapan Mukherjee
National Science Foundation
Division of Advanced Engineering
Research and Technology
1800 G Street, N.W.
Washington, D.C. 20550

Franck F. Oettinger
Electron Devices Section
National Bureau of Standards
Washington, D.C. 20234

John Pollack
NASA Lewis Research Center
21000 Brookpark Road
Cleveland, Ohio 44135

E. L. Ralph
Spectrolab
12484 Gladstone
Sylmar, Calif. 91342

Anthony Ratajczak
NASA Lewis Research Center
21000 Brookpark Road
Cleveland, Ohio 44135

David Redfield
RCA Laboratories
201 Washington Road
Princeton, N. J. 08540

Kent A. Reed
University of Chicago
Chicago, Ill. 60637

Michael Riches W142
NOAA/NWS
8060 13th Street
Silver Spring, Md. 20910

Louis Rosenblum
NASA Lewis Research Center
21000 Brookpark Road
Cleveland, Ohio 44135

Allen Rothwarf
Institute of Energy Conversion
University of Delaware
Newark, Del. 19711

Peter M. Sandow
Penn State University
University Park, Pa. 16802

Edwin Scheibner
Georgia Institute of Technology
Atlanta, Ga. 30332

Larry Scudder
NASA Lewis Research Center
21000 Brookpark Road
Cleveland, Ohio 44135

Alfred Seck
Centralab
Globe-Union, Inc.
4501 N. Arden Drive
El Monte, Calif. 91734

Katsunori Shimada
Jet Propulsion Laboratory
California Institute of Technology
4800 Oak Grove Drive
Pasadena, Calif. 91103

Donald Staggs
University of Illinois
Box 232
Urbana, Ill. 61801

Jacques St. Pierre
Brown Univeristy
Providence, R. I. 02906

Cliff Swartz
NASA Lewis Research Center
21000 Brookpark Road
Cleveland, Ohio 44135

Albert H. Terp
Tetra Tech
1911 Ft. Myer Drive
Arlington, Va. 22209

Philip Thacher
Sandia Labs
Albuquerque, N. Mex. 87115

Daniel Trivich
Department of Chemistry
Wayne State University
Detroit, Mich. 48202

Orlando Ugucini
NASA Lewis Research Center
21000 Brookpark Road
Cleveland, Ohio 44135

Douglas Warschauer
Naval Weapons Center
China Lake, Calif. 93555

Irving Weinberg
NASA Lewis Research Center
21000 Brookpark Road
Cleveland, Ohio 44135

Ronald Wichner
Lawrence Livermore Lab.
P. O. Box 808
Livermore, Calif. 94550

Victor Weizer
NASA Lewis Research Center
21000 Brookpark Road
Cleveland, Ohio 44135

George Wise
NASA Lewis Research Center
21000 Brookpark Road
Cleveland, Ohio 44135

Charles Wrigley
Solarex
1335 Piccard Drive
Rockville, Md. 20850

Kenneth Yass
NASA Lewis Research Center
21000 Brookpark Road
Cleveland, Ohio 44135

Robert Yasui
Jet Propulsion Laboratory
California Institute of Technology
4800 Oak Grove Drive
Pasadena, Calif. 91103

National Aeronautics and Space Administration

WASHINGTON, D. C. 20546

POSTAGE AND FEES PAID
NATIONAL AERONAUTICS AND
SPACE ADMINISTRATION
NASA-451



OFFICIAL BUSINESS
Penalty For Private Use, \$300.00

SPECIAL FOURTH CLASS MAIL
BOOK

150 001 C1 U E 751215 S00903DS
DEPT OF THE AIR FORCE
AF WEAPONS LABORATORY
ATTN: TECHNICAL LIBRARY (SUL)
KIRTLAND AFB NM 87117